

USE OF DIAGONAL GRIDS (DIAGRIDS) AS AN EARTHQUAKE-RESISTANT SYSTEM FOR TALL BUILDINGS HAVING A CIRCULAR PLAN

by

Samuel Roeslin

A thesis submitted to the faculty Civil Engineering at the Ostbayerische Technische Hochschule, Regensburg (Germany) in partial fulfillment of the requirements for the degree of Master of Engineering in Civil Engineering - Building and Infrastructure Rehabilitation

Author: Samuel Roeslin
B.Eng., Civil Engineering (2014)
sroeslin@hotmail.com
4 rue des Iris
67500 Haguenau - France

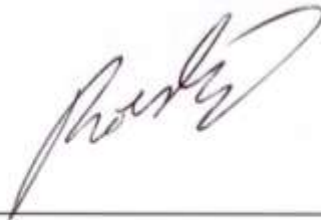
Thesis Supervisor: Dr. Amador Terán Gilmore
Professor, Department of Materials, Area of Technological Development and Sustainability in Civil Engineering
Universidad Autónoma Metropolitana Azcapotzalco, Mexico City
atergil@aol.com

November 15

DECLARATION OF AUTHORSHIP

I hereby declare that the thesis submitted is my own unaided work, unless stated otherwise. No other person's work has been used without due acknowledgement. All references and verbatim extracts have been quoted, and all sources of information, have been specifically acknowledged.

This paper was not previously presented to another examination board and has not been published.



Samuel Roeslin

Faculty of civil engineering

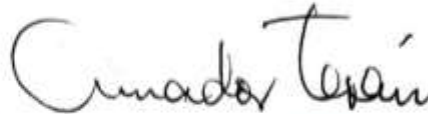
APPROVAL

The undersigned, appointed by the dean of the faculty Civil Engineering at the Ostbayerische Technische Hochschule, Regensburg (Germany), have examined the thesis entitled

Use of diagonal grids (diagrids) as an earthquake-resistant system for tall buildings having a circular plan

presented by Samuel Roeslin

a candidate for the degree of Master of Engineering in Civil Engineering – Building Redevelopment and hereby certify that, in their opinion, it is worthy of acceptance.

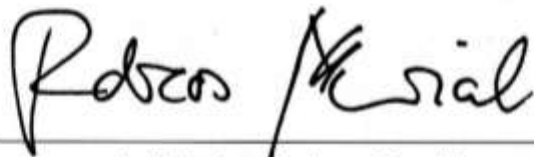


Dr. Amador Terán Gilmore

Professor, Department of Materials

Area of Technological Development and Sustainability in Civil Engineering

Universidad Autónoma Metropolitana Azcapotzalco, Mexico City (Mexico)



Prof. Dr.-Ing. Andreas Maurial

Dean, Faculty Civil Engineering

Ostbayerische Technische Hochschule, Regensburg (Germany)

ABSTRACT

Samuel Roeslin: Use of diagonal grids (diagrids) as an earthquake-resistant system for tall buildings having a circular plan

(Under the direction of Amador Terán Gilmore)

The general purpose targeted is to offer an alternative, from the point of view of the structural system, to reduce the environmental cost of tall buildings located in high seismicity zones.

The work presented in this thesis achieves two particular goals. First, a displacement-based approach was used in order to design a diagrid structural system, earthquake-resistant, for a 24-story building having a circular plan. After the fulfillment of the first target, the focus was set on the study of the dynamic response of the building under earthquake ground motion.

ACKNOWLEDGMENTS

I express my warm thanks to my supervisor Amador Terán Gilmore for his guidance during the time I worked at the Universidad Autónoma Metropolitana Azcapotzalco (UAM) in Mexico City. His selfless contribution will forever be appreciated.

I would also like to extend my gratitude to Arturo Quiroz Ramírez for his patient support and his helpful comments and suggestions. His participation to my professional progress has been invaluable.

I would like to thank Andreas Maurial for the time he devoted to help me for the preparation of this exchange. His thoughtful advice and unwavering support provided me the encouragement to continue. His foreign experience and Spanish skills contributed a lot to the accomplishment of this exchange between the Universidad Autónoma Metropolitana Azcapotzalco in Mexico City (Mexico) and the Ostbayerische Technische Hochschule in Regensburg (Germany).

I wish to express my appreciation to the Universidad Autónoma Metropolitana Azcapotzalco, which provide me access to the facilities in order to accomplish my work.

A special thank you to my parents and family-members, who despite the distance, gave me a steadfast support.

Special thanks to Maïke for her prodigious advice, to Maud for her support emails and to Annabelle and Andreas for their great company during my stay in Mexico City. I thank all my friends from Mexico and also from Germany and France, who were not present in person but called and wrote me often.

Table of Contents

LIST OF FIGURES.....	IX
LIST OF TABLE	XI
1. INTRODUCTION.....	1
2. DIAGRIDS: EXPLANATION	2
2.1 What is a diagrid system?	2
2.2 How do diagrids behave?.....	2
2.3 Points of attention.....	3
2.4 Diagrids application	3
2.5 Diagrids vs braces	4
2.6 Diagrids as sustainable system.....	5
2.7 History.....	5
2.8 Reference buildings based on (Boake 2014).....	6
3. DIAGRID BUILDING WITH A CIRCULAR PLAN SHAPE.....	10
3.1 Why work with a circular shape?	10
3.2 Building parameters	10
3.3 Choice of diagrid parameters.....	12
3.3.1. Help for design	12
3.3.2. Choice for our project.....	13
4. GRAVITATIONAL SYSTEM	15
4.1 Loads for one floor	15
4.2 Slab: steel-deck (Losacero).....	15
4.3 Steel design: beams.....	17
4.3.1. Beam sections	17
4.3.2. Properties of structural steel: A992Fy50	18
4.3.3. Design check with SAP2000	19
4.4 Steel design: columns	20
4.4.1. Columns sections.....	20
4.4.2. Design check with SAP2000	21
4.5 Core design: reinforced concrete.....	22
4.5.1. Capacity design.....	22
4.5.2. Properties of concrete: 6000Psi	23

4.5.3. Properties of rebar steel: A615Gr60.....	23
4.5.4. Columns	24
4.5.5. Beams	25
5. DISPLACEMENT BASED DESIGN.....	26
6. DIAGRIDS.....	30
6.1 Methodology for the preliminary design of diagrids.....	30
6.1.1. Fundamental period of vibration	30
6.1.2. Factor k (FEMA 356)	30
6.1.3. Lateral force F_i	31
6.1.4. Initial value for the area of the diagonals	31
6.1.5. Lateral stiffness in shear and lateral displacement	31
6.1.6. Lateral bending stiffness	32
6.1.7. Curvatures and rotations	32
6.1.8. Period.....	34
6.1.9. Final values of the area	34
6.2 Design of the diagrids for the circular building	35
6.2.1. Definition of performance	35
6.2.2. Coefficient of distortion	35
6.2.3. Factor α	36
6.2.4. Period $T_{T \text{ required}}$	37
6.2.5. Factor k	37
6.2.6. Factor for the percentage of mass moved by the first eigenmode.....	38
6.2.7. Lateral forces and moments	38
6.2.8. Initial value of the diagrids area A^0	39
6.2.9. Lateral stiffness in shear and lateral displacement	40
6.2.10. Lateral bending stiffness	43
6.2.11. Curvatures and rotations	44
6.2.12. Lateral displacement	46
6.2.13. Iteration	47
6.2.14. Period T_T^0 (after iteration).....	47
6.2.15. Areas for the diagrids (after iteration).....	47
6.2.16. Ductility of the building (verification of the assumption).....	48

6.2.17. Factor α (verification of the assumption)	49
7. MODEL FEATURES IN SAP2000.....	50
7.1 Modeling of the main elements	51
7.2 Release at the end of the diagonals	52
7.3 Plastic hinges	52
7.3.1. Computation of the plastic hinges properties for the diagonals	53
7.3.2. Computation of the plastic hinges properties for the steel elements	54
7.3.3. Computation of the plastic hinges properties for the concrete elements	57
8. MODAL ANALYSIS	62
9. PUSH-OVER ANALYSIS	63
9.1 Push-over curve.....	63
9.2 Plastic hinges in the diagrids	64
9.3 Plastic hinges in the core	66
9.4 Lateral displacement	68
9.5 Interstory drift	69
9.6 Interstory ductility	70
9.7 Maximal plastic hinges in the diagrids.....	71
10. TIME-HISTORY ANALYSIS.....	72
10.1 Lateral displacement	72
10.2 Interstory drift	73
10.3 Base shear vs displacement	74
11. INITIAL PROPOSAL/POSSIBLE OPTIMIZATION.....	81
12. NEW COEFFICIENT OF DISTORTION FOR DIAGRID BUILDINGS	82
13. CONCLUSION	85
14. APPENDIX	86
Appendix A. Design of the Losacero (steel-deck).....	87
Appendix B. Live loads according to the Mexican proposal	89
Appendix C. Areas designation	90
Appendix D. Loads on one floor	91
Appendix E. Tables for concrete design (U.S. Customary Units)	93
15. PUBLICATION BIBLIOGRAPHY	95

LIST OF FIGURES

Figure 1: Main parts of a diagrid system (Boake 2014)	2
Figure 2: Braced tube vs diagrid structure (Moon et al. 2007)	4
Figure 3: Pictures of reference buildings (1/4)	6
Figure 4: Pictures of reference buildings (2/4)	7
Figure 5: Pictures of reference buildings (3/4)	8
Figure 6: Pictures of reference buildings (4/4)	9
Figure 7: Elevation view - units in [cm] - no scale.....	11
Figure 8: Cross section - floor area (yellow) and core area (blue) - units in [cm] - no scale	11
Figure 9: Building top displacement versus diagrid angle (redrawn from Moon et al., 2007) taken from (Mele et al. 2014)	12
Figure 10: Optimal diagrid inclination for different building heights (Mele et al. 2014)	13
Figure 11: Diagrid module - units in [cm] - no scale	14
Figure 12: Losacero Section 4 with dimensions in [cm] (IMSA).....	16
Figure 13: Cross section with the Losacero caliber 24 (red) and caliber 22 (blue) - no scale	16
Figure 14: W14x43 [mm] Figure 15: W18x35 [mm]	17
Figure 16: W18*40 [mm] Figure 17: W18*46 [mm]	18
Figure 18: Design check of the steel beams with SAP2000 (Computers & Structure).....	19
Figure 19: W14*132 [mm] Figure 20: W14*211 [mm]	20
Figure 21: W14*283 [mm]	20
Figure 22: Design check of the steel columns with SAP2000 (Computers & Structure).....	21
Figure 23: Column reinforcement [cm].....	24
Figure 24: Beam reinforcement [cm].....	25
Figure 25: Displacement based methodology (Terán Gilmore et al. 2014)	26
Figure 26: Different levels of damage in a building after an earthquake	27
Figure 27: Performance levels	27
Figure 28: Displacement based design spectra for $\mu=1$, $\mu=2$ and $\mu=4$	37
Figure 29: Angle ϕ of the diagrids modules	41
Figure 30: Distance to the centroid axe	43
Figure 31: 3D-Model of the building - SAP2000 (Computers & Structure)	50
Figure 32: Diagrids sections with different area.....	51
Figure 33: Diagonals with released ends.....	52
Figure 34: Force-Displacement diagram for the hinges.....	53
Figure 35: Plastic moment capacity M_p (Segui 2007)	54
Figure 36: Successive stages of loading for a simply supported beam with a concentrated load at midspan (Segui 2007).....	55
Figure 37: Interaction diagram P-M for the steel columns in the base part of the building.....	56
Figure 38: Simplification of the stresses in the concrete compression zone (Terán Gilmore).....	58
Figure 39: Column interaction diagram (McCormac, Brown 2013, p. 291)	60
Figure 40: Column interaction diagram (Terán Gilmore)	60
Figure 41: Interaction diagramm P-M.....	61
Figure 42: Displacement based design spectra for $\mu=1$, $\mu=2$ and $\mu=4$	62

Figure 43: Push-over curve (capacity curve)	63
Figure 44: First plastic hinges in the diagrids	64
Figure 45: Color scale for the plastic hinges (left: small damage, right: heavy damage).....	64
Figure 46: Definition of the points for a plastic hinge	65
Figure 47: Plastic hinges in the diagrids for a roof displacement of 1 m	65
Figure 48: Plastic hinges in the core for a roof displacement of 75 cm	66
Figure 49: Plastic hinges in the concrete core for a roof displacement of 1 m	67
Figure 50: Plastic hinges in the steel elements for a roof displacement of 1 m.....	67
Figure 51: Deformed shape of the building for different roof displacements	68
Figure 52: Nonlinear static analysis: lateral displacement.....	68
Figure 53: Nonlinear static analysis: interstory drift.....	69
Figure 54: Nonlinear static analysis: interstory ductility.....	70
Figure 55: Nonlinear static analysis: plastic deformation in the diagrids	71
Figure 56: Time-analysis maximal roof displacement.....	72
Figure 57: Time-analysis: interstory drift	73
Figure 58: Overview of the base shear vs displacement diagrams for the 10 ground motions.....	74
Figure 59: Base shear vs Roof displacement - Ground motion 1.....	75
Figure 60: Base shear vs Roof displacement - Ground motion 2.....	75
Figure 61: Base shear vs Roof displacement - Ground motion 3.....	76
Figure 62: Base shear vs Roof displacement - Ground motion 4.....	76
Figure 63: Base shear vs Roof displacement - Ground motion 5.....	77
Figure 64: Base shear vs Roof displacement - Ground motion 6.....	77
Figure 65: Base shear vs Roof displacement - Ground motion 7.....	78
Figure 66: Base shear vs Roof displacement - Ground motion 8.....	78
Figure 67: Base shear vs Roof displacement - Ground motion 9.....	79
Figure 68: Base shear vs Roof displacement - Ground motion 10.....	79
Figure 69: Displacement based design spectra for $\mu=1$, $\mu=1,5$, $\mu=2$ and $\mu=4$	83
Figure 70: Values of Modulus of Elasticity for Normal-Weight Concrete (McCormac, Brown 2013, p. 631)	93
Figure 71: Designations, Areas, Perimeters, and Weights of Standard Bars (McCormac, Brown 2013, p. 631)	93
Figure 72: Areas of Groups of Standard Bars (in ²) (McCormac, Brown 2013, p. 634)	94

LIST OF TABLE

Table 1: Opposition Braced vs Diagrid systems, based on (Boake 2014).....	4
Table 2: References diagrids buildings.....	9
Table 3: Geometric parameters for the diagrid structure.....	10
Table 4: Load on the gravitational system (for one floor).....	15
Table 5: Design of the steel-deck (Losacero).....	15
Table 6: Beam sections and self-weight.....	17
Table 7: Structural steel properties	18
Table 8: Column sections and self-weight.....	20
Table 9: Concrete properties.....	23
Table 10: Rebar steel properties	24
Table 11: Steel reinforcement in the columns	24
Table 12: Steel reinforcement in the beams	25
Table 13: Values of coefficient of distortion (Terán Gilmore, Coeto 2011, p. 159).....	35
Table 14: Suggested values of α for regular buildings (Terán Gilmore, Coeto 2011, p. 161).....	36
Table 15: Percentage of mass moved by the first mode (normalized by 100).....	38
Table 16: Computation of the lateral forces and moments (before iteration)	39
Table 17: Initial values for the diagrids areas (before iteration)	40
Table 18: Lateral stiffness and lateral displacement (before iteration).....	42
Table 19: Lateral bending stiffness (before iteration)	44
Table 20: Curvatures and rotations (before iteration).....	45
Table 21: Lateral displacement (before iteration)	46
Table 22: Definitive areas for the diagrids	48
Table 23: Computation of the yield force and yield displacement in the diagrids.....	53
Table 24: Steel main beam section properties.....	56
Table 25: Steel column section properties.....	56
Table 26: Computation of the COD for the diagrid building	82
Table 27: Comparison of the diagrids area with a COD of 1,5 and 1,2	84

1. INTRODUCTION

Today, sustainability plays a key role in the conception, design and construction of buildings. Sustainability encompasses many factors like: energy efficiency, low environmental cost and an efficient use of available resources.

In furtherance of reducing the environmental cost of tall buildings and providing an efficient use of available resources, the structural system known as diagrid has been recently used in many high-rise edifices situated in areas of low seismic activity. Despite the great advantages that this represents from the point of view of sustainability, its use has often been ignored for the design of structural systems of tall constructions in areas of high seismicity, where structural material savings could be higher.

For the sake of a significant reduction of the environmental cost and the amount of structural materials, it is urgent to raise the use of innovative structural systems, like diagrids, for the design and construction of skyscrapers located in seismic areas.

Based on the experience gained through buildings using diagrids in non-seismic areas, it is considered that there are two main design requirements for diagrids located in zones of low seismic activity: on one hand the resistance and on the other the stiffness. Moreover, the use of diagrids in high seismic zones requires explicit consideration of lateral deformation capacity and energy dissipation.

This thesis studies the lateral response of a 24-story diagrid building with circular cross section. The aim is to understand how to control the demand for lateral deformation during an earthquake and find appropriate design requirements to stabilize the lateral response of the structure when the building enters its range of plastic behavior. A displacement-based approach is used in order to enable the preliminary design (also based on performance concepts). This is followed by the study of the dynamic response of the building when subjected to earthquake ground motion.

2. DIAGRIDS: EXPLANATION

2.1 What is a diagrid system?

A diagrid system is a lattice structural system with a triangular pattern that differs from conventional triangular systems due to its narrow members. It is a particular form of space truss mixed with tubular system (Kim, Lee 2012). The term diagrid is a mix of the words “diagonal” and “grid”. Sometimes diagrids are also called “exodiagonal systems” (Mele et al. 2014).

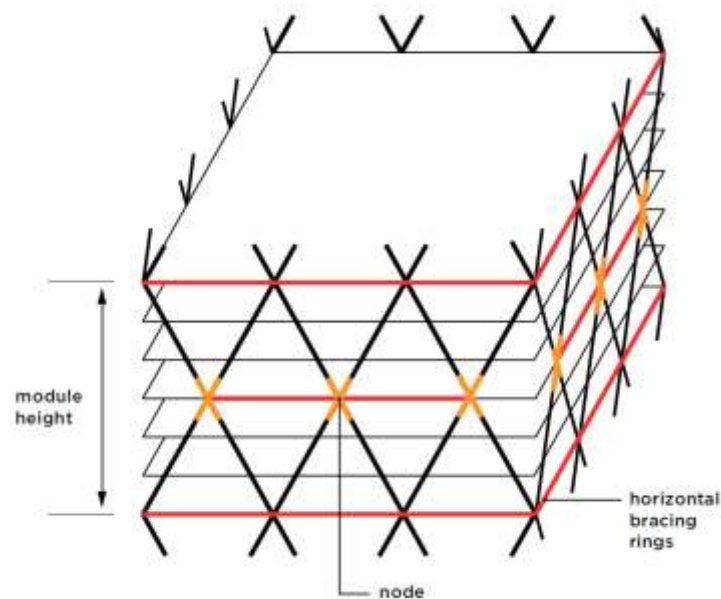


Figure 1: Main parts of a diagrid system (Boake 2014)

As shown in Figure 1, the diagrid system is composed of two main parts: diagonal braces and horizontal bracing rings. The diagonal grids (or braces) have a double function and act as bracing elements as well as inclined columns. The horizontal bracing rings provide stability to the structure by connecting, and thus, integrating the work of the braces (Kim, Lee 2012).

2.2 How do diagrids behave?

The diagrids have a double function because they act as bracing elements as well as inclined columns. Therefore diagrids are able to carry both lateral forces and gravity loads.

The triangulation gives a huge stability to the structure. Because of the triangular shape, the load distribution in the diagrid structural system is similar to the one in trusses. Only axial forces -tension

and compression - but no bending moment develop in the diagrid elements thus diminishing shear racking effects. That's why diagrids show an enormous efficiency. (Mele et al. 2014).

Because of this enormous structural integrity and since diagrids are able to resist the lateral loads of the entire building, the core can be discharged of its function to resist horizontal forces (Boake 2014).

Due to the larger lateral stiffness of diagrids, the response under dynamic loads is also better. (Moon et al. 2007)

In contrast to tubular structures, the shear lag effect developed by diagrids is considerably low. Therefore the in-plane shear stiffness of the surface of the diagrid structure is also higher compared to that of other tubular structures (Kim, Lee 2012).

2.3 Points of attention

When using diagrids, attention must be paid to joints since they are more complicated than those of conventional braced structures. Due to this they are also more expensive to build.

Pin connections are sufficient since only axial forces have to be transferred. The construction of rigid connections which are able to transmit overturning moment is not necessary (Moon et al. 2007).

Compared to a tubular structure diagrids have higher strength, but if buckling of the diagonals is not prevented, they tend to exhibit unstable nonlinear behavior when subjected to lateral loading (Kim, Lee 2012).

2.4 Diagrids application

Diagrids can be used in the interior part of a building in order to create a span free space (for roof lobby for example), but most are used as external systems located at the perimeter of the edifice. The steel structure of the diagrids can be exposed or concealed, in order to fit architecturally requirements (Boake 2014).

A diagrid system can be planar but this is not a necessity. It can also be developed in three-dimensions and achieve multiple and capricious forms (Boake 2014). Another main advantage of diagrids is that they don't rely on a particular building shape and can therefore be customized to follow the building geometry (Moon et al. 2007).

2.5 Diagrids vs braces

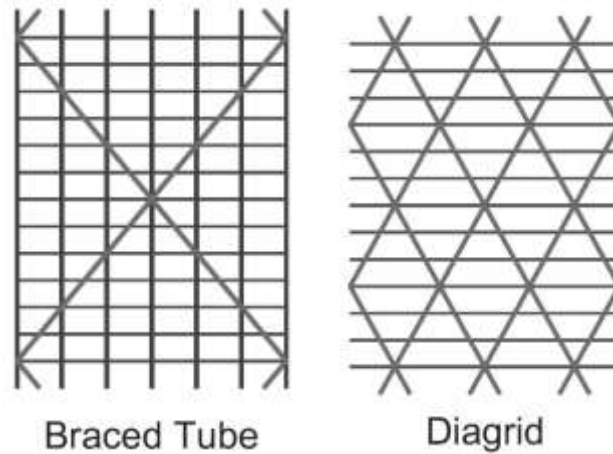


Figure 2: Braced tube vs diagrid structure (Moon et al. 2007)

Figure 2 depicts two sketches of possible structural systems. The one on the left is typical for a braced tube system. As can be seen, there are columns and beams that are stiffened with braces in order to carry the lateral load. The one on the right shows a diagrid system with a module height of 6 stories. Columns are not present since the diagrids are able to withstand vertical as well as horizontal loads.

Table 1: Opposition Braced vs Diagrid systems, based on (Boake 2014)

Braces	Diagrids
Carry only lateral loads	Carry gravity as well as lateral loads
Vertical columns are mandatory	No need of vertical columns
Works well for building with a rectilinear form	The form/shape of the building doesn't matter. Diagrids suit either rectilinear, highly angular, or curved shapes
Need of a core to stabilize the building	No need of core since diagrids are capable of withstanding vertical and horizontal loads
	The triangular pattern provides structural integrity
	Due to the triangular design, redundancy is created over the building since the load can be transmitted through several elements
	Use less structural material

2.6 Diagrids as sustainable system

Steel is principally used because this material behaves in a good way under both tension and compression stress. Steel also offers advantages from a sustainable point of view as explained by Dr. Edwin Basson in the foreword of the book *Diagrid structures - Systems, connections, details* from Terri Meyer Boake (2014):

Sustainable steel is at the core of a green economy. Steel, created as long ago as 150 years, can be recycled and reused in new products and applications. The amount of energy required to produce a tonne of steel has been reduced by 50% in the past 30 years, making it a good choice for building structures. 97% of steel by-products can be reused. As we look to the future life of our buildings through “design for disassembly”, steel will allow for the immediate reuse of structural elements. What cannot be reused as is can be recycled into a closed-loop, cradle-to-cradle system. Steel does not waste.

2.7 History

The late nineteenth century saw the emerging of high-rise buildings in the United States of America. Although at that time skyscrapers were representative of America, nowadays this type of structures expanded all over the globe since they possess economic advantages for dense urban areas. The use of steel in structural systems was a major turning in the building history. Steel rigid frames with wind bracing were used in most high-rise building at the beginning of the twentieth century. The reach of an important height was not achieved through a major technological evolution but rather through an enormous usage of structural material, which led to an over-design of the building structure (Ali, Moon 2007).

The 1960s marked a new area in the design of structural systems for tall buildings with the abandonment of the conventional rigid frames and the use of new systems, like tubular forms. This period saw also the emergence of the use of concrete (Ali, Moon 2007).

The concept of diagrid was born at the end of the nineteenth century, and debuted in the twentieth century in Russia when the engineer Vladimir Grigoryevich Shukhov designed several structures with only diagonal elements. The most know is probably the Shukhov’s Shabolovka Radio Tower (Terán Gilmore et al. 2014).

After that, a long period without building of diagrids followed. Only in 1963, with the IBM Building located in Pittsburgh, USA, the diagrid system found renewed interest. Some buildings like the John Hancock Center in Chicago or the Bank of China Tower in Hong Kong followed in period, which expanded till the end of the twentieth century.

The great enthusiasm for diagrids came at the beginning of the twenty-first century with the buildings designed by Sir Norman Foster. In 2002 and 2004, the London City Hall and Swiss Re (30 St. Mary Axe), respectively, both located in London; and in 2006, the Hearst Magazine Tower,

located in New York. Many other skyscrapers, high-rise buildings and towers, with various shapes and forms, followed.

2.8 Reference buildings based on (Boake 2014)

The following list contain some of the important buildings, which were built with diagrids, from the first tower designed by the Russian engineer Vladimir Shukhov to skyscrapers of our modern world.

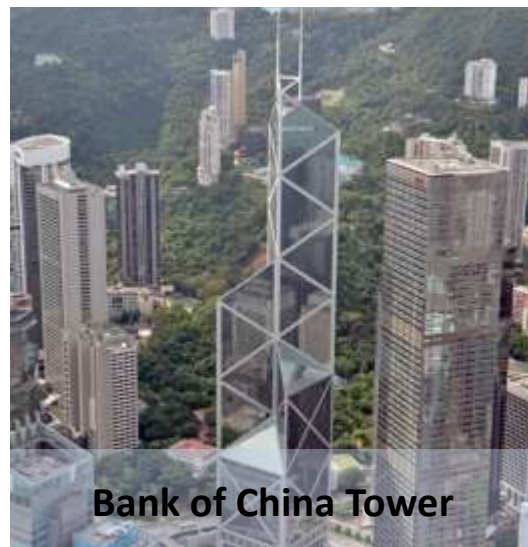
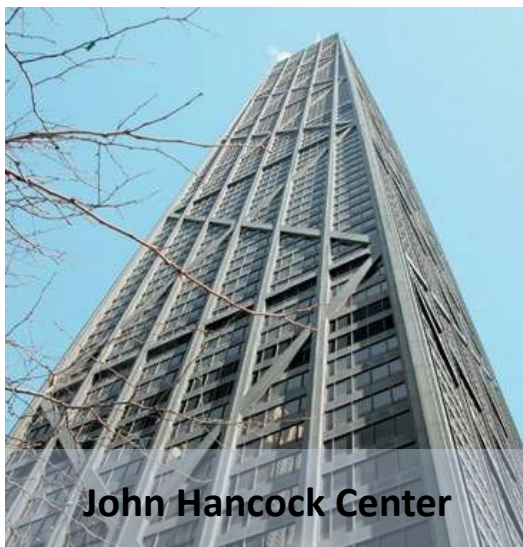


Figure 3: Pictures of reference buildings (1/4)



Puerta de Europa



London City Hall



Swiss Re (30 St. Mary Axe)



Hearst Magazine Tower



Tornado Tower



Guangzhou IFC

Figure 4: Pictures of reference buildings (2/4)



Figure 5: Pictures of reference buildings (3/4)



Figure 6: Pictures of reference buildings (4/4)

Table 2: References diagrids buildings

Building name	Opening	Location	Illustration credits
Shukhov Towers	End of the 19 th , beginning of the 20 th century	Russia	Book (Boake 2014)
IBM Building (United Ironworkers)	1963	Pittsburgh, PA, USA	Terri Meyer Boake
John Hancock Center	1969	Chicago, IL, USA	Terri Meyer Boake
Bank of China Tower	1990	Hong Kong, China	Terri Meyer Boake
Puerta de Europa	1996	Madrid, Spain	Terri Meyer Boake
London City Hall	2002	London, England	Terri Meyer Boake
Swiss Re (30 St. Mary Axe)	2004	London, England	Terri Meyer Boake
Hearst Magazine Tower	2006	New York City, NY, USA	Terri Meyer Boake
Tornado Tower	2008	Doha, Qatar	Alexey Sergeev
Guangzhou IFC	2010	Guangzhou, China	Terri Meyer Boake
O-14	2010	Dubai, UAE	RUR Architecture PC
Aldar Headquarters	2011	Abu Dhabi, UAE	William Hare
Capital Gate	2011	Abu Dhabi, UAE	Terri Meyer Boake
Al Bahar Towers	2012	Abu Dhabi, UAE	Terri Meyer Boake
Doha Tower	2012	Doha, Qatar	Ateliers Jean Nouvel and CSECEC
CCTV	2012	Beijing, China	Terri Meyer Boake
One Shelley Street	2012	Sydney, Australia	Terri Meyer Boake
The Leadenhall Building	2014	London, England	Paul Raftery

3. DIAGRID BUILDING WITH A CIRCULAR PLAN SHAPE

3.1 Why work with a circular shape?

First of all, Kim, Lee (2012) showed in their article that structures with circular plan behave in a better manner than square structures. They compared the maximum displacements for square and circular plan structures having a similar member force/strength ratio and found that circular structures displace less than a square one.

They also noticed that the deformation capacity of square plan buildings is lower than that of edifices having a round plan, and explained that the main reason for this is that the shear lag effect is smaller in a circular plan structure. Thus the structural members are able to carry the loads in a more efficient manner, leading to a higher strength and stiffness.

Previous research have already been done for tall steel buildings using diagrids and located in areas of high seismicity. For more information on this particular topic please refer to the article “Uso de rejillas perimetrales (Diagrid) para estructurar edificios altos de acero ubicados en zonas de alta sismicidad¹” from Terán Gilmore, Amador; Quiroz Ramírez, Arturo and Díaz Martínez, Gerardo (2014) and the thesis entitled “Uso de rejillas rígidas como sistema estructural en edificios altos ubicados en zonas sísmicas²” (Amaya Aguilar 2015).

Based on these facts, an interest for the study of diagrid buildings with a circular plan structure arose. The thesis “Bases para un diseño sísmico basado en rigidez de rejillas rígidas de planta circular para edificios de gran altura ubicados en zonas de alta sismicidad³” written by Josimar Salvador Olivera González (2015) present a simple methodology aimed at making possible the preliminary design of diagrids having circular plan cross section.

3.2 Building parameters

Table 3: Geometric parameters for the diagrid structure

Description	Value
Number of story	24
Height	84 m
Outer diameter	36,50 m
Inner diameter	34,20 m
Story height	3,5 m
Core area (per story)	100 m ²
Floor area (per story)	918 m ²

¹ Use of perimetral grids (Diagrid) to structure tall steel edifices located in areas of high seismicity

² Use of rigid grids as structural system for tall buildings located in seismic zones

³ Basis for a stiffness-based seismic design of rigid grids with a circular plan for high-rise buildings located in high seismicity zones

(Translations supplied without guarantee)

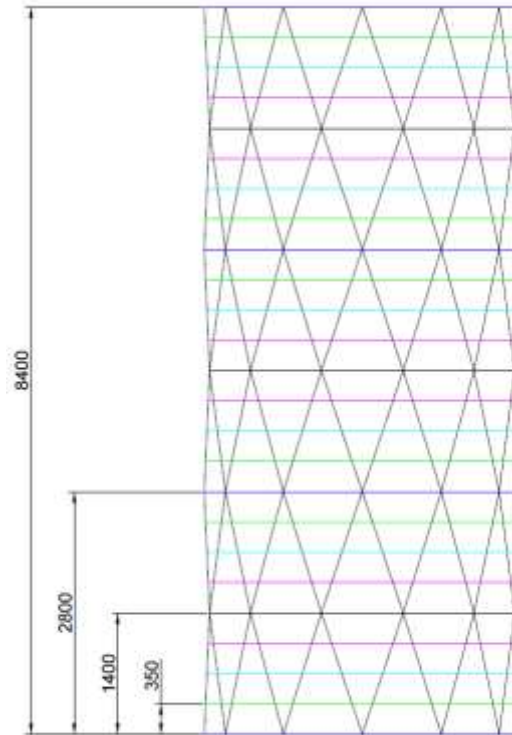


Figure 7: Elevation view - units in [cm] - no scale

Remark: Plans realized with AutoCad 2016 (Autodesk)

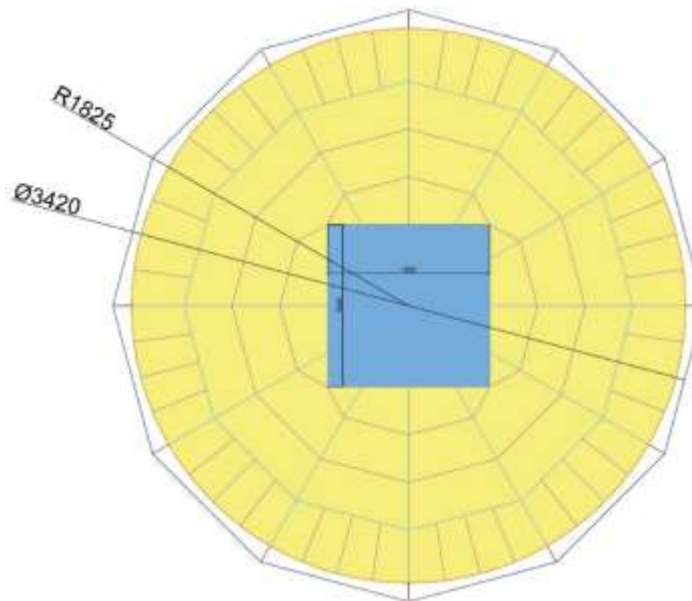


Figure 8: Cross section - floor area (yellow) and core area (blue) - units in [cm] - no scale

3.3 Choice of diagrid parameters

3.3.1. Help for design

Moon et al. (2007) and Mele et al. (2014) showed that the choice for the module angle is a balance between two contradictory necessities. On one hand, a small module angle provides a high shear rigidity. On the other hand, an angle equal to 90° (vertical columns) delivers the maximum bending stiffness. Diagrids must contribute to shear rigidity as well as bending stiffness since vertical columns are not present.

The demand for shear and bending stiffness is not the same for all buildings since it depends on the aspect ratio of the edifice. Stocky buildings are governed by shear whereas slender ones are more influenced by bending behavior. To fit this characteristic, the angle of a module's diagonal should increase as the building slenderness increases (Mele et al. 2014).

In the article: "Diagrid structures for tall buildings: case studies and design considerations" written by Mele et al. (2014), graphs which depict the optimal angle in dependence on the number of stories provide support for the design of a diagrid system.

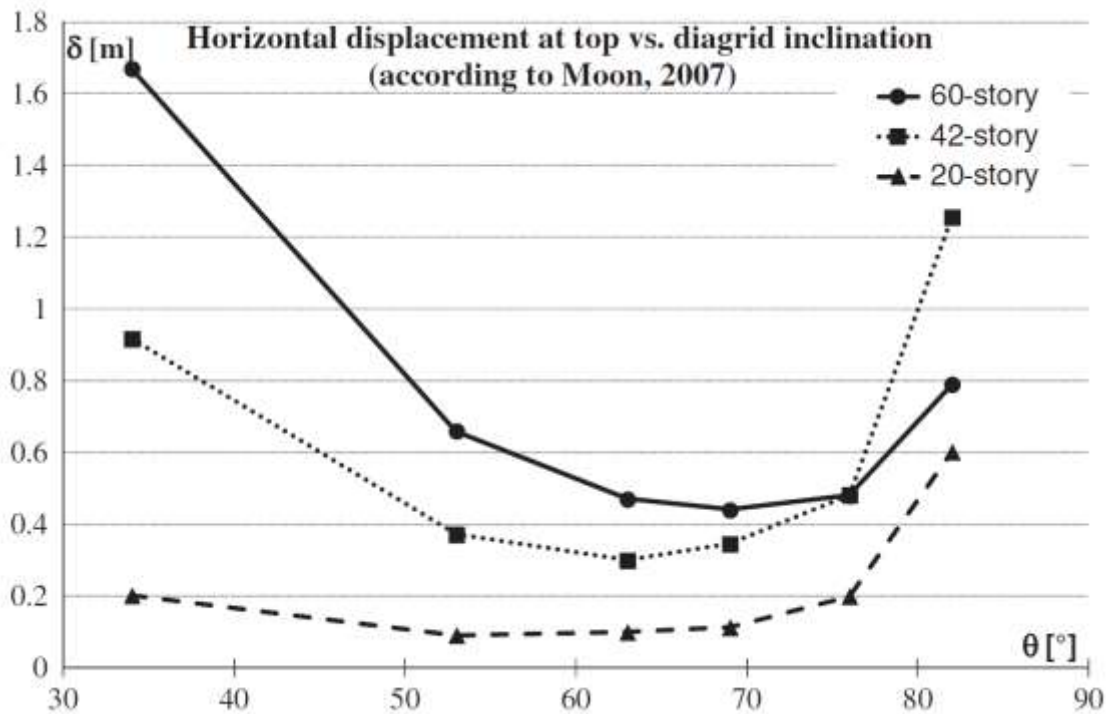


Figure 9: Building top displacement versus diagrid angle (redrawn from Moon et al., 2007) taken from (Mele et al. 2014)

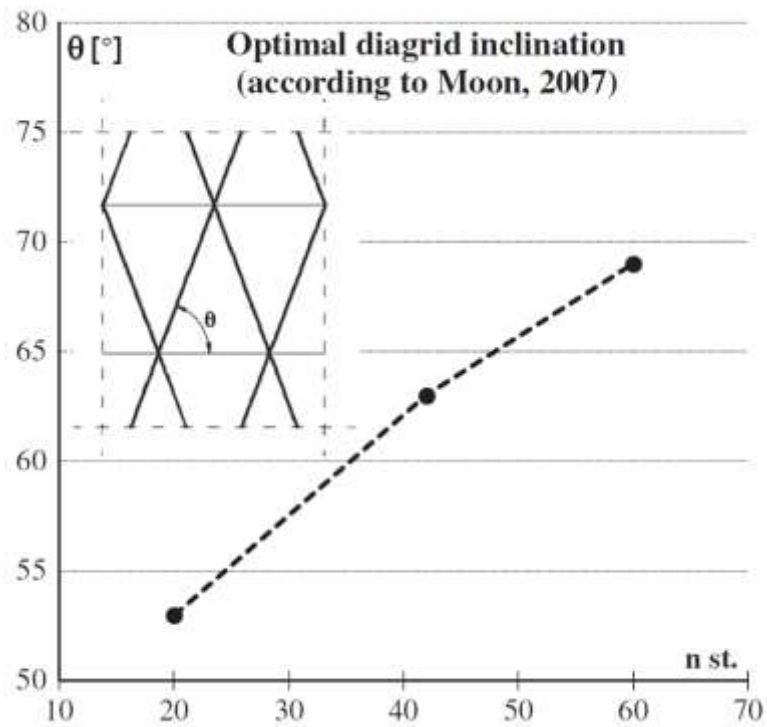


Figure 10: Optimal diagrid inclination for different building heights (Mele et al. 2014)

3.3.2. Choice for our project

Description	Value
Story height	3,5 m
Module height	8 stories (28 m)
Triangle height	4 stories (14 m)
Base angle	71,36°
Angle at the top	37,29°
Length of the base	9,45 m
Total length of a diagonal	29,55 m
Length of the diagonal for an interstory	3,69 m

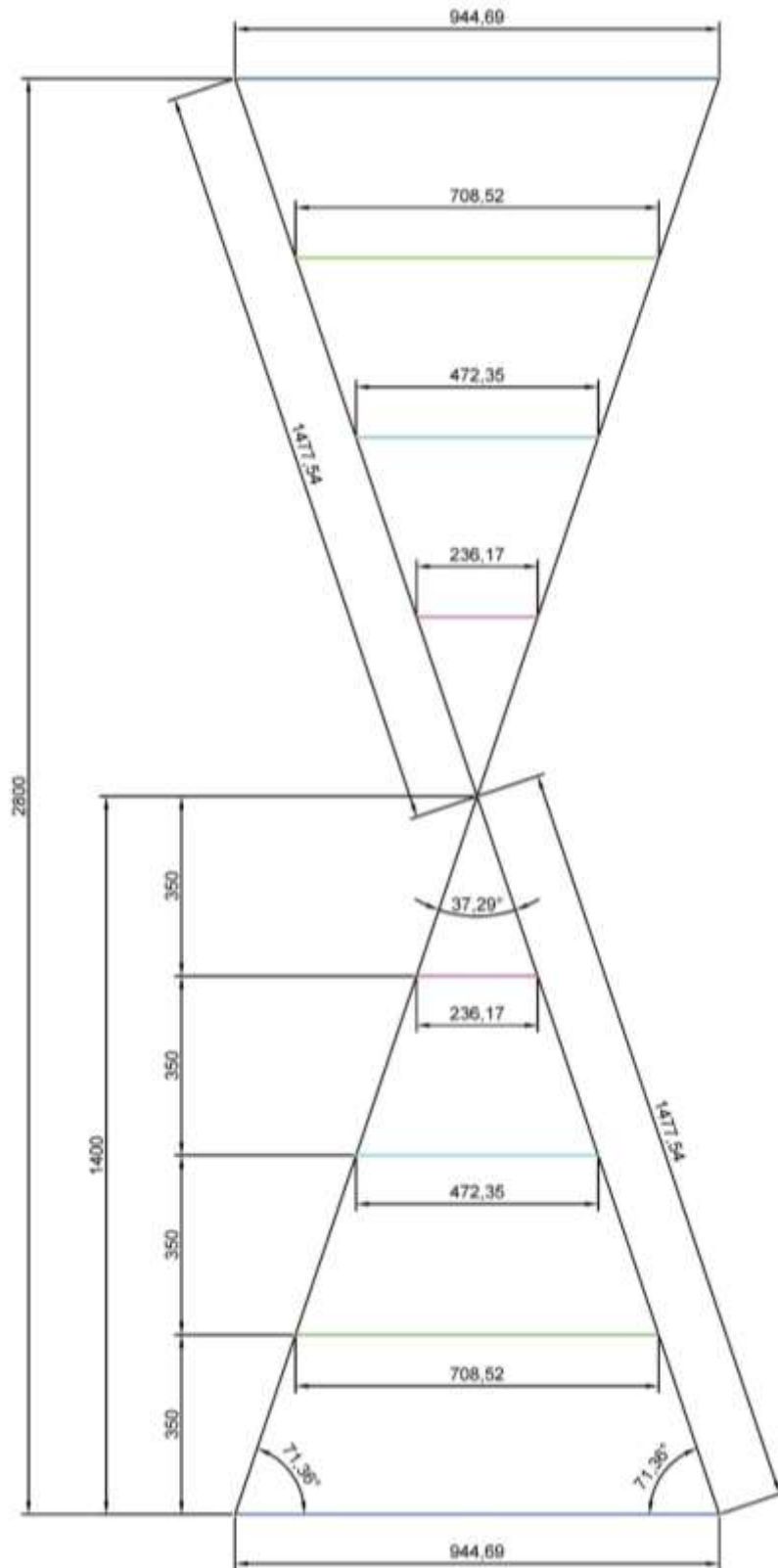


Figure 11: Diagrid module - units in [cm] - no scale

4. GRAVITATIONAL SYSTEM

This chapter deals only with the gravitational system, i.e. the concrete core, the steel members and the slab (not the diagrids). First of all, preliminary sections and dimensions for the steel members and reinforced concrete core elements were established through a hand calculation. After this, the results found were inserted in the software SAP2000 (Computers & Structure) for strength checks. The final design was chosen in order to fulfill the strength checks and also satisfy some requirements to stabilize the response of the gravitational system when subjected to lateral deformation.

Since the diagrids are designed to withstand the lateral loads, the gravitational system doesn't need to accomplish this task. The design of the gravitational system is therefore mainly governed by vertical loads.

4.1 Loads for one floor

Table 4: Load on the gravitational system (for one floor)

	Dead load [t]	Live load [t]	Combination for Mexico (load factor 1.4) [t]
Roof	298	82	532
Story	298	205	704,2

Note: The self-weight of the steel beams and columns and the self-weight of the concrete core is not included in the dead loads given in the upper table

4.2 Slab: steel-deck (Losacero)

All the tables used for the design of the steel-deck are present in the appendix A and are taken from the leaflet "Losacero Sección 4 y Sección 36/15" (IMSA).

Table 5: Design of the steel-deck (Losacero)

	Middle part of the cross-section (between the core and the beams supported by the columns)	Outer part of the cross-section (between the beams supported by the columns and the belt)
Losacero Section	4	4
Caliber	22	24
Concrete thickness [cm]	5	5
Weight [t/m²]	0,212	0,2097

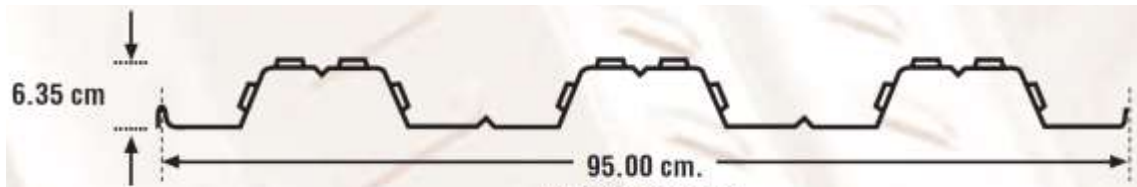


Figure 12: Losacero Section 4 with dimensions in [cm] (IMSA)

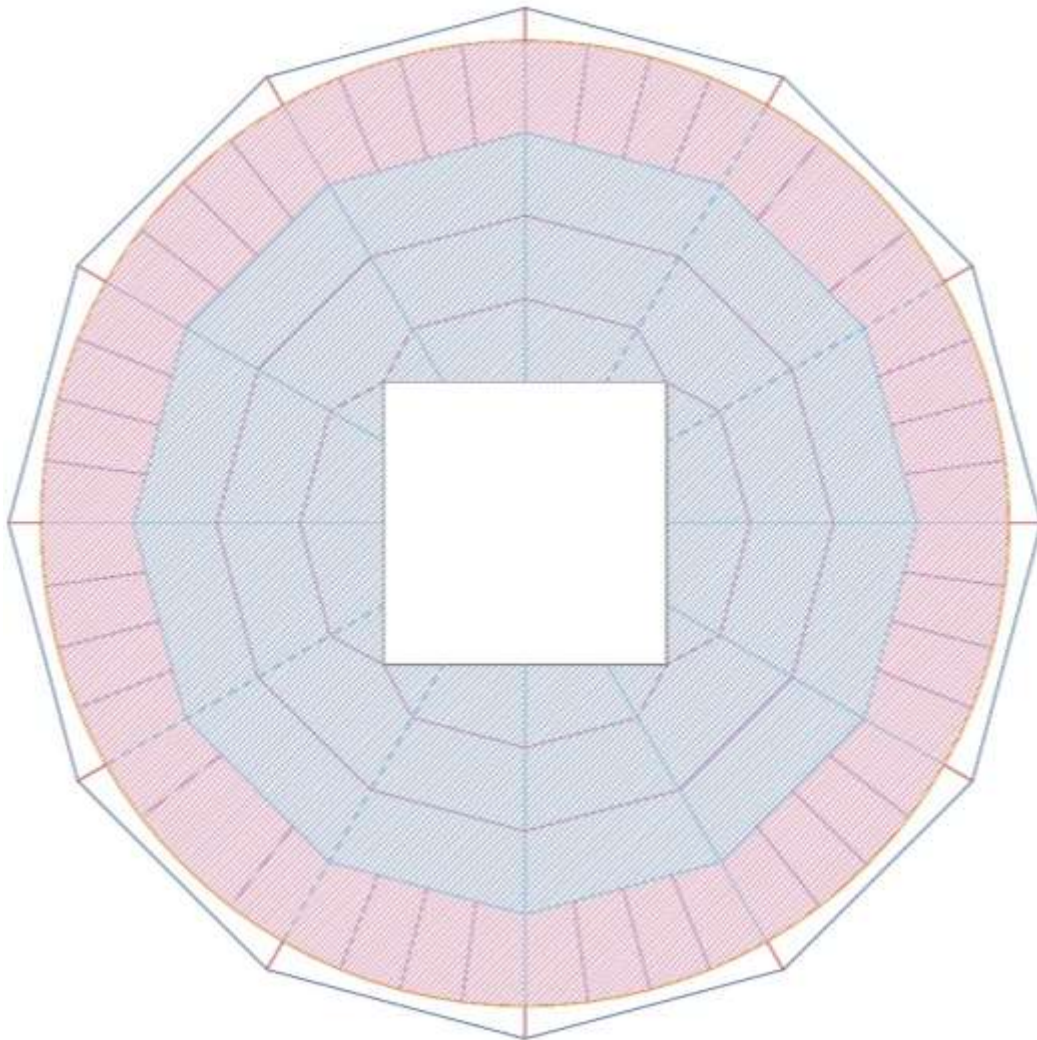


Figure 13: Cross section with the Losacero caliber 24 (red) and caliber 22 (blue) - no scale

4.3 Steel design: beams

4.3.1. Beam sections

Table 6: Beam sections and self-weight

Beam section	Self-weight [lb/ft]	Self-weight [t/m]	Length [m]	Self-weight [t]	Number of beams/floor	Total weight [t]
W18X46	46	0,068356	2,95	0,2017	28	5,646
W18X46	46	0,68356	2,1765	1,4878	8	11,902
W18X46	46	0,68356	3,25	2,2216	12	26,659
W18X46	46	0,68356	7,1693	4,9006	12	58,808
W18X40	40	0,5944	5,6423	3,3538	12	40,245
W18X40	40	0,5944	4,1152	2,4461	8	19,569
W18X40	40	0,5944	2,1456	1,2753	8	10,203
W18X40	40	0,5944	3,7219	2,2123	12	26,548
W18X40	40	0,5944	3,6026	2,1414	24	51,393
W18X35	35	0,5201	1,119	0,5820	96	55,871
W14X43	43	0,63898	1,15	0,7348	12	8,818
					Σ	315,662

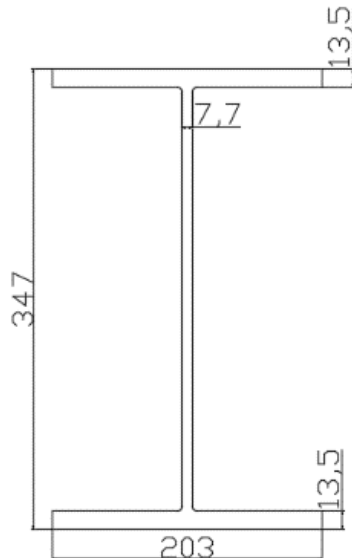


Figure 14: W14x43 [mm]

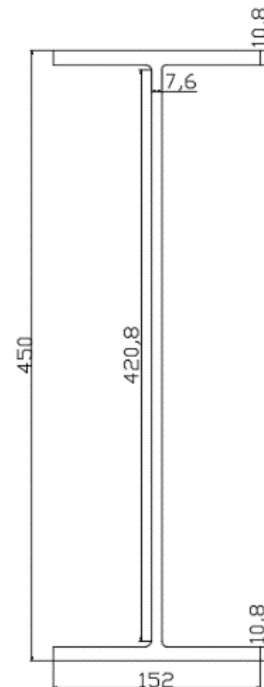


Figure 15: W18x35 [mm]

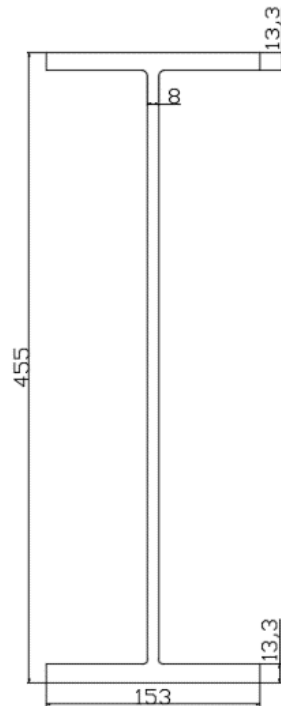


Figure 16: W18*40 [mm]

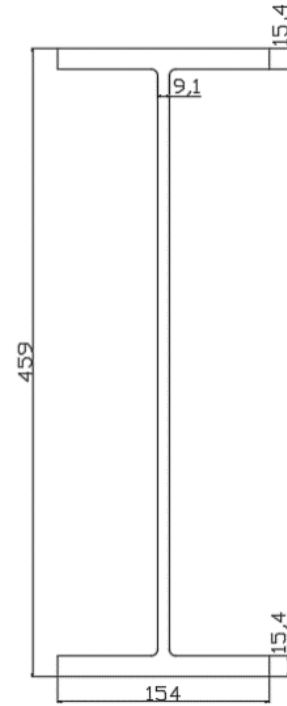


Figure 17: W18*46 [mm]

4.3.2. Properties of structural steel: A992Fy50

Table 7: Structural steel properties

	US-customary units	Mexican customary units	SI-Units
Weight per unit volume	490 lb/ft ³	7,849 tonf/m ³	76,9729 kN/m ³
Modulus of Elasticity, E	29000 ksi	20389019 tonf/m ²	199900 MPa
Poisson's Ratio, U	0,3	0,3	0,3
Shear Modulus, G	11154 ksi	7841930 tonf/m ²	76903 MPa
Minimum Yield Stress, F_y	50 ksi	35153,48 tonf/m ²	345 MPa
Minimum Tensile Stress, F_u	65 ksi	45699,53 tonf/m ²	448 MPa
Effective yield stress, F_{ye}	55 ksi	38668,83 tonf/m ²	379 MPa
Effective Tensile stress, F_{ue}	71,5 ksi	50269,48 tonf/m ²	493 MPa

4.3.3. Design check with SAP2000

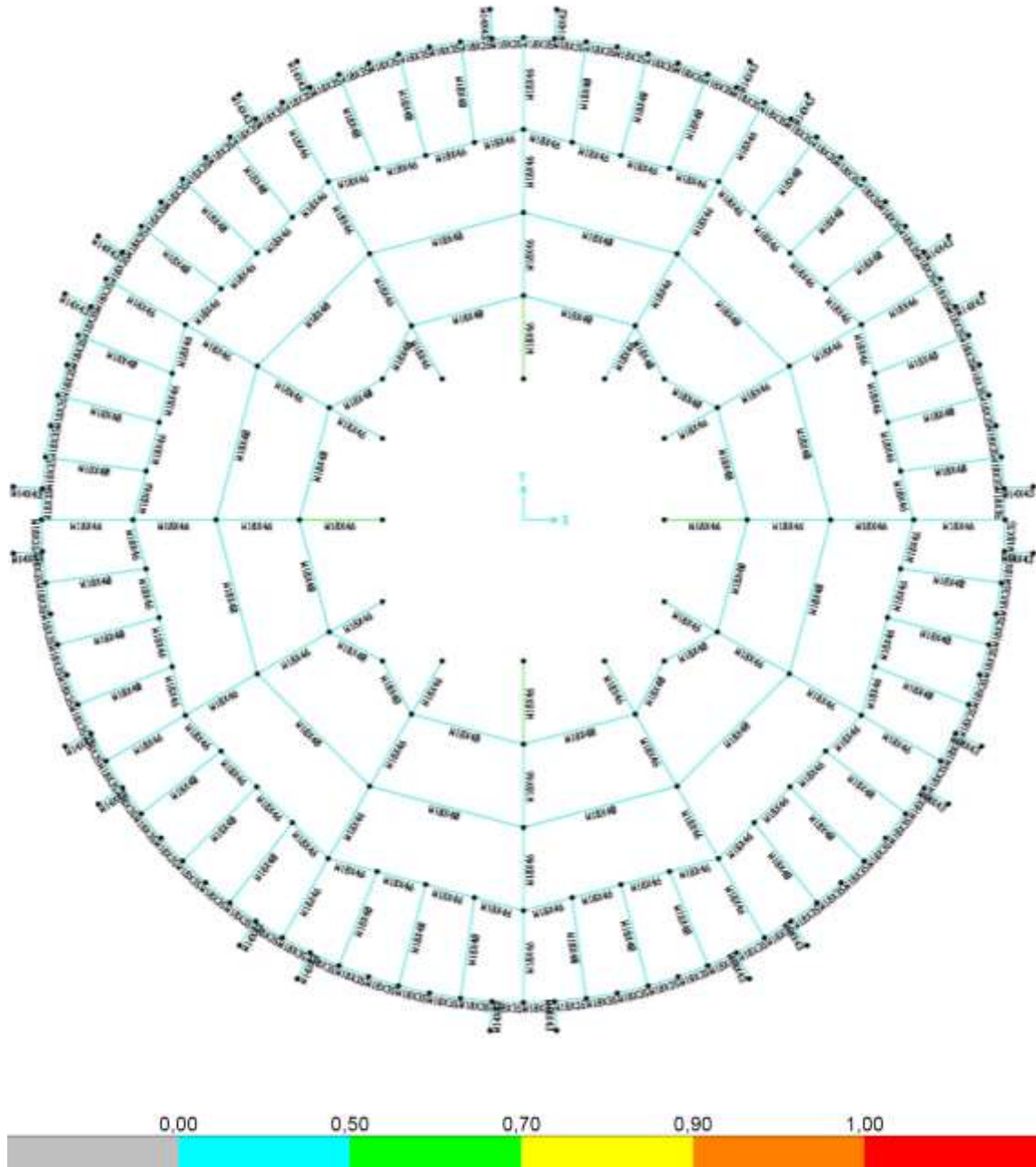


Figure 18: Design check of the steel beams with SAP2000 (Computers & Structure)

4.4 Steel design: columns

4.4.1. Columns sections

Table 8: Column sections and self-weight

Column Section	Self-weight [lb/ft]	Self-weight [t/m]	Height [m]	Self-weight [t]	Number of columns/floor	Total weight [t]
W 14x132	132	0,196152	3,5	0,6865	12	8,238
W 14x211	211	0,313546	3,5	1,0974	12	13,169
W 14x283	283	0,420538	3,5	1,4719	12	17,663

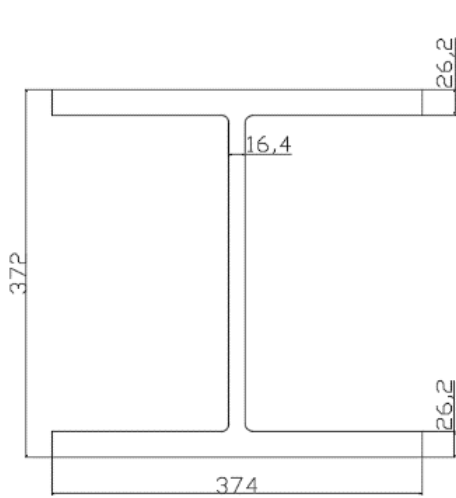


Figure 19: W14*132 [mm]

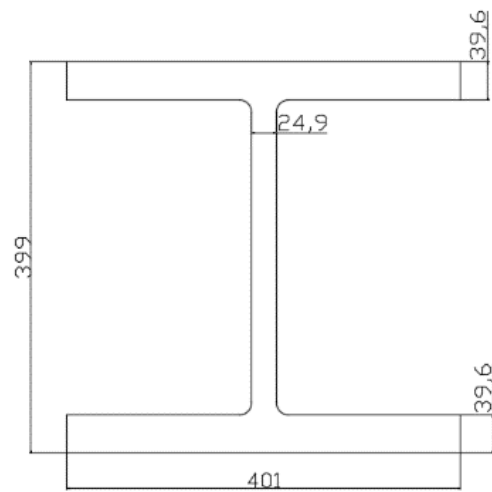


Figure 20: W14*211 [mm]

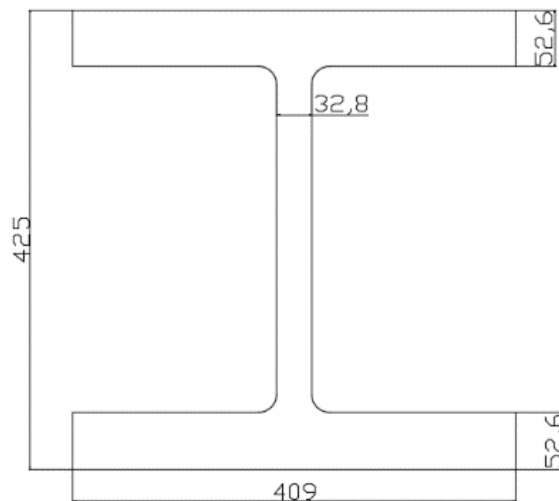


Figure 21: W14*283 [mm]

4.4.2. Design check with SAP2000

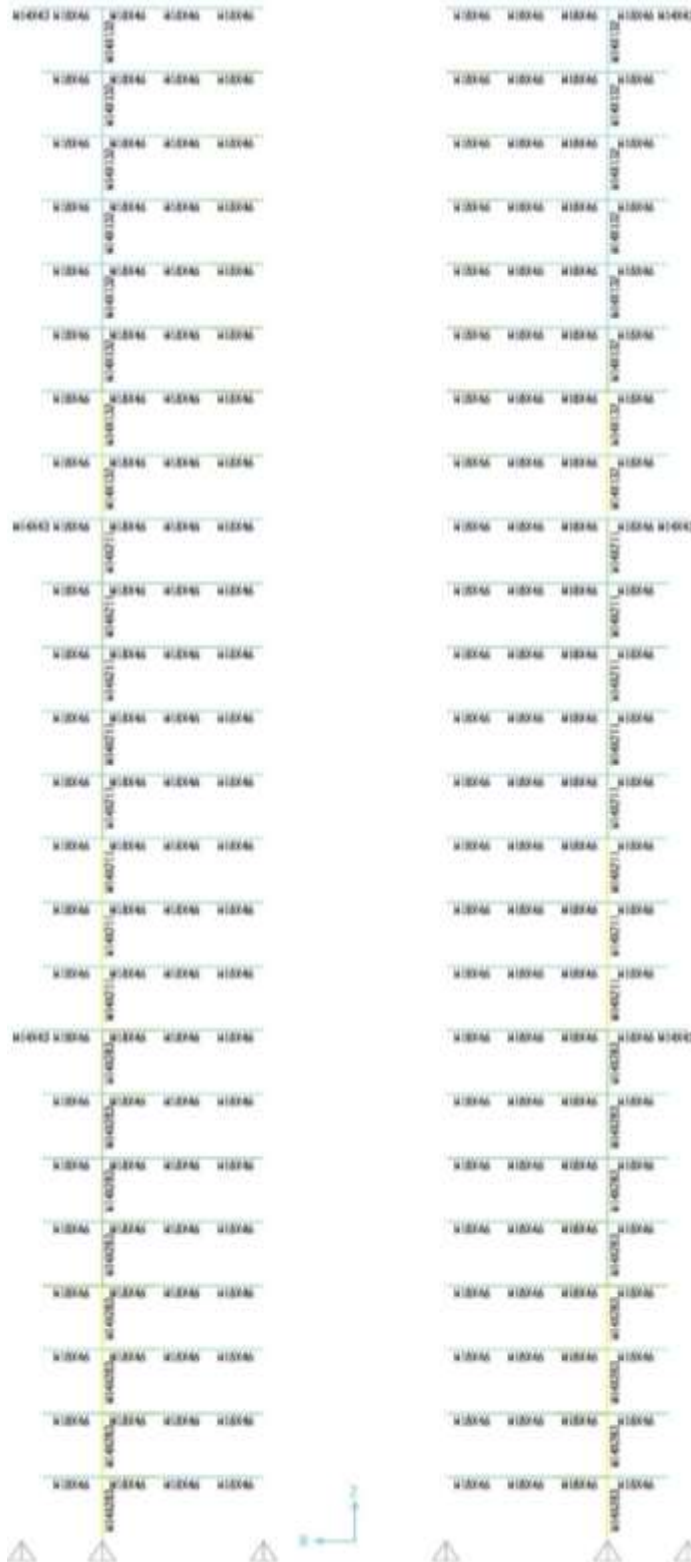


Figure 22: Design check of the steel columns with SAP2000 (Computers & Structure)

4.5 Core design: reinforced concrete

Since the American building code is widely accepted in Mexico (McCormac, Brown 2013, p. 7), the design of the concrete elements is based on the standard ACI 318. Thus the sizing units match with the US-customary units. In order to give a feeling to people who are accustomed to work with other units, the main properties are also given in the customary units used in Mexico and in SI-Units.

4.5.1. Capacity design

A reinforced concrete structure is designed to develop plastic behavior during severe seismic excitations. Plastic demands tend to concentrate in specific locations. It is important to limit the amplitude and number of plastic cycles. Different experimental tests have been devised to promote different behaviors in reinforced concrete structural members. From what has been observed in these tests, it can be said that it is convenient to promote a stable plastic behavior for earthquake-resistant reinforced concrete structures, through a bending-dominated behavior. Shear and axial behavior need of course to be controlled and torsion can be ignored. Nevertheless, this is not enough. It is also required to provide adequate detailing to the structural member and to control its plastic deformation demands (Amador Terán Gilmore).

In a reinforced concrete member, the flexural resisting mechanism depends on a force couple between compression and tension. The bending capacity is lost if one of these forces is lost or significantly degraded. There are two possible manners to reach failure: crushing of the compression strut (concrete) and fracture of steel in tension. One way of protecting the compression strut is to delay crushing of concrete by means of adequate confinement. In an actual reinforced concrete element, the confinement is provided by longitudinal and transverse reinforcement. Another way of protecting the compression strut is to provide negative steel to reduce the compression demands on the concrete. An adequate balance between negative and positive steels stabilizes the bending-resisting mechanism. To protect the steel in tension, it is necessary to avoid its fracture. This is achieved by providing a minimum area of steel. Another aspect to consider for stable bending behavior is the control of shear effects. Among other things, this requires the use of slender members. Finally, a stable bending behavior requires the control of the level of axial force in the reinforced concrete structural member (Amador Terán Gilmore).

The objective of capacity design is to allow for the conception of structures that are capable of developing a stable and consistent plastic mechanism. This approach applies to the seismic design of ductile structures. An important aspect of capacity design is the recognition of the difficulties involved during the prediction of the dynamic response of a structure, particularly when it develops significant plastic behavior (Amador Terán Gilmore).

A capacity design has three main stages:

- 1) Identification and hierarchization of behavior and failure modes
- 2) Selection of an acceptable plastic mechanism
- 3) Design of plastic mechanism

To promote a stable comportment in flexion, the following points should be considered:

- Appropriate use of transverse reinforcement (confinement and delay of local buckling)
- Adequate balance of positive and negative steel
- Control of shear effects through the use of slender members
- Control of axial loads on structural members

According to the Mexican standards, capacity design has the following requirements in terms of the structural materials:

- Concrete
 - Class I
 - $f'_c = 250 \text{ kg/cm}^2$
- Steel
 - Corrugated
 - $f_{ynominal} = 4200 \frac{\text{kg}}{\text{cm}^2}$
 - $f_{yactual} \leq f_{nominal} + 1300 \text{ kg/cm}^2$

4.5.2. Properties of concrete: 6000Psi

For all the elements, the concrete used has a 6000-psi compressive strength.

Table 9: Concrete properties

	US- customary units	Mexican customary units	SI-Units
Weight per unit volume	150 lb/ft ³	2,4028 tonf/m ³	23,5631 kN/m ³
Modulus of Elasticity, E	4415,201 ksi	3104193,7 tonf/m ²	30442 MPa
Poisson's Ratio, U	0,2	0,2	0,2
Shear Modulus, G	1840 ksi	1293414,1 tonf/m ²	12684 MPa
Specified Concrete Compressive Strength, f'_c	6 ksi	4218,418 tonf/m ²	41 MPa

4.5.3. Properties of rebar steel: A615Gr60

The rebar steel is an ASTM A615Gr60. This is the steel, which is nowadays the most widely used for reinforcing bars (McCormac, Brown 2013, p. 24).

The grade GR60 give the minimum yield strength which is 60 ksi (or 60,000 psi).

Table 10: Rebar steel properties

	US- customary units	Mexican customary units	SI-Units
Weight per unit volume	490 lb/ft ³	7,849 tonf/m ³	76,9729 kN/m ³
Modulus of Elasticity, E	29000 ksi	20389019 tonf/m ²	199900 MPa
Minimum Yield Stress, F_y	60 ksi	42184,18 tonf/m ²	414 MPa
Minimum Tensile Stress, F_u	90 ksi	63276,27 tonf/m ²	621 MPa
Effective yield stress, F_{ye}	66 ksi	46402,6 tonf/m ²	455 MPa
Effective Tensile stress, F_{ue}	99 ksi	69603,89 tonf/m ²	683 MPa

4.5.4. Columns

Table 11: Steel reinforcement in the columns

	US customary units	SI-units
Longitudinal reinforcement	12#10 (A _{st} = 15,19 in ²)	12Ø32 (A _{st} = 9650 mm ²)
Ties (stirrups)	#3 every 18 inches	Ø32 every 45,72 cm

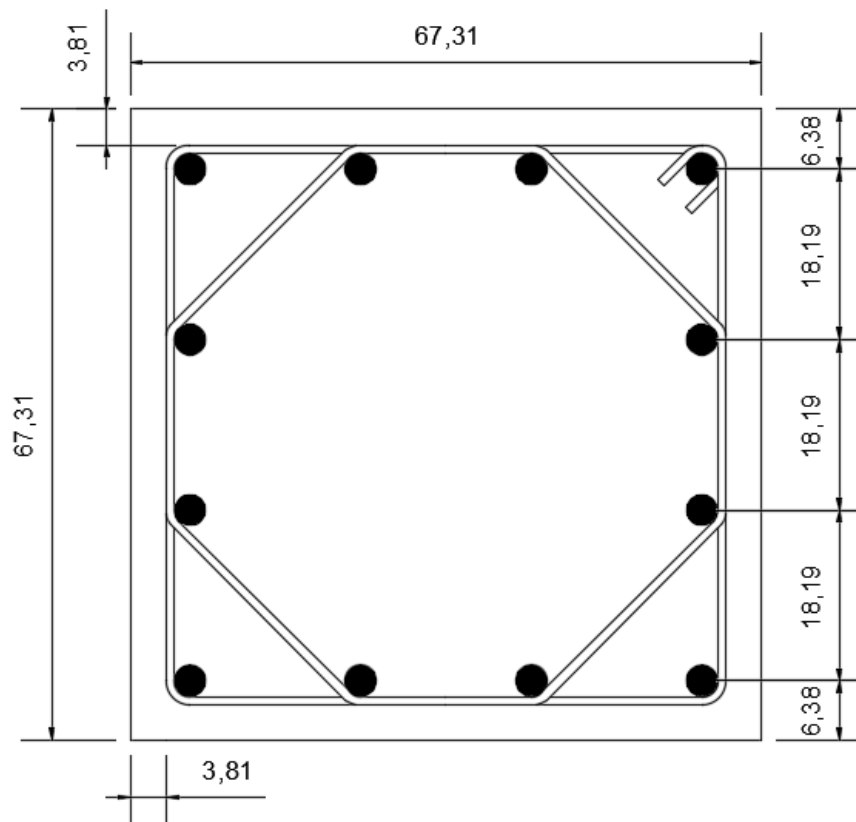


Figure 23: Column reinforcement [cm]

To avoid shear weaknesses the stirrups must provide a shear force resistance equal to:

$$V_{design} = \frac{2M_R}{H}$$

where M_R is the “actual” moment strength of the column and H the height of the column (Amador Terán Gilmore).

4.5.5. Beams

The bending moments on the core beams are very low. The shear and torsion are so small that the minimum amount of mandatory stirrups in order to satisfy the standard is also sufficient to withstand shear and torsion forces.

Table 12: Steel reinforcement in the beams

	US customary units	SI-units
Longitudinal reinforcement (bottom)	3#7 ($A_s=1,80 \text{ in}^2$)	3Ø22 ($A_{st} = 1140 \text{ mm}^2$)
Longitudinal reinforcement (top)	3#7 ($A_s=1,80 \text{ in}^2$)	3Ø22 ($A_{st} = 1140 \text{ mm}^2$)
Ties (stirrups)	#3 every 3,78 inches	Ø32 every 9,6 cm

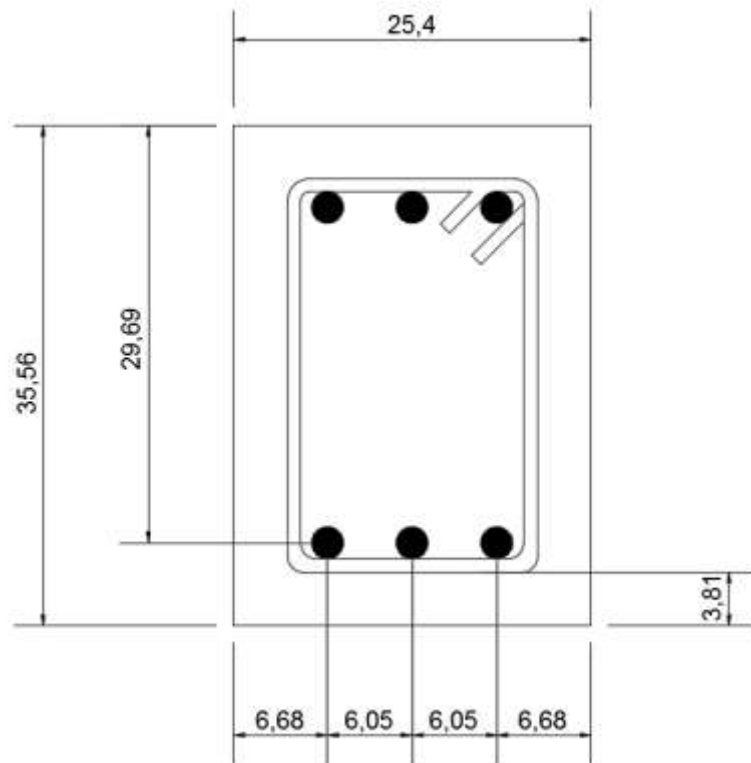


Figure 24: Beam reinforcement [cm]

5. DISPLACEMENT BASED DESIGN

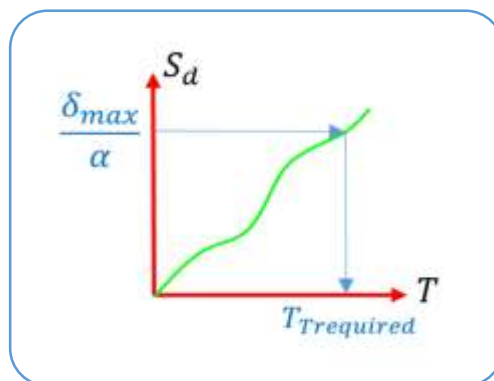
1. Qualitative definition of performance:
Description of acceptable damage thresholds
in the relevant sub-systems



2. Quantitative definition of performance:
 $IDI_{max} = f(\text{damage threshold})$



3. $\delta_{max} = f(IDI_{max})$



5. Stiffness based design of the structural system's
elements

Figure 25: Displacement based methodology (Terán Gilmore et al. 2014)

Some research works have shown that the conception of low-rise buildings is usually controlled by gravity and vertical loads. However, as the height of the building increases, the design begins to be controlled by lateral drift. Strength is not the main feature anymore but stiffness (Ali, Moon 2007). The dynamic response of high-rise buildings is mainly governed by a global flexural drift modes (Terán Gilmore, Coeto 2011).

A displacement-based methodology has five main steps as shown in figure 25 (based on Terán Gilmore et al. 2014).

1. **Establishment of a qualitative definition for an adequate performance.** This is achieved through the specific consideration of acceptable levels of damage for the different sub-systems - structural and nonstructural - which compose the building.

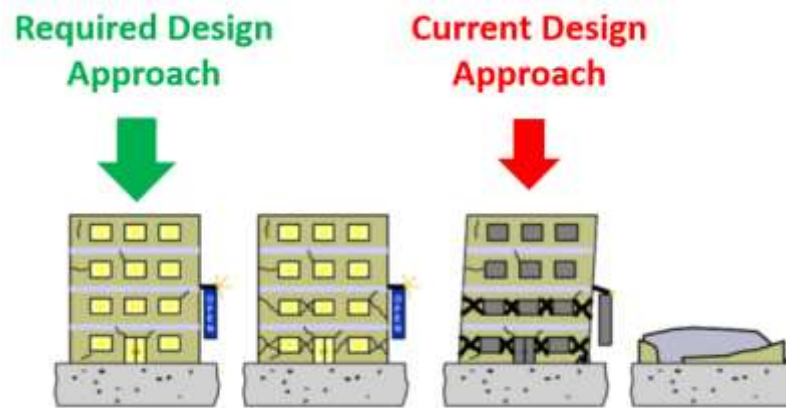


Figure 26: Different levels of damage in a building after an earthquake

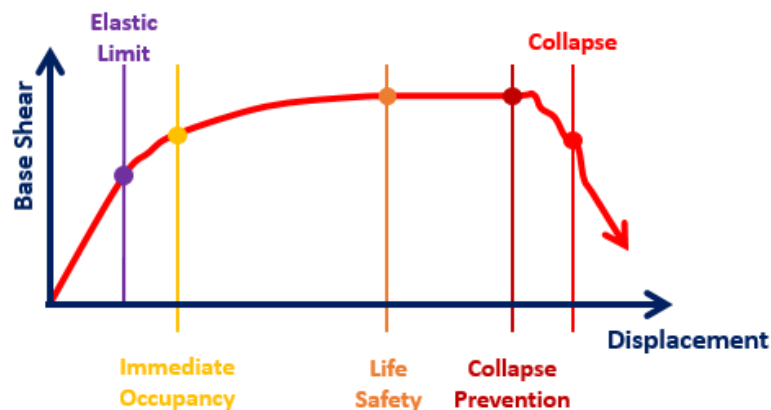


Figure 27: Performance levels

The performance levels are depicted in the graph “base shear vs displacement” on figure 27.

A building or a building part can be designed to remain operational after a ground motion. Therefore the elements should be undamaged and remain in the elastic range without the development of plastic hinges. The maximal threshold to achieve this is defined by the elastic limit.

If a very little damage, in terms of nonlinear behavior, is allowed the performance level to reach is immediate occupancy. Some elements will be damaged but taken in a point of view of the entire building it remains pretty undamaged. Repair and replacement of the damaged portions is easy and affordable.

Further away from the elastic limit and showing greater plastic deformations is the level called life safety. Several parts of the edifice are damaged and show nonlinear behavior but the security for the building occupant is not at risk.

The last performance level is called collapse prevention. At this level the building is severely damaged and the security for the occupant becomes critical. After an earthquake with severe intensity, the edifice is not able to fulfill its function anymore and reparations in a reasonable amount of money are barely possible.

For a standard occupancy structure the design objectives can be formulate in relation with the earthquake intensity:

- Withstand without damage seismic motions of low intensity;
- Withstand without structural damage, although possibly with some type of nonstructural damage, seismic motions of moderate intensity;
- Withstand without collapse, although with some type of structural and nonstructural damage, severe seismic motions.

2. **Performance quantification by establishing response thresholds that are consistent with the acceptable damage level considered for the different sub-systems.** Usually the thresholds are formulated in terms of maximum allowable interstory drift index (*IDI*) for the building. They also should consider the performance of the structural and nonstructural sub-systems.

For one given story, the *IDI* can be defined as the ratio of the story displacement in the horizontal direction Δh over the story height h :

$$IDI = \frac{\Delta h}{h}$$

The lateral roof displacement doesn't permit an adequate definition of damage in a building since a large displacement for a skyscraper is not comparable with a large roof displacement for a small edifice. The *IDI* however, a value without unit, takes into account the lateral story displacement reported to height of a story or the lateral roof displacement in conjunction with the entire building height. The damage can be therefore quantified for any given structure.

3. **Computation of $\delta_{roof,max}$, the maximum demand for the roof displacement.** The maximum allowable interstory drift index (IDI_{max}) threshold found in the step number 2 is used to find $\delta_{roof,max}$. A new coefficient called coefficient of distortion (COD) need to be computed. It considers that interstory drift is not constant along the height of the building. Typical values for the *COD* coefficient are given in table 13. With the definition of the *IDI* and *COD*, the maximal roof displacement for the building can be calculated with the following formula:

$$\delta_{roof,max} = \frac{IDI_{max}}{COD}$$

4. **Definition of $T_{Trequired}$ for the fundamental period of vibration of the building.** With the help of a design displacement spectrum, a target value $T_{Trequired}$ for the fundamental period of vibration of the building is established ($T_{Trequired}$, quantifies the global lateral stiffness requirements). A distortion controlled based design is a difficult task because it sets a standard of review for the entire structural system, which requires the simultaneous consideration of all structural elements of the building.

To be able to use a displacement based design spectra, the maximal roof displacement $\delta_{roof,max}$ found for the building - a multiple degree of freedom system - need to be expressed for a single degree of freedom system. The factor α considers this transformation. Table 14 gives values for α_S (shear) and α_B (flexure) dependent on the number of story and the ductility of the building.

By dividing the roof displacement of the building by the factor α , the roof displacement S_d expressed for a single degree of freedom is obtained:

$$S_d = \frac{\delta_{roof,max}}{\alpha}$$

With the result of S_d and a design displacement spectrum (a graph of S_d vs the period T), it is possible to define a target value $T_{Trequired}$ for the fundamental period of vibration of the building.

5. **Stiffness based design of the structural system's elements.** The dimensions of the structural elements of the earthquake resistant subsystem are designed in such a way that the actual fundamental period of vibration of the structural system is as close as possible to the target value $T_{Trequired}$. The dimensions of these elements define the available capacity of the system in terms of structural local rigidity.

6. DIAGRIDS

6.1 Methodology for the preliminary design of diagrids

The preliminary design of diagrids is based on the article “Uso de rejillas perimetrales (Diagrid) para estructurar edificios altos de acero ubicados en zonas de alta sismicidad⁴” (Terán Gilmore et al. 2014) in combination with the thesis “Bases para un diseño sísmico basado en rigidez de rejillas rígidas de planta circular para edificios de gran altura ubicados en zonas de alta sismicidad⁵” written by Josimar Salvador Olivera González (2015). In conjunction, they present a simple methodology to find a preliminary area for the diagonals of diagrid building.

6.1.1. Fundamental period of vibration

Under the assumption that the global shear and bending deformations can be considered as separate components (as would in the case of a cantilever beam), the fundamental period of vibration of a structural system must satisfy the following condition (Terán Gilmore, Coeto 2011):

$$T_T^2 = T_S^2 + T_B^2$$

T_T is the fundamental period of vibration of the entire building

T_S is the fundamental period of vibration associated with the global behavior in shear

T_B is the fundamental period of vibration associated with the global behavior in bending

6.1.2. Factor k (FEMA 356)

According to the suggestions made by FEMA 356 (Federal Emergency Management Agency 2000), k can be estimated as:

$$k = \begin{cases} 1 & \text{if } T \leq 0,5 \text{ s} \\ \frac{(T + 1.5)}{2} & \text{if } 0,5 \text{ s} < T < 2,5 \text{ s} \\ 2 & \text{if } T \geq 2,5 \text{ s} \end{cases}$$

⁴ Use of perimetral grids (Diagrid) to structure tall steel edifices located in areas of high seismicity

⁵ Basis for a stiffness-based seismic design of rigid grids with a circular plan for high-rise buildings located in high seismicity zones

(Translations supplied without guarantee)

6.1.3. Lateral force F_i

The lateral force F_i depends on the base shear V_b , and the weight and height of the stories, and is defined as follow:

$$F_i = V_b \frac{w_i H_i^k}{\sum_{j=1}^n w_j H_j^k}$$

V_b is the base shear

w_i is the weight of the studied story

H_i is the height from the studied story to the ground level

n is the number of floors

6.1.4. Initial value for the area of the diagonals

A variation through height is established for the areas of the diagonals that compose the diaphragms. An initial value A^0 for the diagonals is assigned. The only condition that must be satisfied by the diagonal areas is to follow the variation in height chosen for them.

6.1.5. Lateral stiffness in shear and lateral displacement

Once the preliminary sizing of the diagonals has been done, the laterals deformations of the diaphragms due to their global behavior in shear are estimated. Under consideration of the presence of rigid diaphragms which limit the axial deformation of the horizontal elements of the structural system, the lateral stiffness in shear provided by the diagonals can be estimated as:

$$K_{Si} = \sum_{j=1}^{N_i} \frac{EA_j^0}{L_j} \cos^2 \theta_j \cos^2 \phi_j$$

N_i is the total number of diagonals located in the i-th interstory

A_j^0 is the area initially proposed for the j-th diagonal located at the interstory

θ_j is the base angle of the j-th diagonal with respect to a horizontal axis

ϕ_j is the angle in plan formed by the j-th diagonal with respect to the direction of analysis

L_j is the total interstory length of a diagonal

The relative lateral displacement $\Delta\delta_{Si}$ in the i -th interstory can be estimated as:

$$\Delta\delta_{Si} = \frac{V_i}{K_{Si}}$$

V_i is the shear at an interstory under a supposition of a distribution over the height of the lateral forces.

The lateral displacement δ_{Si} in the i -th level is the addition of the relative lateral displacements $\Delta\delta_{Si}$ of the stories under it plus its own relative displacement:

$$\delta_{Si} = \sum_{j=1}^i \Delta\delta_{Sj}$$

6.1.6. Lateral bending stiffness

To estimate the lateral deformation due to the overall flexural behavior it is reasonable to assume that the diagrid behaves as a cantilever beam. Within this context, the lateral bending stiffness I_{Bi} in the i -th interstory can be estimated by considering the cross-sectional areas of the diagonals and the distance that separate them to the centroid of the interstory floor. Since the diagonals are not vertical, the lateral bending stiffness I_{Bi} can be computed with the following formula:

$$I_{Bi} = \sum_{j=1}^{N_i} A_j \sin^2 \theta_j d_j^2$$

N_i is the total number of diagonals located in the i -th interstory

A_j is the area of the j -th diagonal

θ_j is the base angle of the j -th diagonal with respect to a horizontal axis

d_j is the distance that separates the diagonal from the centroid of the i -th floor interstory

6.1.7. Curvatures and rotations

The curvatures at the upper and lower ends of the diagrids located in the i -th interstory can be estimated as:

$$\varphi_i^{above} = \frac{M_{i+1}}{EI_{Bi}}$$

$$\varphi_i^{down} = \frac{M_i}{EI_{Bi}}$$

M_i is the overturning moment at the interstory i

M_{i+1} is the overturning moment at the interstory $i+1$

Note that they are estimated according to the distribution along height of lateral forces used to determine the value of V_i .

The rotations at the upper θ_i^{above} and lower θ_i^{down} ends of the diaphragms located in the i -th interstory can be estimated as:

$$\theta_i^{above} = \left(\frac{2\varphi_i^{above} + \varphi_i^{down}}{6} \right) h_i$$

$$\theta_i^{down} = \left(\frac{\varphi_i^{above} + 2\varphi_i^{down}}{6} \right) h_i$$

h_i is the height of the i -th interstory

The total increase of rotation in the slab located in the i -th level due to global flexural behavior $\Delta\theta_i^{tot}$ can be estimated as the sum of the contributions of the upper and lower portions:

$$\Delta\theta_i^{tot} = \theta_i^{above} + \theta_i^{down}$$

The total rotation of the slab located in the i -th level θ_i^{tot} can be found by adding the contributions of all interstories located below it:

$$\theta_i^{tot} = \sum_{j=1}^i \Delta\theta_j^{tot}$$

Finally, the relative displacement of the i -th interstory due to global flexural behavior $\Delta\delta_{Bi}$ can be estimated as:

$$\Delta\delta_{Bi} = \theta_i^{tot} h_i$$

And the lateral displacement in the i -th level:

$$\delta_{Bi} = \sum_{j=1}^i \Delta\delta_{Bj}$$

6.1.8. Period

Once the lateral deformations due to global behavior in shear and bending are established, an initial estimate of the values of T_S and T_B is made:

$$T_S^0 = 2\pi \sqrt{\frac{\sum_{i=1}^n w_i \delta_{Si}^2}{g \sum_{i=1}^n F_i \delta_{Si}}} \quad T_B^0 = 2\pi \sqrt{\frac{\sum_{i=1}^n w_i \delta_{Bi}^2}{g \sum_{i=1}^n F_i \delta_{Bi}}}$$

g is the acceleration of gravity

w_i is the weight in the i -th interstory

F_i is the lateral force in the i -th interstory

If δ_{Si} and δ_{Bi} are estimated from the assumed distribution of alleged lateral force within the context of a stiffness design, an arbitrary value for the base shear can be chosen.

Once initial values have been estimated for T_S^0 and T_B^0 , an initial value for the fundamental period of vibration T_T^0 can be computed:

$$(T_T^0)^2 = (T_S^0)^2 + (T_B^0)^2$$

6.1.9. Final values of the area

The final value of the areas of the diagonals is estimated as:

$$A = A^0 \left(\frac{T_T^0}{T_{T \text{ required}}} \right)^2$$

6.2 Design of the diagrids for the circular building

6.2.1. Definition of performance

In order to keep the gravitational system undamaged and allow for efficient damage control in the diagrids, the following levels of performance were chosen:

Gravitational system: operational (no development of non-linear behavior)

Diagrids: life safety

To achieve these objectives, the maximal interstory drift index (IDI_{max}) associated to life safety was set to 0,01:

$$IDI_S^{LS} = 0,01$$

6.2.2. Coefficient of distortion

To compute the coefficient of distortion (COD) the ductility of the building is needed. At the beginning the building's ductility is not known so an assumption has to be made. It was assumed that the building possess a ductility of $\mu = 2$. This supposition need to be verified at the end.

The coefficient of distortion considers that interstory drift is not constant along the height of the building.

Table 13: Values of coefficient of distortion (Terán Gilmore, Coeto 2011, p. 159)

Global ductility μ	Stiffness distribution through height		
	Regular	Irregular	Highly irregular
1	1,2	1,5	> 1,5
2 +	1,5	$\geq 2,0$	> 2,0

A regular building is designed in such a manner that the stiffness distribution along height is regular. This means that the structural elements are sized, for example linearly along height, in order to achieve a regular stiffness distribution along height.

With the definition of the IDI and COD , the maximal roof displacement for the building can be computed as:

$$\delta_S^{LS} = \frac{IDI_S^{LS}(H)}{COD^{LS}} = \frac{0,01(84m)}{1,5} = 0,56 \text{ m} = 56 \text{ cm}$$

6.2.3. Factor α

To be able to use a displacement based design spectra, the roof displacement found for the building - a multiple degree of freedom system - need to be expressed for a single degree of freedom system. The factor α considers this transformation. Table 14 gives values for α_S (shear) and α_B (flexure) dependent on the number of story and the ductility of the building.

The particularity in a diagrid construction is that the diagonals acts for both the shear and flexural behavior of the building. This has to be taken in account for the choice of the factor α since only one factor $\alpha_{Diagrids}$ will be defined as a combination of α_S and α_B . At this point of the design, the issue is that the ratio between the shear and flexure the diagonals will withstand at the end is not known. Therefore an assumption has to be made. This value need to be confirmed once the design of the diagrids is done.

Table 14: Suggested values of α for regular buildings (Terán Gilmore, Coeto 2011, p. 161)

Number of story	Shear (α_S)		Flexural (α_B)
	$\mu = 1$	$\mu = 2 +$	$\mu = 1$
1	1,00	1,00	1,00
2	1,20	1,10	1,20
3	1,30	1,20	1,30
4	1,35	1,20	1,35
5	1,40	1,20	1,40
10	1,40	1,20	1,50
15	1,40	1,20	1,55
20 +	1,40	1,20	1,60

The building studied has 24 stories and a ductility of $\mu = 2$ is assumed. Table 14 gives a value of $\alpha_S = 1,20$ for shear and $\alpha_B = 1,60$ for flexure.

Under an assumption that the diagrids acts 50% in shear and 50% in flexure, the mean value is taken: $\alpha_{Diagrids} = 1,4$

By dividing the roof displacement of the building by the factor $\alpha_{Diagrids}$, the roof displacement S_d expressed for a single degree of freedom is obtained:

$$S_d = \frac{\delta_S^{LS}}{\alpha_{Diagrids}} = \frac{0,56 \text{ m}}{1,4} = 0,40 \text{ m} = 40 \text{ cm}$$

For a single degree of freedom system the corresponding roof displacement is 40 cm.

6.2.4. Period T_T required

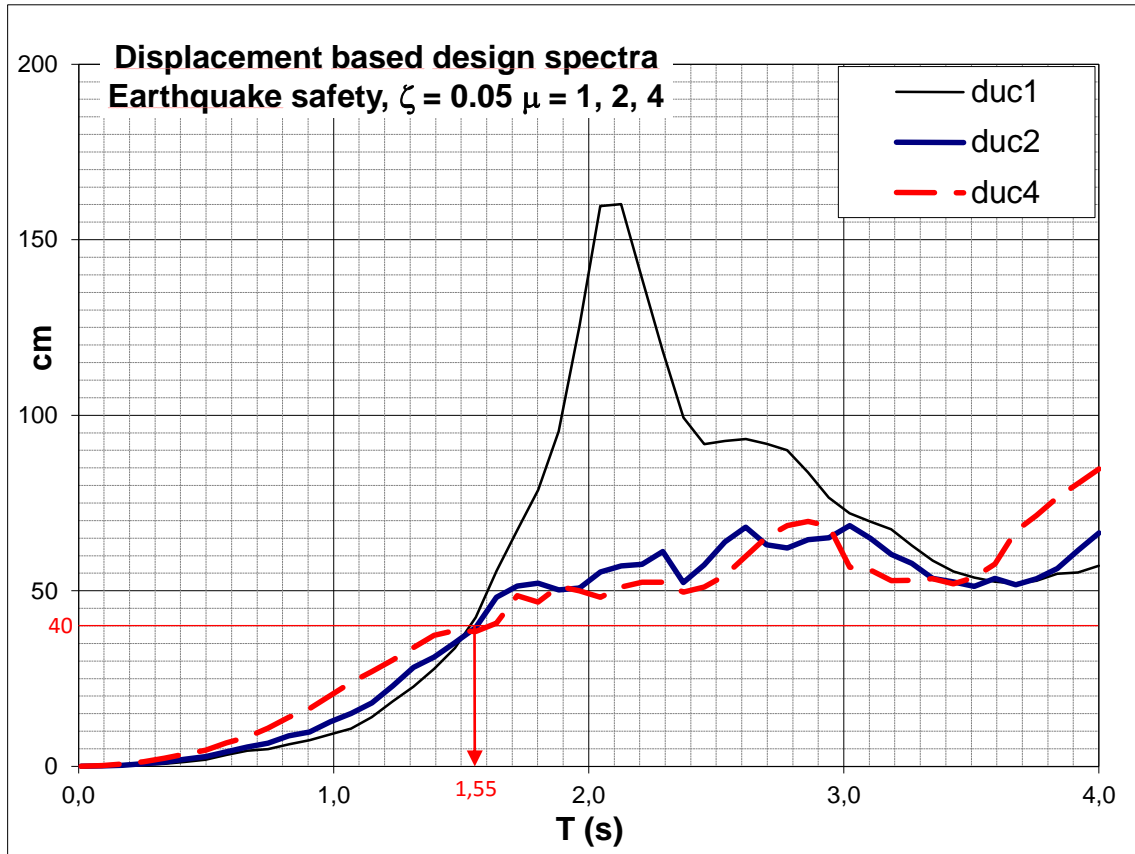


Figure 28: Displacement based design spectra for $\mu=1$, $\mu=2$ and $\mu=4$

The design spectra shown in figure 28 is one for the lake zone of Mexico City. The spectra was determined by establishing the mean + one standard deviation spectra corresponding to ten ground motions generated according to the article “A Two-Stage Method for Ground-Motion Simulation Using Stochastic Summation of Small Earthquakes” from Kohrs-Sansorny (2005). The dominant (corner) period is at about 2 seconds. The three curves correspond to ductilities of $\mu = 1$, $\mu = 2$ and $\mu = 4$, and a percentage of critical damping of 5% ($\zeta=0.05$).

With a roof displacement of 40 cm and a ductility of $\mu = 2$ the period obtained is $T_{T\text{required}}= 1,55\text{s}$

6.2.5. Factor k

According to the suggestions made by FEMA 356 (Federal Emergency Management Agency 2000), k can be estimated as:

$$k = \begin{cases} 1 & \text{if } T \leq 0,5 \text{ s} \\ \frac{(T + 1,5)}{2} & \text{if } 0,5 \text{ s} < T < 2,5 \text{ s} \\ 2 & \text{if } T \geq 2,5 \text{ s} \end{cases}$$

Here $T_{T \text{ required}} = 1,55 \text{ s}$ so

$$k = \frac{T_{T \text{ required}} + 1,5}{2} = \frac{1,55 + 1,5}{2} = 1,525$$

6.2.6. Factor for the percentage of mass moved by the first eigenmode

The number of eigenmode will influence the percentage of mass taken by each one. The percentage of mass moved by the first mode depends on the number of stories of the building. For a building with one story there is only one eigenmode. Thus the factor is 1 for shear and bending since all the building mass has to be taken by the first mode. The more the number of stories increases, the more the factors will decrease since the percentage of mass taken by the first mode will reduce.

Table 15: Percentage of mass moved by the first mode (normalized by 100)

Stories	m_s/m	m_b/m
1	1	1
2	0,9	0,78
3	0,85	0,71
4	0,84	0,68
5	0,83	0,66
10	0,79	0,63
15+	0,75	0,6

6.2.7. Lateral forces and moments

Lateral force:

$$F_i = V_b \frac{w_i H_i^k}{\sum_{j=1}^n w_j H_j^k} m_s/m$$

Moment:

$$\Delta M_i = V_i * h_i * \frac{m_b/m}{m_s/m}$$

V_i is the shear at an interstory under a supposition of a distribution over the height of the lateral forces. It is the sum of F_i from the top of the building to the studied story.

h_i is the interstory height

m_s/m and m_b/m are the % of mass moved by the first mode for shear and bending respectively

$$M_i = \sum \Delta M_i \text{ (from the top of the building)}$$

Table 16: Computation of the lateral forces and moments (before iteration)

Story	Story height h_i [m]	Structure's weight w_i [ton]	Total height H_i [m]	Lateral force per story F_i [ton]	Total lateral force $V_i = \sum F_i$ [ton]	ΔM_i [ton.m]	M_i [ton.m]
24	3,50	455,982267	84,00	105,39	105,39	295,08	295,08
23	3,50	587,056212	80,50	98,76	204,15	571,62	866,71
22	3,50	587,056212	77,00	92,29	296,44	830,04	1696,74
21	3,50	587,056212	73,50	85,97	382,41	1070,76	2767,50
20	3,50	587,056212	70,00	79,81	462,22	1294,21	4061,71
19	3,50	587,056212	66,50	73,80	536,02	1500,86	5562,57
18	3,50	587,056212	63,00	67,96	603,98	1691,14	7253,71
17	3,50	587,056212	59,50	62,29	666,27	1865,55	9119,26
16	3,50	587,056212	56,00	56,79	723,05	2024,55	11143,81
15	3,50	592,082254	52,50	51,46	774,52	2168,65	13312,47
14	3,50	592,082254	49,00	46,32	820,84	2298,36	15610,82
13	3,50	592,082254	45,50	41,37	862,22	2414,21	18025,03
12	3,50	592,082254	42,00	36,62	898,84	2516,74	20541,77
11	3,50	592,082254	38,50	32,07	930,91	2606,54	23148,31
10	3,50	592,082254	35,00	27,73	958,64	2684,18	25832,49
9	3,50	592,082254	31,50	23,61	982,25	2750,30	28582,80
8	3,50	592,082254	28,00	19,73	1001,98	2805,56	31388,35
7	3,50	596,662952	24,50	16,10	1018,08	2850,63	34238,98
6	3,50	596,662952	21,00	12,72	1030,81	2886,26	37125,24
5	3,50	596,662952	17,50	9,64	1040,44	2913,24	40038,47
4	3,50	596,662952	14,00	6,86	1047,30	2932,43	42970,90
3	3,50	596,662952	10,50	4,42	1051,72	2944,81	45915,72
2	3,50	596,662952	7,00	2,38	1054,10	2951,49	48867,20
1	3,50	596,662952	3,50	0,83	1054,93	2953,80	51821,01

6.2.8. Initial value of the diagrids area A^0

According to a linear variation through the height, an initial value for the diagonals area A^0 was first assumed. Due to practical reasons the area of the diagrids was changed every four stories and not at each story as a theoretical linear variation would suggest.

Table 17: Initial values for the diagrids areas (before iteration)

Story	Triangle number	Diatrids pattern	Diatrids area	
			Theory [m ²]	Practical [m ²]
24	6	0	0,0417	0,1667
23	6	1	0,0833	0,1667
22	6	2	0,1250	0,1667
21	6	3	0,1667	0,1667
20	5	4	0,2083	0,3333
19	5	3	0,2500	0,3333
18	5	2	0,2917	0,3333
17	5	1	0,3333	0,3333
16	4	0	0,3750	0,5000
15	4	1	0,4167	0,5000
14	4	2	0,4583	0,5000
13	4	3	0,5000	0,5000
12	3	4	0,5417	0,6667
11	3	3	0,5833	0,6667
10	3	2	0,6250	0,6667
9	3	1	0,6667	0,6667
8	2	0	0,7083	0,8333
7	2	1	0,7500	0,8333
6	2	2	0,7917	0,8333
5	2	3	0,8333	0,8333
4	1	4	0,8750	1,0000
3	1	3	0,9167	1,0000
2	1	2	0,9583	1,0000
1	1	1	1,0000	1,0000

6.2.9. Lateral stiffness in shear and lateral displacement

Lateral stiffness:

$$K_{Si} = \sum_{j=1}^{N_i} \frac{EA_j^0}{L_j} \cos^2 \theta_j \cos^2 \phi_j$$

ϕ_j is the angle in plan formed by the j-th diagonal with respect to the direction of analysis

$$\tan \alpha_1 = \frac{R(1 - \cos 30^\circ)}{R \sin 30^\circ} = 0,2680$$

$$\alpha_1 = \tan^{-1}(\tan \alpha_1) = 15^\circ$$

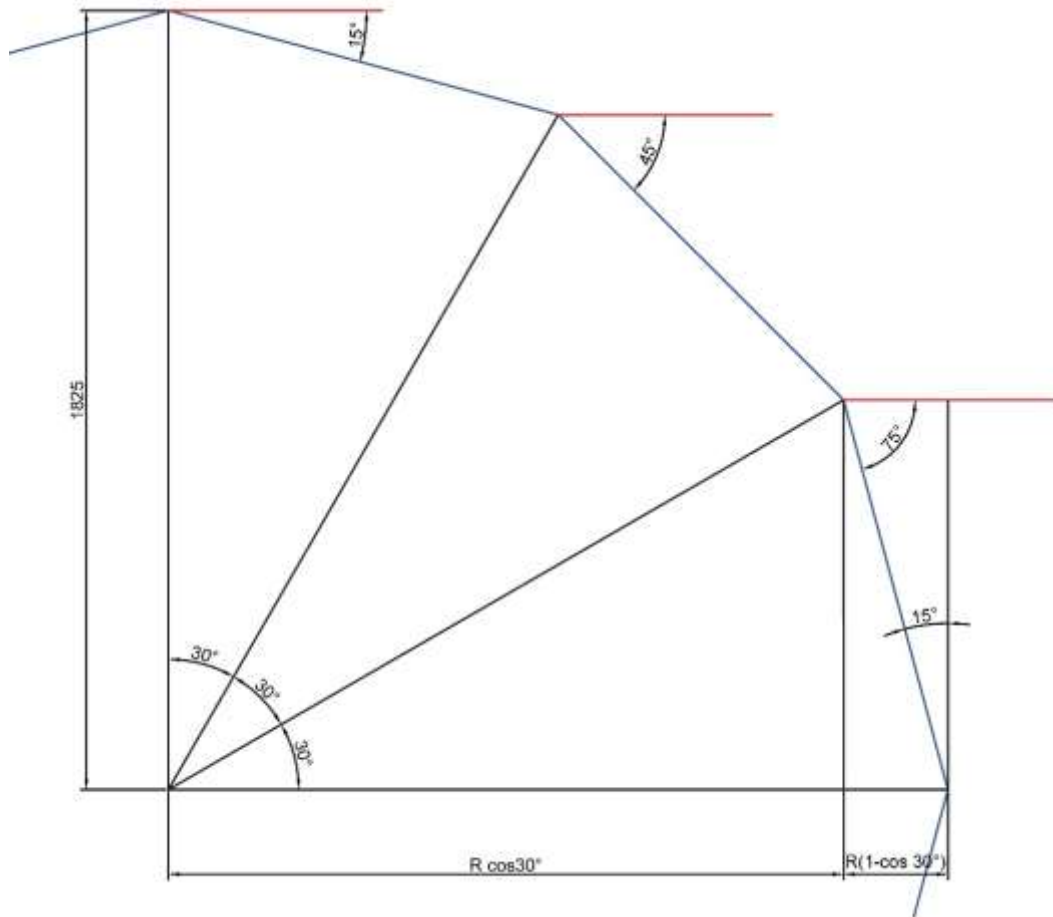


Figure 29: Angle ϕ of the diagrids modules

The Young modulus, the area of the diagonal and the base angle don't change within an interstory. In a circle there are four quadrants and in a diagrid module there are two diagonals so:

$$K_{Si} = \frac{EA^0}{L_{diagonal}} * \cos^2 \theta_j * 8 * \sum \cos^2 \phi_j$$

$$K_{Si} = \frac{20389019 \frac{t}{m^2} * A^0}{3,695 m} * \cos^2 71,36^\circ * 8 * (\cos^2 75^\circ + \cos^2 45^\circ + \cos^2 15^\circ)$$

Lateral displacement:

$$\Delta\delta_{Si} = \frac{V_i}{K_{Si}}$$

$$\delta_{Si} = \sum_{j=1}^i \Delta\delta_{Si}$$

Table 18: Lateral stiffness and lateral displacement (before iteration)

Story	K_s individual [ton/m]	K_s total [ton/m]	$\Delta\delta_s$ [m]	δ_s [m]
24	93969,69651	1082988,593	0,0000973	0,0052135
23	93969,69651	1082988,593	0,0001885	0,0051162
22	93969,69651	1082988,593	0,0002737	0,0049277
21	93969,69651	1082988,593	0,0003531	0,0046539
20	187883,0225	2165327,523	0,0002135	0,0043008
19	187883,0225	2165327,523	0,0002475	0,0040874
18	187883,0225	2165327,523	0,0002789	0,0038398
17	187883,0225	2165327,523	0,0003077	0,0035609
16	281852,719	3248316,116	0,0002226	0,0032532
15	281852,719	3248316,116	0,0002384	0,0030306
14	281852,719	3248316,116	0,0002527	0,0027922
13	281852,719	3248316,116	0,0002654	0,0025395
12	375822,4155	4331304,709	0,0002075	0,0022740
11	375822,4155	4331304,709	0,0002149	0,0020665
10	375822,4155	4331304,709	0,0002213	0,0018516
9	375822,4155	4331304,709	0,0002268	0,0016302
8	469735,7415	5413643,638	0,0001851	0,0014035
7	469735,7415	5413643,638	0,0001881	0,0012184
6	469735,7415	5413643,638	0,0001904	0,0010303
5	469735,7415	5413643,638	0,0001922	0,0008399
4	563705,438	6496632,231	0,0001612	0,0006477
3	563705,438	6496632,231	0,0001619	0,0004865
2	563705,438	6496632,231	0,0001623	0,0003246
1	563705,438	6496632,231	0,0001624	0,0001624

6.2.10. Lateral bending stiffness

Since the diagonals are not vertical, the lateral bending stiffness I_{Bi} can be computed with the following formula:

$$I_{Bi} = \sum_{j=1}^{N_i} A_j \sin^2 \theta_i d_j^2$$

$$I_{Bi} = 2A^0 * [d_1^2 + 2d_2^2 + 2d_3^2] * \sin^2 71,36^\circ$$

$$I_{Bi} = 2A^0 * [18,25^2 + 2(R\cos 30^\circ)^2 + 2(R\cos 60^\circ)^2] * \sin^2 71,36^\circ$$

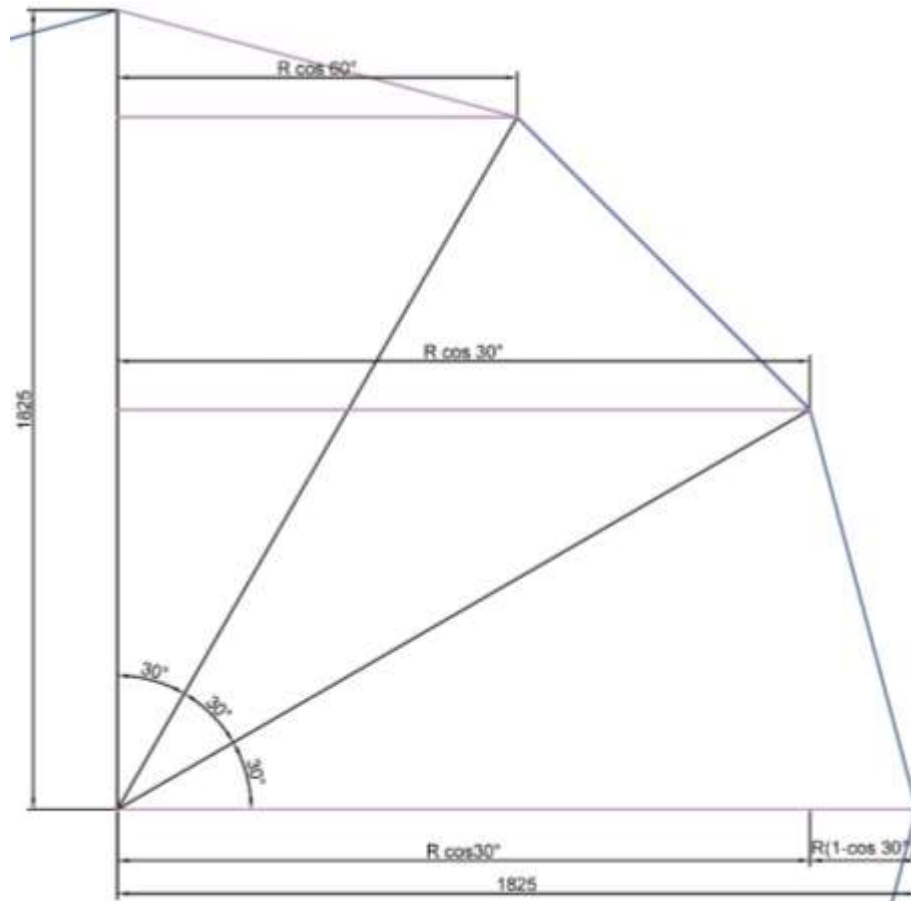


Figure 30: Distance to the centroid axe

Table 19: Lateral bending stiffness (before iteration)

Story	Diagrids area Practical [m ²]	I _B [m ⁴]
24	0,1667	299,097469
23	0,1667	299,097469
22	0,1667	299,097469
21	0,1667	299,097469
20	0,3333	598,015515
19	0,3333	598,015515
18	0,3333	598,015515
17	0,3333	598,015515
16	0,5000	897,112984
15	0,5000	897,112984
14	0,5000	897,112984
13	0,5000	897,112984
12	0,6667	1196,21045
11	0,6667	1196,21045
10	0,6667	1196,21045
9	0,6667	1196,21045
8	0,8333	1495,1285
7	0,8333	1495,1285
6	0,8333	1495,1285
5	0,8333	1495,1285
4	1,0000	1794,22597
3	1,0000	1794,22597
2	1,0000	1794,22597
1	1,0000	1794,22597

6.2.11. Curvatures and rotations

Curvatures at the upper and lower ends of the diagrids located in the i-th interstory:

$$\varphi_i^{above} = \frac{M_{i+1}}{EI_{Bi}} \qquad \varphi_i^{down} = \frac{M_i}{EI_{Bi}}$$

Rotations at the upper θ_i^{above} and lower θ_i^{down} ends of the diagrids located in the i-th interstory:

$$\theta_i^{above} = \left(\frac{2\varphi_i^{above} + \varphi_i^{down}}{6} \right) h_i \qquad \theta_i^{down} = \left(\frac{\varphi_i^{above} + 2\varphi_i^{down}}{6} \right) h_i$$

Total increase of rotation in the slab located in the i-th level due to global flexural behavior:

$$\Delta\theta_i^{tot} = \theta_i^{above} + \theta_i^{down}$$

Total rotation of the slab located in the i-th level:

$$\theta_i^{tot} = \sum_{j=1}^i \Delta\theta_j^{tot}$$

Table 20: Curvatures and rotations (before iteration)

φ^{above} [1/m]	φ^{down} [1/m]	θ^{above} [rad]	θ^{down} [rad]	$\Delta\theta^{tot}$ [rad]	θ^{tot} [rad]
0	4,83878E-08	2,82262E-08	5,64524E-08	2,82262E-08	6,3449E-05
4,83878E-08	1,42123E-07	1,39357E-07	1,94036E-07	1,9581E-07	6,34208E-05
1,42123E-07	2,78232E-07	3,28112E-07	4,07509E-07	5,22148E-07	6,3225E-05
2,78232E-07	4,53815E-07	5,8933E-07	6,91753E-07	9,96839E-07	6,27029E-05
2,26975E-07	3,3312E-07	4,59125E-07	5,21042E-07	1,15088E-06	6,1706E-05
3,3312E-07	4,56212E-07	6,54763E-07	7,26567E-07	1,17581E-06	6,05552E-05
4,56212E-07	5,9491E-07	8,79278E-07	9,60186E-07	1,60585E-06	5,93793E-05
5,9491E-07	7,47913E-07	1,13034E-06	1,2196E-06	2,09053E-06	5,77735E-05
4,98559E-07	6,09243E-07	9,37043E-07	1,00161E-06	2,15664E-06	5,5683E-05
6,09243E-07	7,27805E-07	1,13534E-06	1,2045E-06	2,13695E-06	5,35263E-05
7,27805E-07	8,53458E-07	1,34696E-06	1,42025E-06	2,55145E-06	5,13894E-05
8,53458E-07	9,85445E-07	1,57054E-06	1,64754E-06	2,9908E-06	4,88379E-05
7,39047E-07	8,42236E-07	1,35353E-06	1,41372E-06	3,00106E-06	4,58471E-05
8,42236E-07	9,49107E-07	1,53626E-06	1,5986E-06	2,94998E-06	4,28461E-05
9,49107E-07	1,05916E-06	1,72514E-06	1,78934E-06	3,32373E-06	3,98961E-05
1,05916E-06	1,17193E-06	1,91931E-06	1,98509E-06	3,70865E-06	3,65724E-05
9,37627E-07	1,02966E-06	1,69453E-06	1,74822E-06	3,67963E-06	3,28637E-05
1,02966E-06	1,12317E-06	1,85645E-06	1,911E-06	3,60467E-06	2,91841E-05
1,12317E-06	1,21785E-06	2,02078E-06	2,07601E-06	3,93178E-06	2,55794E-05
1,21785E-06	1,31342E-06	2,18699E-06	2,24273E-06	4,263E-06	2,16476E-05
1,09447E-06	1,17463E-06	1,96208E-06	2,00884E-06	4,20482E-06	1,73846E-05
1,17463E-06	1,25513E-06	2,10256E-06	2,14952E-06	4,1114E-06	1,31798E-05
1,25513E-06	1,33581E-06	2,24354E-06	2,2906E-06	4,39305E-06	9,06842E-06
1,33581E-06	1,41655E-06	2,38476E-06	2,43186E-06	4,67536E-06	4,67536E-06

6.2.12. Lateral displacement

Relative displacement of the i -th interstory due to global flexural behavior:

$$\Delta\delta_{Bi} = \theta_i^{tot} h_i$$

Lateral displacement in the i -th level:

$$\delta_{Bi} = \sum_{j=1}^i \Delta\delta_{Bj}$$

Table 21: Lateral displacement (before iteration)

Story	$\Delta\delta_{Bi}$ m	δ_{Bi} m
24	0,000222072	0,003571376
23	0,000221973	0,003349304
22	0,000221288	0,003127331
21	0,00021946	0,002906044
20	0,000215971	0,002686584
19	0,000211943	0,002470613
18	0,000207828	0,00225867
17	0,000202207	0,002050842
16	0,00019489	0,001848635
15	0,000187342	0,001653744
14	0,000179863	0,001466402
13	0,000170933	0,001286539
12	0,000160465	0,001115607
11	0,000149961	0,000955142
10	0,000139636	0,00080518
9	0,000128003	0,000665544
8	0,000115023	0,000537541
7	0,000102144	0,000422518
6	8,95279E-05	0,000320374
5	7,57667E-05	0,000230846
4	6,08462E-05	0,000155079
3	4,61294E-05	9,42326E-05
2	3,17395E-05	4,81032E-05
1	1,63638E-05	1,63638E-05

6.2.13. Iteration

Since the self-weight of the diagrids is neglected for the first computation, some iterations steps need to be accomplished in order to include the weight of the diagonals.

In our example, after two iteration steps the results converged in an acceptable manner. These results are the definite values that will be taken for the diagrids sizing and design.

6.2.14. Period T_T^0 (after iteration)

Once the values for all the parameters needed for the computation of T_S and T_B are definitive, it is possible to find the period for shear and bending and thus find the period T_T^0 :

$$T_S = 0,3629 \text{ s} ; T_B = 0,279 \text{ s}$$

$$T_T^2 = T_S^2 + T_B^2 \Rightarrow T_T^0 = \sqrt{T_S^{02} + T_B^{02}} = 0,4578 \text{ s}$$

6.2.15. Areas for the diagrids (after iteration)

$$A = A^0 \left(\frac{T_T^0}{T_{T \text{ required}}} \right)^2$$

To keep the system sustainable in terms of material savings and not to have over-dimensioned elements at the top of the building, a linear variation along height for the diagonal areas was chosen. Table 22 gives the definitive areas of the diagrids elements. The last column shows the weight under the fact that the diagrids are constructed in structural steel with a weight of 7,8 ton/m³.

To give an idea of a possible section, the dimensions for a full square and full circle are also written in column four and five respectively. Of course the design of the diagonals elements is not limited to these two section types.

Table 22: Definitive areas for the diagrids

Story	Diagrids area required [m ²]	Diagrids area Required [cm ²]	Side (square) [cm]	Diameter (circle) [cm]	Diagrids weight [ton]
24	0,01455	146	12,1	13,6	10,065
23	0,01455	146	12,1	13,6	10,065
22	0,01455	146	12,1	13,6	10,065
21	0,01455	146	12,1	13,6	10,065
20	0,02909	291	17,1	19,2	20,125
19	0,02909	291	17,1	19,2	20,125
18	0,02909	291	17,1	19,2	20,125
17	0,02909	291	17,1	19,2	20,125
16	0,04365	436	20,9	23,6	30,190
15	0,04365	436	20,9	23,6	30,190
14	0,04365	436	20,9	23,6	30,190
13	0,04365	436	20,9	23,6	30,190
12	0,05820	582	24,1	27,2	40,255
11	0,05820	582	24,1	27,2	40,255
10	0,05820	582	24,1	27,2	40,255
9	0,05820	582	24,1	27,2	40,255
8	0,07274	727	27,0	30,4	50,314
7	0,07274	727	27,0	30,4	50,314
6	0,07274	727	27,0	30,4	50,314
5	0,07274	727	27,0	30,4	50,314
4	0,08729	873	29,5	33,3	60,380
3	0,08729	873	29,5	33,3	60,380
2	0,08729	873	29,5	33,3	60,380
1	0,08729	873	29,5	33,3	60,380

6.2.16. Ductility of the building (verification of the assumption)

To find a value for the coefficient of distortion, we assumed that the building has a ductility of $\mu=2$. The design of the diagrids is now done so the assumption has to be proven.

For a diagrid with a plastic hinge the longitudinal yield displacement can be expressed as:

$$\Delta A = \frac{F_y}{\frac{EA}{L}} = 0,00764 \text{ m}$$

Since the diagonal is tilted, we have to consider the base angle to find the horizontal displacement after yield:

$$\Delta H = \frac{\Delta A}{\cos\theta}$$

The interstory drift at yield can then be expressed as:

$$IDI_y = \frac{\Delta H}{h} = \frac{\Delta A / \cos \theta}{h} = \frac{0,00764 \text{ m} / \cos 71,36^\circ}{3,5 \text{ m}} = 0,0068$$

where h is the interstory height.

$$\mu = \frac{IDI_S^{LS}}{IDI_y} = \frac{0,01}{0,0068} = 1,47 \approx 1,5$$

After checking for the consequences of having an actual value of μ of 1,5 with respect to the value of μ of 2,0 originally assumed, it is seen that the preliminary design will barely change in such a manner that the preliminary design is kept unchanged.

6.2.17. Factor α (verification of the assumption)

To express the roof displacement for a single degree of freedom, $\alpha_{Diagrids}$ was assumed equal to 1,4. The design of the diagrids is now done so the assumption has to be proven.

The period T_T for the diagrid system found with a modal analysis in SAP2000 is equal to $T_T = 1,63 \text{ s}$.

$$\frac{T_S}{T_T} = \frac{1}{\sqrt{1 + \frac{S_{dB}}{S_{dS}}}} = \frac{1,28}{1,63} = 0,79$$

$$\sqrt{1 + \frac{S_{dB}}{S_{dS}}} = \frac{1}{0,79} = 1,27$$

$$1 + \frac{S_{dB}}{S_{dS}} = 1,27^2 = 1,61$$

$$\frac{S_{dB}}{S_{dS}} = 0,61$$

$$S_{dB} \approx 0,6 * S_{dS}$$

With $S_{dB} = 0,61 * S_{dS}$ the factor $\alpha_{Diagrids}$ will reduce a little bit:

$$\alpha_{Diagrids} = 0,6 * \alpha_S + 0,4 * \alpha_B = 0,6 * 1,2 + 0,4 * 1,6 = 1,36$$

Initially it was assumed that $S_{dB} = 0,5 * S_{dS}$ and so $\alpha_{Diagrids} = 0,5 * \alpha_S + 0,5 * \alpha_B = 1,4$

With this small difference the end results will barely change, so it is considered that the assumption is verified.

7. MODEL FEATURES IN SAP2000

The building was modeled in the Integrated Software for Structural Analysis and Design SAP2000 (Computers & Structure).

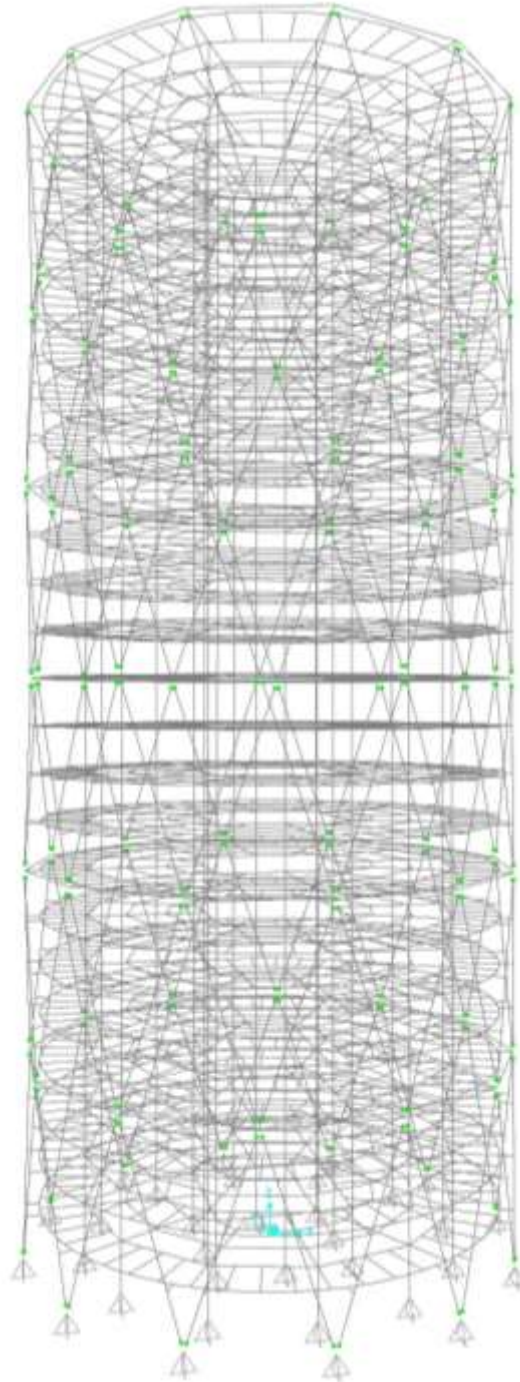


Figure 31: 3D-Model of the building - SAP2000 (Computers & Structure)

7.1 Modeling of the main elements

The model include the diagrid system, the concrete core elements and all the steel main beams, secondary beams and columns. The steel deck was not modelled as a surface but the weight was included in the dead load. The stories and roof dead and live loads were computed and assigned to the model.

As discussed before the diagrids' areas change every 4 story. To match the reality, the model should also reflect this change every 4 stories.

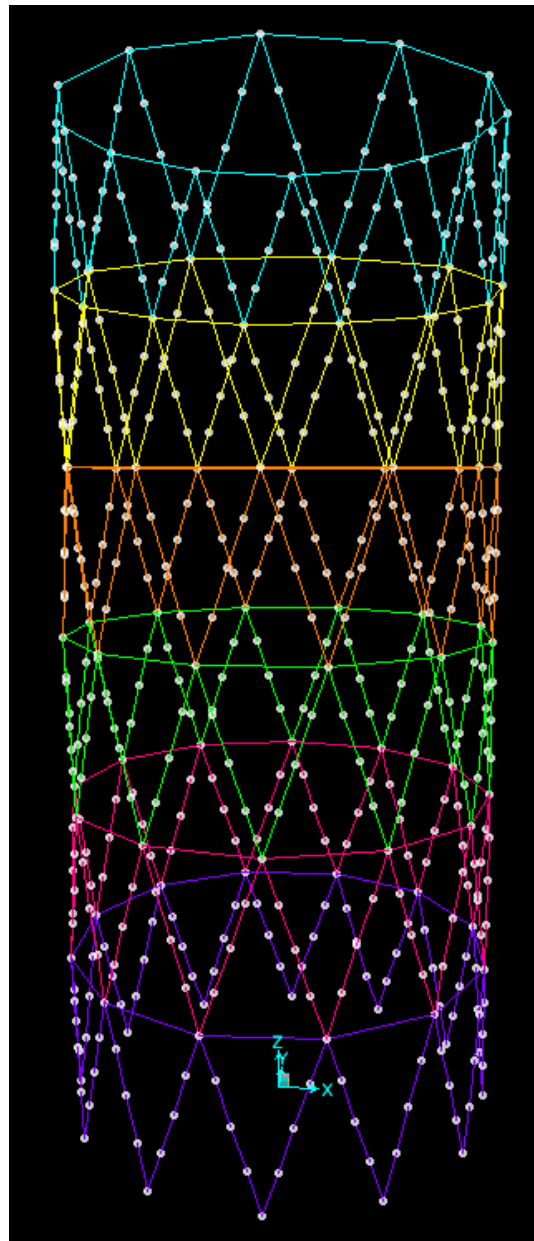


Figure 32: Diagrids sections with different area

7.2 Release at the end of the diagonals

Since diagrids only works in axial action, releases were introduced at the end of the diagonal members in order to simulate the pin-end-connection.

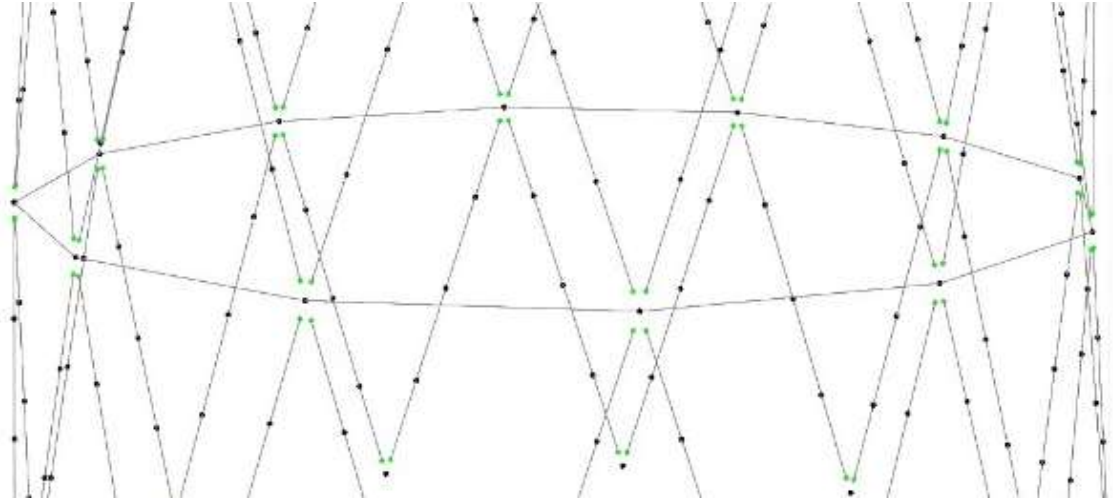


Figure 33: Diagonals with released ends

7.3 Plastic hinges

Plastic hinges which work in an axial direction were introduced in the diagonals; and plastic hinges which work in rotation were assigned to the main steel beams, steel columns, concrete columns and concrete beams.

For the computation of the plastic hinges properties all the material characteristics are taken without any reduction factor and the material overstrength is used. The overstrength is considered in order to avoid non-ductile behavior and prevent or delay an inadequate comportment. The consideration of the overstrength enables also a reasonable estimation of the global response of the structure and makes possible a rational strength design. The tensile strength and compressive strength for steel and concrete are multiplied by the factors 1,2 and 1,1 respectively to obtain the strength which take into account the overstrength of the material.

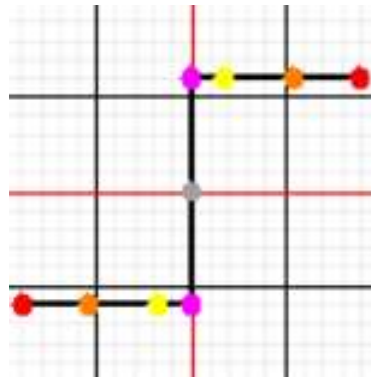


Figure 34: Force-Displacement diagram for the hinges

As shown on figure 34, the displacement control parameter for the hinges was assumed symmetric. The hinges don't show a strain hardening comportment. Once the yield force is reached, the max value for the load of the plastic hinge is reached. After the yield point the displacement will increase but the force remains the same.

7.3.1. Computation of the plastic hinges properties for the diagonals

$$f_{design\ value} = 3515 \frac{kg}{cm^2}$$

$$Steel\ overstrength = 1,2$$

$$f_y = 1,2 * f_{design\ value} = 4218 \frac{kg}{cm^2} = 42180\ ton/m^2$$

$$Yound\ modulus\ steel = 20389019\ t/m^2$$

$$Length\ of\ a\ diagonal = 3,365\ m$$

Table 23: Computation of the yield force and yield displacement in the diagrids

Stories	A _{brace} [m ²]	F _y = A _{brace} * f _y [tonf]	EA/L [ton/m]	Yield disp. [m]
21-24	0,01363	574,91340	75210,37320	0,00764
17-20	0,02725	1149,40500	150365,56637	0,00764
13-16	0,04087	1723,89660	225520,75955	0,00764
9-12	0,05450	2298,81000	300731,13275	0,00764
5-8	0,06812	2873,30160	375886,32592	0,00764
1-4	0,08175	3448,21500	451096,69912	0,00764

7.3.2. Computation of the plastic hinges properties for the steel elements

(1) Steel beams.

The bending moment that brings the beam to the point of yielding is M_y and is defined as:

$$M_y = F_y S_x$$

F_y is the stress at yield

S_x is the elastic section modulus

The plastic moment capacity, denoted M_p , is the bending moment at which a plastic hinge forms.

$$M_p = F_y \frac{A}{2} a = F_y Z_x$$

F_y is the stress at yield

A is the total cross-sectional area

a is the distance between centroid of the two half areas

Z_x is the plastic section modulus

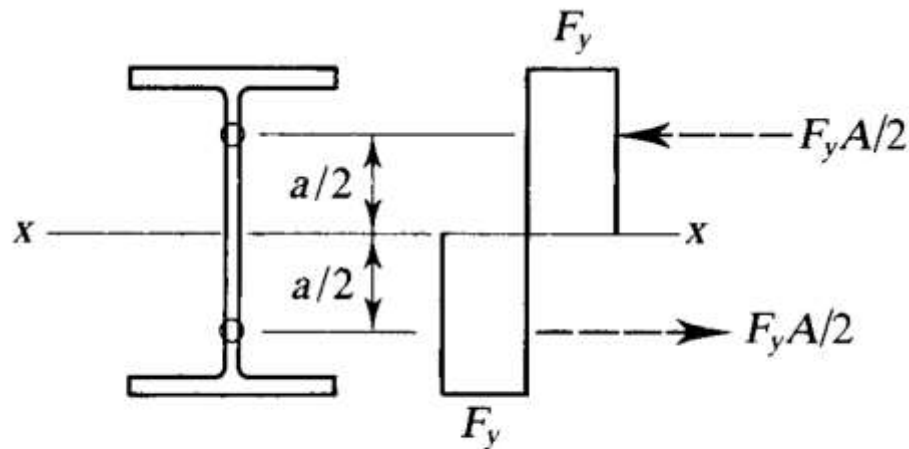


Figure 35: Plastic moment capacity M_p (Segui 2007)

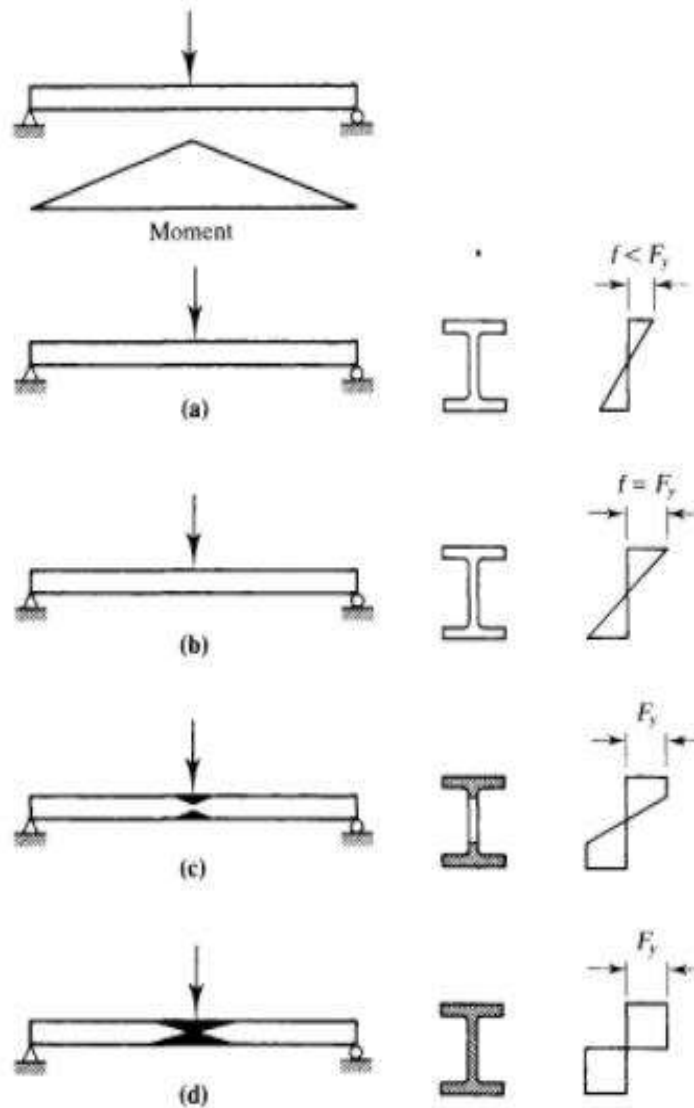


Figure 36: Successive stages of loading for a simply supported beam with a concentrated load at midspan (Segui 2007)

Once yield begins, the distribution of stress on the cross section will no longer be linear, and yielding will progress from the extreme fiber toward the neutral axis. At the same time, the yielded region will extend longitudinally from the center of the beam as the bending moment reaches M_y at more locations. (Segui 2007, p. 175)

When stage d [in figure 36] has been reached, any further increase in the load will cause collapse, since all elements of the cross section have reached the yield plateau of the stress-strain curve and unrestricted plastic flow will occur. A plastic hinge is said to have formed at the center of the beam. (Segui 2007, p. 176)

Plastic hinges are assigned only to the main steel beams. All the secondary beams present in the building remains in the elastic range.

Table 24: Steel main beam section properties

AISC_Manual_Label [in x lb/ft]	Sectional Area [in ²]	I _x [in ⁴]	Z _x [in ³]	S _x [in ³]	I _y [in ⁴]	Z _y [in ³]	S _y [in ³]
W18X46	13,5	712	90,7	78,8	22,5	11,7	7,43

$$M_p = 1,2F_y Z_x = 1,2 * 3515 \frac{kg}{cm^2} * 1487 cm^3 = 6272166 kg.cm = 62,72 ton.m$$

(2) Steel columns

The steel columns are principally subjected to axial loading but in a certain range also to bending. For the computation of the plastic hinges in the columns this phenomenon need to be taken into account. This is possible with an interaction diagram force-moment (P-M).

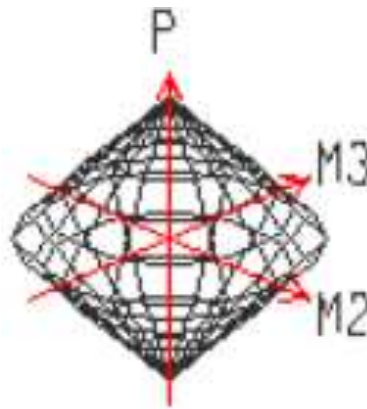


Figure 37: Interaction diagram P-M for the steel columns in the base part of the building

Table 25: Steel column section properties

AISC_Manual_Label [in x lb/ft]	Sectional Area [in ²]	I _x [in ⁴]	Z _x [in ³]	S _x [in ³]	I _y [in ⁴]	Z _y [in ³]	S _y [in ³]
W14X132	38,8	1530	234	209	548	113	74,5
W14X211	62,0	2660	390	338	1030	198	130
W14X283	83,3	3840	542	459	1440	274	179

Columns W14x132:

$$P = 1,2F_y A = 1,2 * 3515 \frac{kg}{cm^2} * 250,32 cm^2 = 1055849,76 kg = 1056 tonf$$

$$M_2 = 1,2F_y Z_x = 1,2 * 3515 \frac{kg}{cm^2} * 3835 cm^3 = 16176030 kg.cm = 162 tonf.m$$

$$M_3 = 1,2F_y Z_y = 1,2 * 3515 \frac{kg}{cm^2} * 1852 cm^3 = 7811736 kg.cm = 78 tonf.m$$

Columns W14x211:

$$P = 1,2F_y A = 1,2 * 3515 \frac{kg}{cm^2} * 400 cm^2 = 1687200 kg = 1687,2 tonf$$

$$M_2 = 1,2F_y Z_x = 1,2 * 3515 \frac{kg}{cm^2} * 6391 cm^3 = 26957238 kg.cm = 270 tonf.m$$

$$M_3 = 1,2F_y Z_y = 1,2 * 3515 \frac{kg}{cm^2} * 3245 cm^3 = 13687410 kg.cm = 136,8 tonf.m$$

Columns W14*x283:

$$P = 1,2F_y A = 1,2 * 3515 \frac{kg}{cm^2} * 537,5 cm^2 = 2267175 kg = 2267,2 tonf$$

$$M_2 = 1,2F_y Z_x = 1,2 * 3515 \frac{kg}{cm^2} * 8882 cm^3 = 37464276 kg.cm = 374,6 tonf.m$$

$$M_3 = 1,2F_y Z_y = 1,2 * 3515 \frac{kg}{cm^2} * 4490 cm^3 = 18938820 kg.cm = 189,4 tonf.m$$

7.3.3. Computation of the plastic hinges properties for the concrete elements

A reinforced concrete structure is designed to develop plastic behavior during severe seismic excitations. Plastic demands tend to concentrate in specific locations. For a “classic” building the critical zones are normally located at both ends of the beams and at the base of the columns located at the first story but in a diagrid building plastic hinges are expected to develop in the steel diagonals. Nevertheless the design of plastic mechanism for the gravitational concrete elements need to take into consideration the following points:

- Design of beams for flexure, $M_R = f(M_u)$
- Design of beams for shear, $V_V = f(M_R)$
- Design of columns for flexure, $M_C = f(M_R)$
- Design of columns for shear, $V_C = f(M_{CR})$
- Design of connections for shear, $V_{node} = f(M_R)$

For the concrete core, the zones where plastic demands may develop should be detailed so the longitudinal steel provides a balance of positive and negative steel with sufficient anchorage. In the plastic zone splices and cuts must be avoided. The transverse steel provides confinement, delay buckling and shear strength. Through adequate detailing it is possible to design in a context of large uncertainty. A good detailing not only promotes an adequate behavior for the life safety performance level, but also promotes damage control during low intensity seismic excitations (Amador Terán Gilmore).

In order to reasonably estimate the flexural capacity of the reinforced concrete elements and loading capacity of the columns, the followings hypotheses should apply:

- A flat section before bending must remain flat after flexion
- The stress distribution is known for the concrete located in the compression zone
- No slip occurs between the steel reinforcement and the concrete that enclose it
- The concrete does not withstand tension
- The resistance element is associated with a maximum strain of compression in the concrete of 0,003 ($\epsilon_{cmax} = 0,003$).

(1) Concrete beams

To enable a simpler calculation method, the compression strut can be determined from an equivalent rectangular stress block in the concrete. The magnitude and location of the corresponding strut C matches which what you would get with more refined models or what would be measured in a real beam.

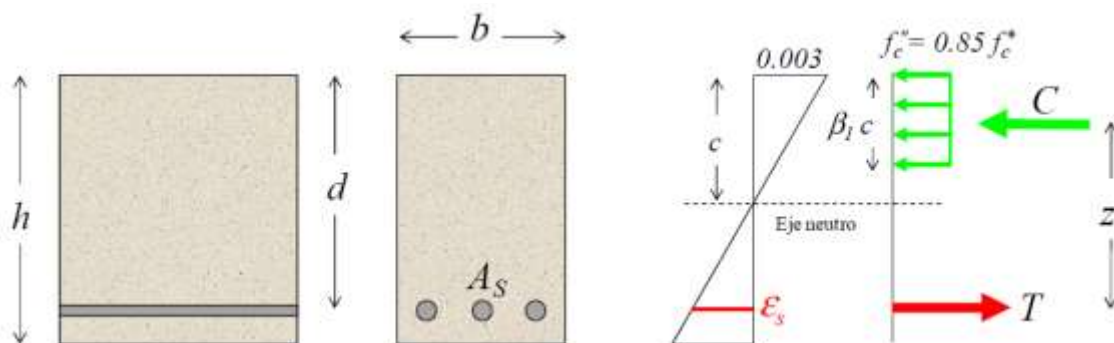


Figure 38: Simplification of the stresses in the concrete compression zone (Terán Gilmore)

For beam only submitted to flexure, no axial force can develop in the beam itself because there is no external axial force to counter act it. So C must be equal to T .

$$C = T$$

where $C = \beta_1 c * f_c'' * b$ and $T = A_s f_y$

$$f_c^* = 0,8 * f_c'$$

$$f_c'' = 0,85 * f_c^*$$

$$\beta_1 = 0,85 \text{ if } f_c^* \leq 280 \text{ kg/cm}^2$$

$$\beta_1 = 1,05 - \frac{f_c^*}{1400} \text{ if } f_c^* \geq 280 \text{ kg/cm}^2$$

$$\text{Concrete: } f_c' = 4218,418 \frac{\text{tonf}}{\text{m}^2} = 421,85 \frac{\text{kg}}{\text{cm}^2}$$

$$\text{so } f_c^* = 0,8 * f_c' = 0,8 * 421,85 \frac{\text{kg}}{\text{cm}^2} = 337,48 \frac{\text{kg}}{\text{cm}^2}$$

$$f_c'' = 0,85 * f_c^* = 0,85 * 337,48 \frac{\text{kg}}{\text{cm}^2} = 287 \frac{\text{kg}}{\text{cm}^2}$$

$$\beta_1 = 1,05 - \frac{f_c^*}{1400} = 1,05 - \frac{337,48 \frac{\text{kg}}{\text{cm}^2}}{1400} = 0,8$$

$$\text{Steel reinforcement: } f_y = 42184,18 \frac{\text{tonf}}{\text{m}^2} = 4218,4 \frac{\text{kg}}{\text{cm}^2}$$

$$M_n = q f_c'' b d^2 (1 - 0,5q)$$

$$\text{where } \rho = \frac{A_s}{bd} = \frac{11,61 \text{ cm}^2}{25,4 \text{ cm} * 29,69 \text{ cm}} = 0,015$$

$$\text{and } q = \frac{\rho f_y}{f_c''} = \frac{0,015 * 1,2 * 4218,4 \frac{\text{kg}}{\text{cm}^2}}{1,1 * 287 \frac{\text{kg}}{\text{cm}^2}} = 0,24$$

$$M_n = 0,24 * 1,1 * 287 * 25,4 * (29,69)^2 * (1 - 0,5 * 0,22)$$

$$M_n = 1509836,6 \text{ kg.cm} = 15,1 \text{ ton.m}$$

(2) Concrete columns

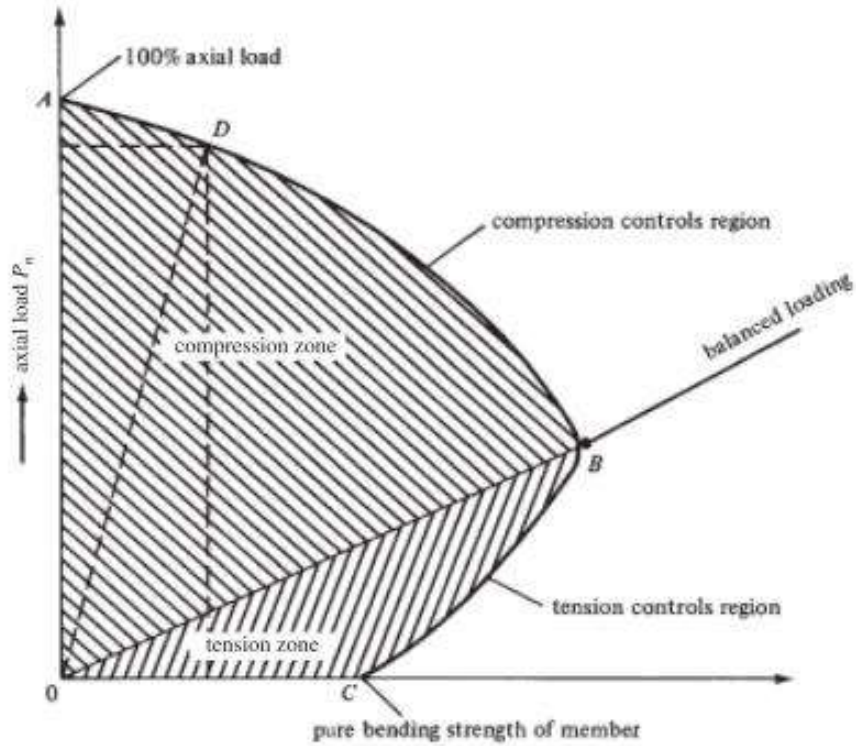


Figure 39: Column interaction diagram (McCormac, Brown 2013, p. 291)

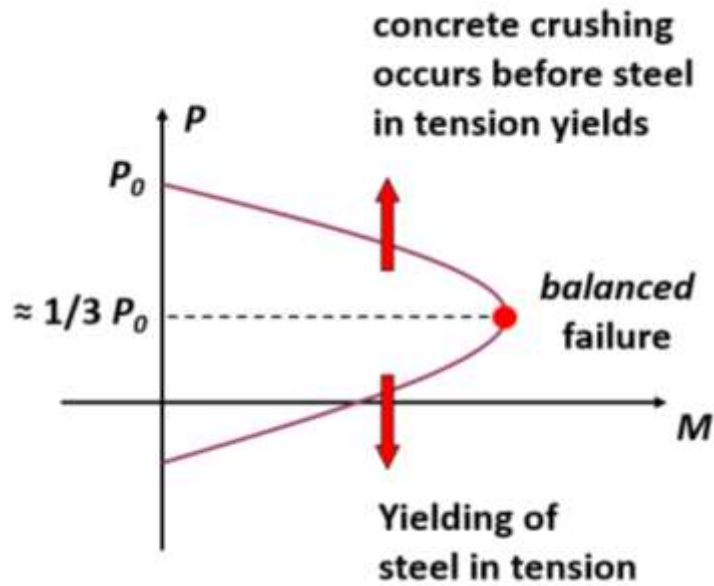


Figure 40: Column interaction diagram (Terán Gilmore)

$$P = A_s f_y + A_c f_c'' = 98 \text{ cm}^2 * 1,2 * 4218 \frac{\text{kg}}{\text{cm}^2} + (67,31^2) * 1,1 * 287 \frac{\text{kg}}{\text{cm}^2}$$

$$P = 1926358 \text{ kg} = 1926 \text{ tonf}$$

With the beam dimensions found through a static analysis (see part 4.5.4 Columns) and with the help of a software it is possible to compute the interaction diagram for the column. Some points can be calculated by hand but some other need an iterative process. So the use of a software is more convenient in order to obtain the interaction diagram.

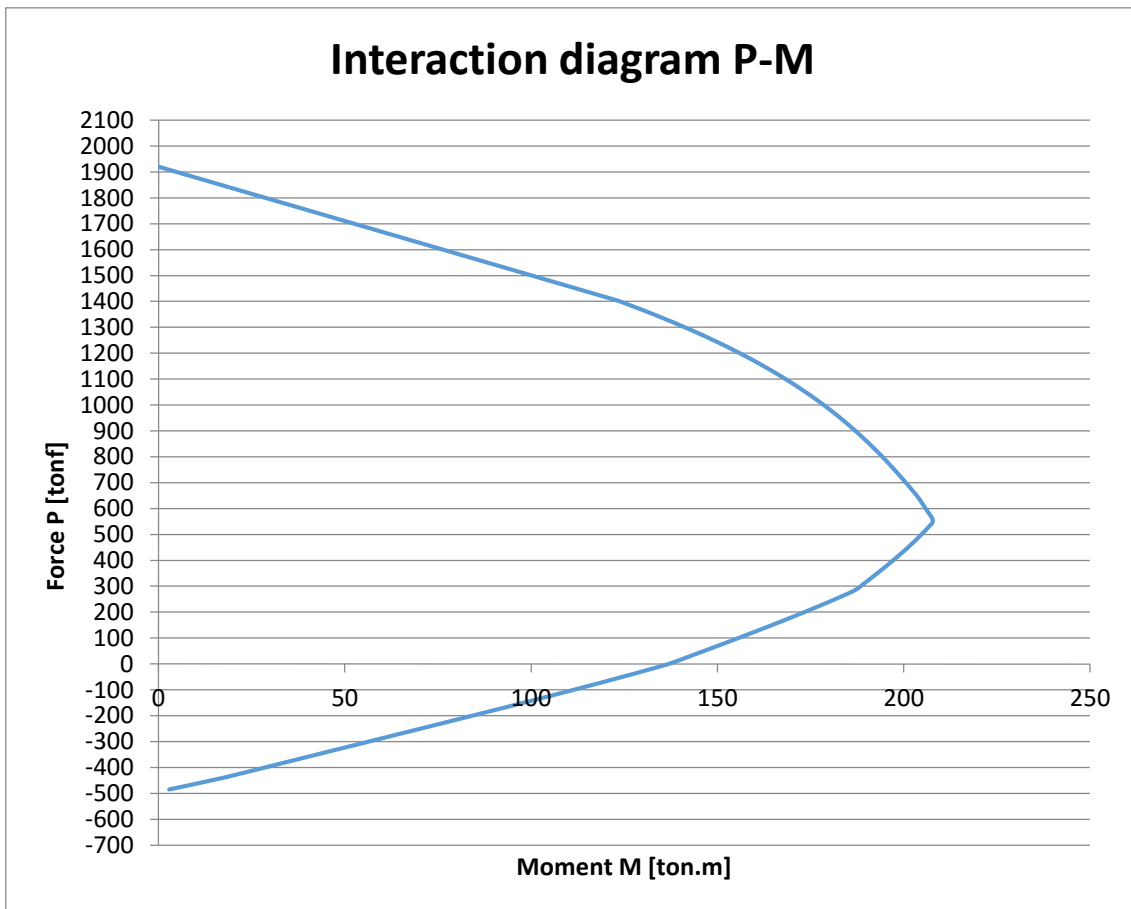


Figure 41: Interaction diagramm P-M

8. MODAL ANALYSIS

Once all the building with its structural elements and core is modeled in the software, it is possible to run a modal analysis to find the period of the building.

The period found for the building is $T_{building} = 1,63$ s

This result should be compared with the period $T_{Required}$ which was established for the design of the diagrid elements. Since $T_{building}$ is greater than $T_{Required} = 1,55$ s the maximal roof displacement at the end will be bigger than assumed. This is not a problem if the IDI_{max} (here 0,01) is not exceeded.

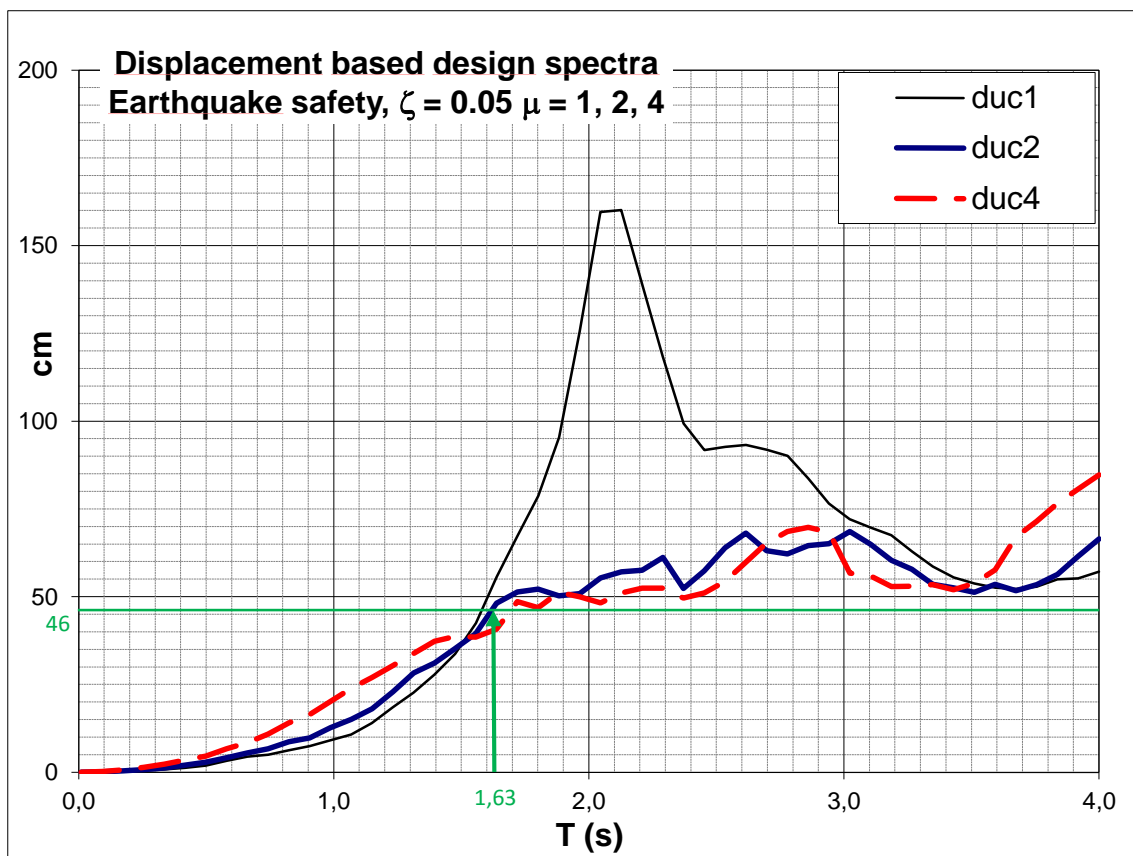


Figure 42: Displacement based design spectra for $\mu=1$, $\mu=2$ and $\mu=4$

If $T_{building}$ is larger than $T_{Required}$, the engineer must ask himself/herself if the value can be kept for the rest of the analysis with the risk that IDI_{max} will be exceeded - what would lead in the obligation to do a new design - or if the value should be adjusted at this point before further computation. For the example developed herein, it was chosen to keep the actual design with a building period of 1,63s to do the push-over and time-history analyses. All the important results are shown in the following chapters.

9. PUSH-OVER ANALYSIS

Pushover is a static-nonlinear analysis method where a structure is subjected to gravity loading and a monotonic displacement-controlled lateral load pattern which continuously increases through elastic and inelastic behavior until an ultimate condition is reached (Pushover).

The building was pushed to reach a maximum roof displacement of 1 m. The push-over analysis take into account the nonlinear behavior of all structural materials.

9.1 Push-over curve

The push-over curve (figure 43) obtained with the software SAP 2000 (Computers & Structure), shows that while the first plastic hinge appears in the diagrid at a roof displacement of $\delta_{roof} = 43 \text{ cm}$ (red line on the left); the first one in the gravitational system appears in the concrete beams at about a δ_{roof} of 70 cm (red line on the right).

The purple line depicts the maximal roof displacement $\delta_S^{LS} = 56 \text{ cm}$ assumed before for $IDI_S^{LS} = 0,01$

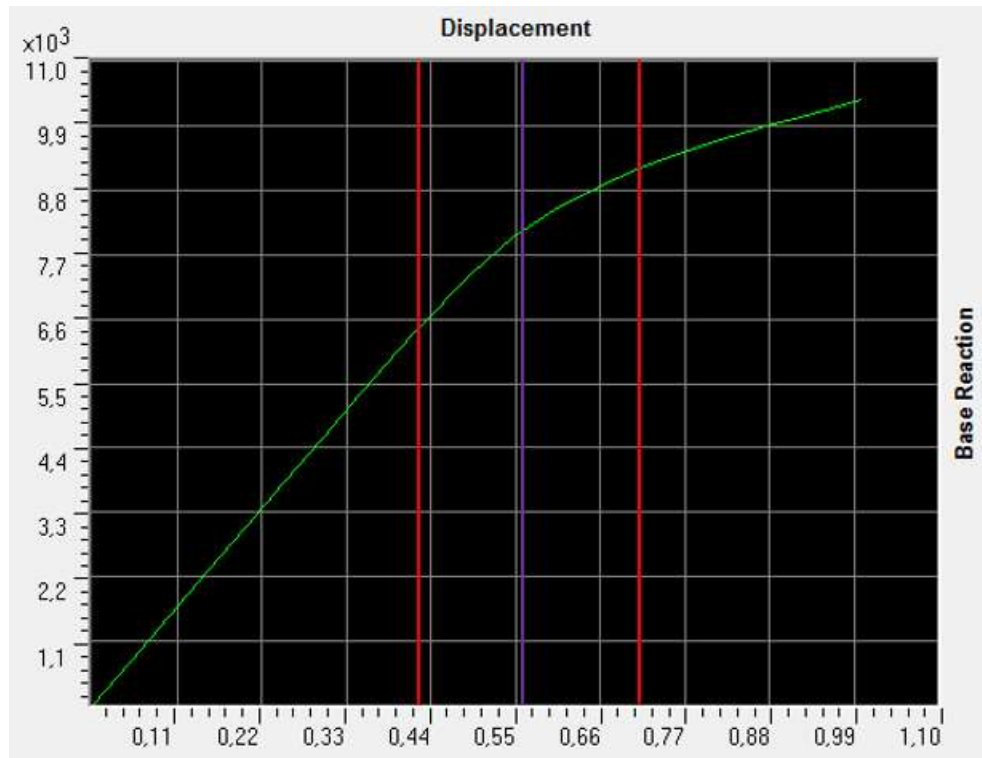


Figure 43: Push-over curve (capacity curve)

9.2 Plastic hinges in the diagrids

Figure 44 shows the location of the two first plastic hinges (in purple) which appear in the diagrids at a roof displacement of 43 cm.

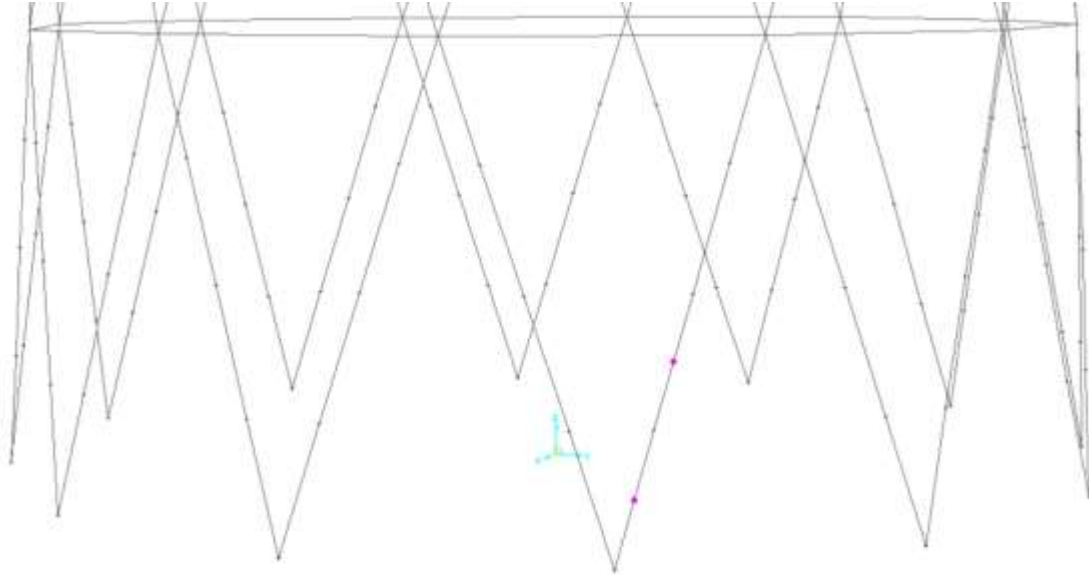


Figure 44: First plastic hinges in the diagrids



Figure 45: Color scale for the plastic hinges (left: small damage, right: heavy damage)

The color give an information about the level of damage which occurs in the plastic hinge. The purple color (left on figure 45) is for a low level of damage and the red (right on figure 45) means that the capacity of the plastic hinge is exceeded. The points C, D and E are defined as shown figure 46.

Points A to E are to be take in relation with figure 34 which depicts the Force-Displacement diagram for the hinges. From point A to B the behavior of the bar is elastic. At point B the hinge starts to develop a plastic behavior. Points C and D represent thresholds for 1 time and 3 times the yield displacement respectively (as shown on figure 46). Point E is the maximal point before failure and is achieved for a displacement of 5 times the yield displacement.

Point	Force/SF	Disp/SF
E-	-1	-5
D-	-1	-3
C-	-1	-1
B-	-1	0
A	0	0
B	1,	0,
C	1,	1,
D	1,	3,
E	1,	5,

Figure 46: Definition of the points for a plastic hinge

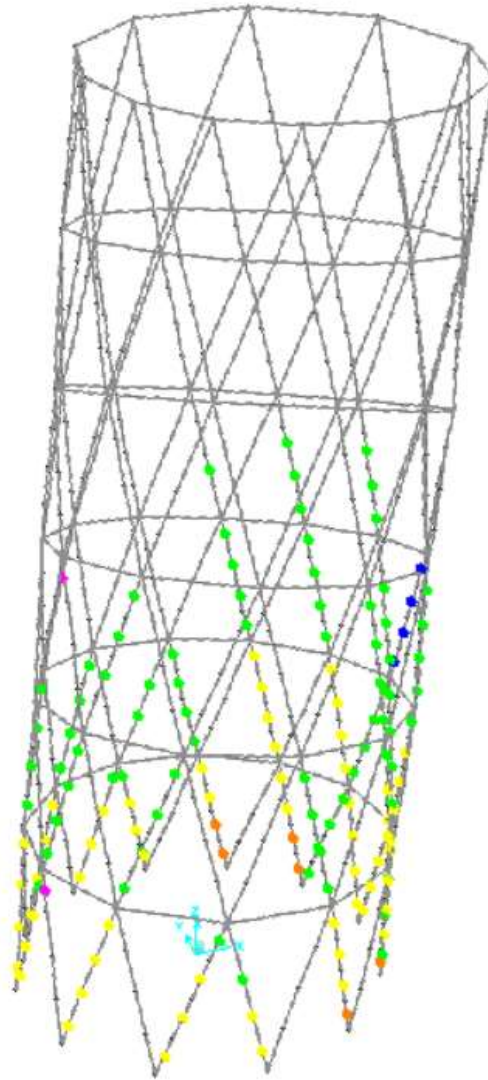


Figure 47: Plastic hinges in the diagrids for a roof displacement of 1 m

9.3 Plastic hinges in the core

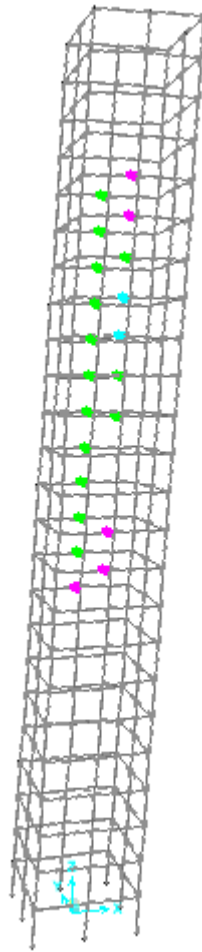


Figure 48: Plastic hinges in the core for a roof displacement of 75 cm

Figure 48 shows the concrete core for a roof displacement of 75 cm. The first plastic hinges appear in the middle part of the building. According to the colors, they stay in a low level of damage. Since it was assumed that the maximal roof displacement should be 56 cm, no plastic hinges will develop into the concrete core. So the performance defined for the core is achieved. However it is always worth to see how a structure behaves beyond the limit expected since nature is unpredictable. Therefore figure 49 gives the plastic hinges in the concrete core for the maximal roof displacement of the push-over analysis (1 m). Here again according to the colors, the level of damage in the plastic hinges is acceptable and even before point C since no hinge is yellow, orange or red. If for any reason the building will displace more than supposed during an earthquake, this won't affect the core in a critical manner.

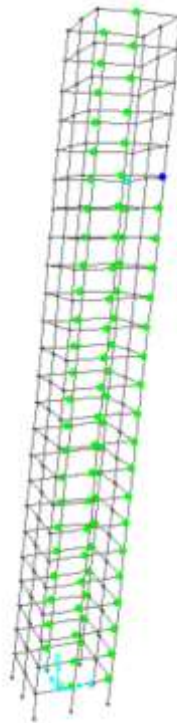


Figure 49: Plastic hinges in the concrete core for a roof displacement of 1 m

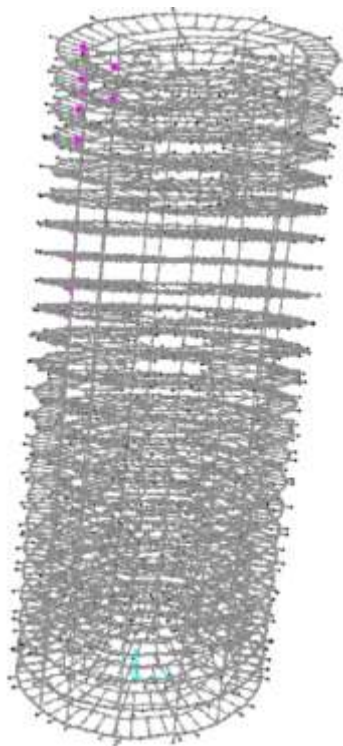


Figure 50: Plastic hinges in the steel elements for a roof displacement of 1 m

9.4 Lateral displacement

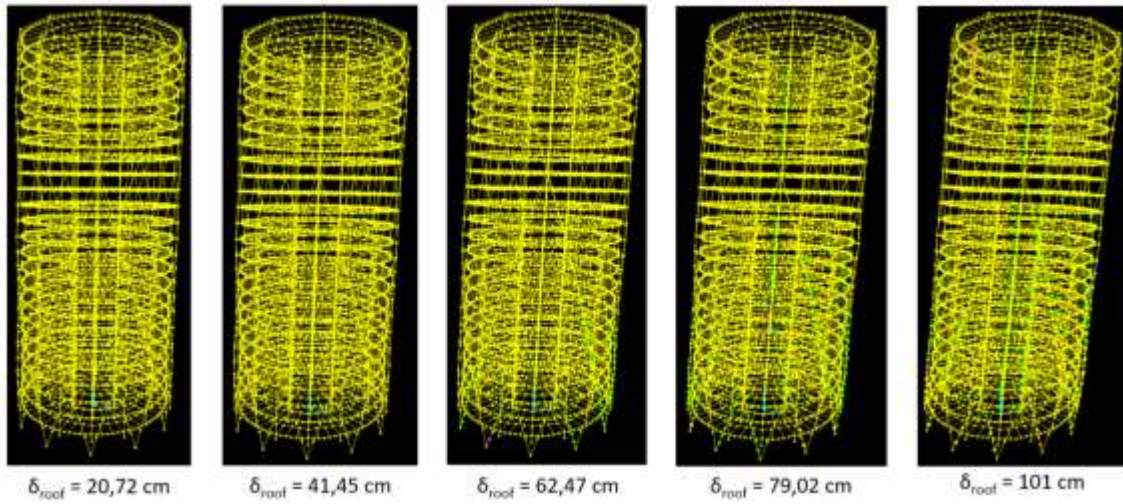


Figure 51: Deformed shape of the building for different roof displacements

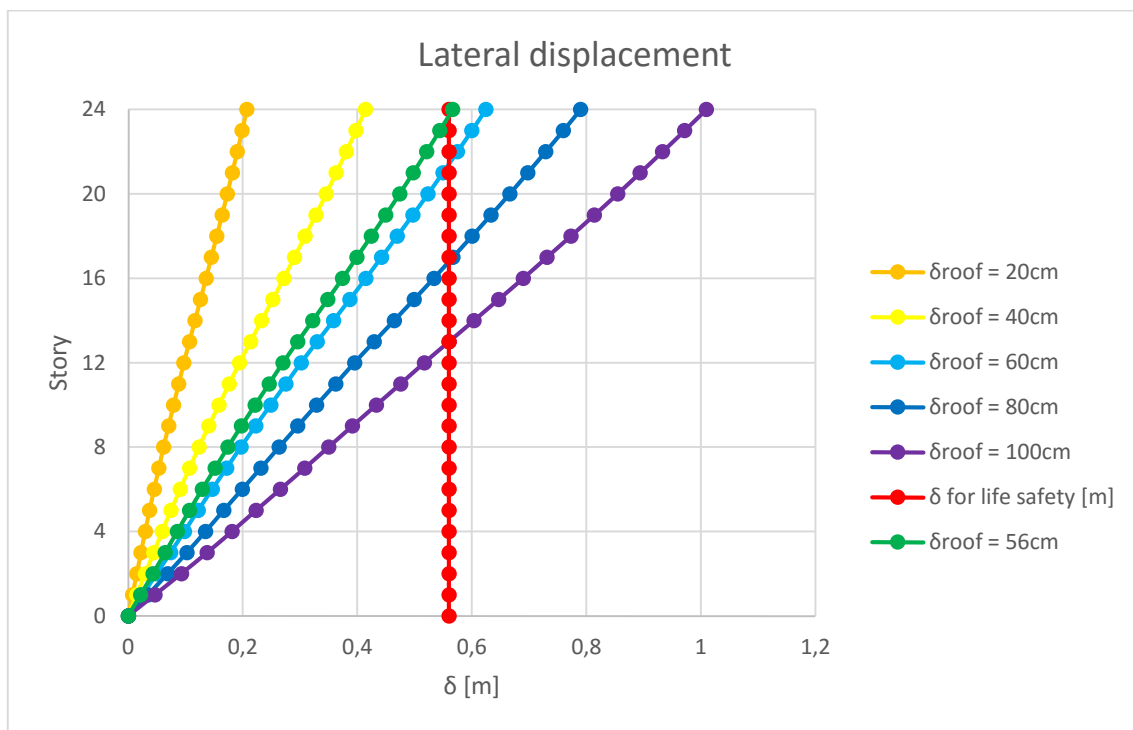


Figure 52: Nonlinear static analysis: lateral displacement

Figure 52 shows the distribution along height of lateral displacement for roof displacements of 20 cm; 40 cm; 56 cm; 60 cm; 80 cm; 1 m and the limit assumed for life safety with an interstory drift

definition of 0,01. The diagrid building reacts in a very good manner since all the curves are almost straight lines. This means that the displacement is spread steadily along the building height.

9.5 Interstory drift

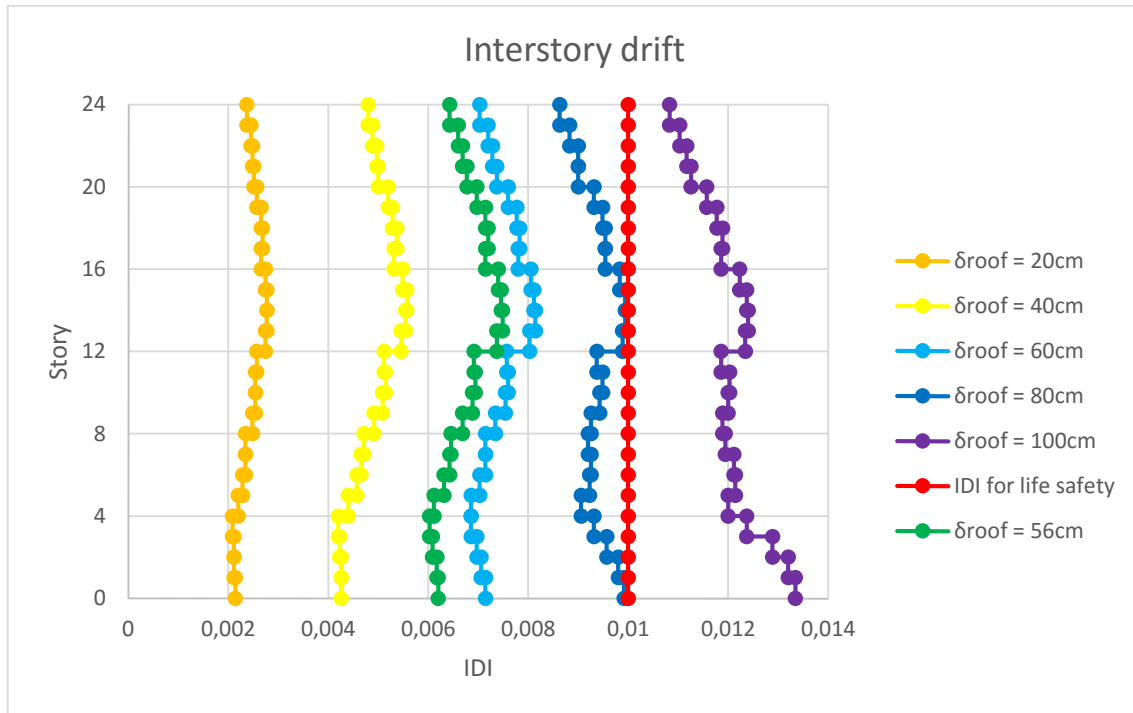


Figure 53: Nonlinear static analysis: interstory drift

As shown in figure 53 the interstory drift for roof displacements of 20 cm; 40 cm; 56 cm; 60 cm; 80 cm; 1 m and the limit assumed for life safety with an interstory drift definition of 0,01 are drawn in the same graph. The curves are almost vertical straight lines which means that the variation in the value of the distortion along height is small. For a roof displacement of 40 cm, 56 cm and 60 cm, the plastic deformations accumulate in the middle stories. But the more the roof displacement increases, the more the curves move away from a vertical shape and are not so straight anymore, and the non-linear distortions tend to gather at the bottom stories. The ultimate line for a roof displacement of 1 m show more internal distortion than the first one. Nevertheless the whole reaction is very good since the distortions are smaller than expected. The building could actually be pushed till a roof displacement of 80 cm and IDI=0,01 will not be exceed.

9.6 Interstory ductility

As shown in figure 54, the diagrids develop maximum ductility of 1,0422 for a roof displacement of 42 cm. Moreover the ductility is almost the same through the height of the building which means that a circular diagrid edifice reacts in a very stable manner.

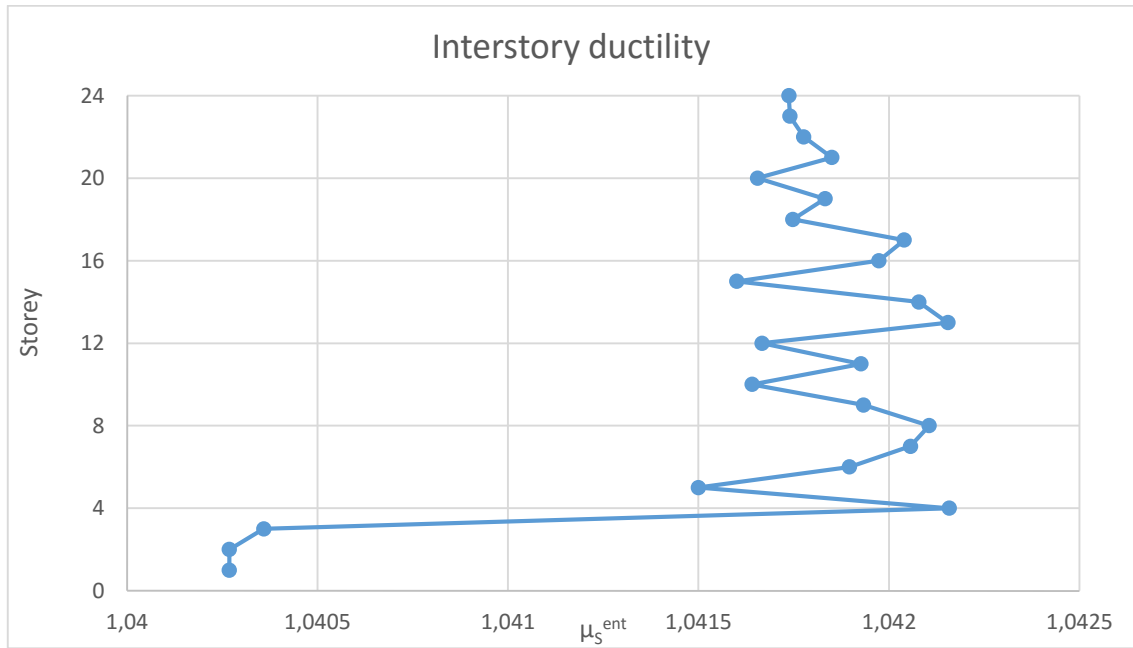


Figure 54: Nonlinear static analysis: interstory ductility

9.7 Maximal plastic hinges in the diagrids

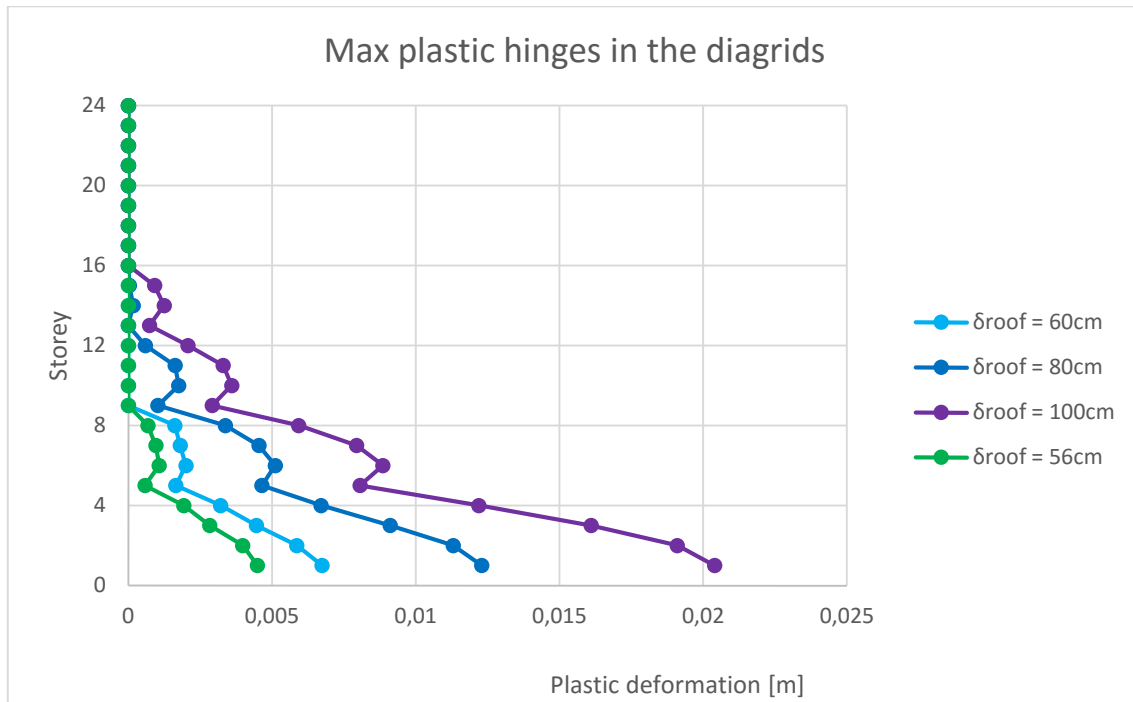


Figure 55: Nonlinear static analysis: plastic deformation in the diagrids

The conclusion of the push-over analysis is that the preliminary design of the diagrids, achieved through the methodology explained in the chapter 6, matches very well the target building performance.

10. TIME-HISTORY ANALYSIS

The time-history analysis enables to evaluate the seismic performance of a building under a real ground motion event.

The building studied in this work is located in the Lake of Mexico City and 5% of critical damping is considered. To evaluate its seismic performance, the same ten ground motions used to establish the design spectra were used. Since it is not possible to predict exactly how the natural earthquake will happen, the building will be put under a scope of 10 ground motions. The average result of these 10 tests matches the roof displacement and interstory drift of the structure which will develop in reality.

10.1 Lateral displacement

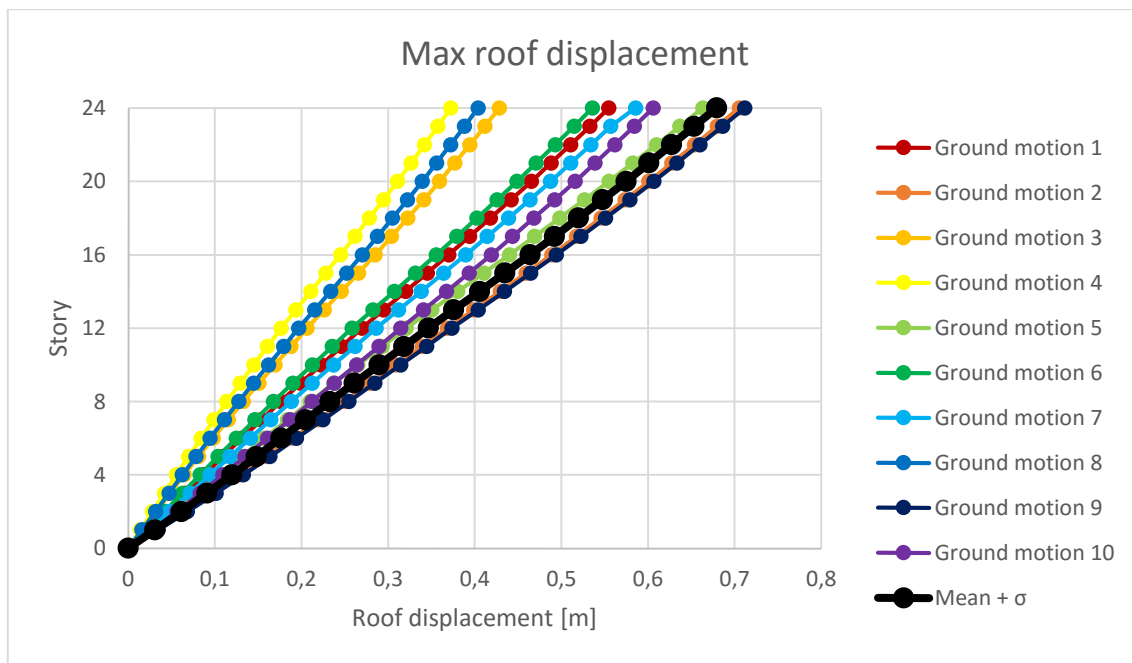


Figure 56: Time-analysis maximal roof displacement

Figure 56 depicts for each ground motion used for the time-analysis, the envelope of lateral displacement for the entire diagrid building. The bold black line shows the average value of all the displacements plus one standard deviation (σ) of the envelopes. In comparison with the roof displacement of $\delta_S^{LS} = 0,56 \text{ m}$ assumed in the design process for an interstory drift 0,01 at a performance level of life safety, the one estimated after the time-history analysis $\delta_S^{LS} = 0,67 \text{ m}$ is greater (this is direct consequence of the fact that $T_{building}$ is larger than $T_{Required}$). Fact is that the entire building will move more than presumed but this is not a problem as long as IDI_{max} itself is not exceed.

10.2 Interstory drift

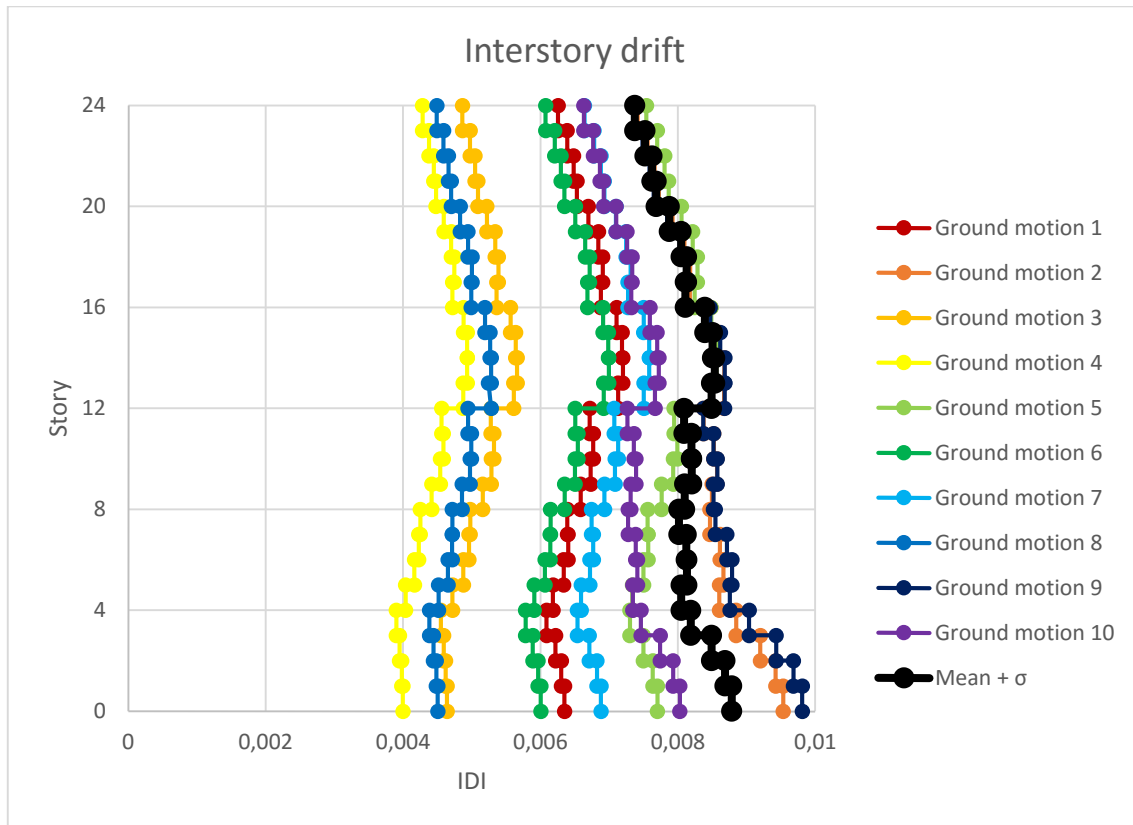


Figure 57: Time-analysis: interstory drift

Figure 57 shows for each ground motion used for the time-analysis, the envelope of interstory drift along height. The bold black line gives the average value of all the IDI plus one standard deviation (σ) of the envelopes.

In comparison with the push-over analysis, the curves pattern is almost the same. The curves are almost vertical straight lines. For small and mid-range roof displacements, the plastic deformations accumulate in the middle stories. But the more the roof displacement increases, the more the curves move away from a vertical shape and are not so straight anymore and the non-linear distortions tend to gather at the bottom stories. The interstory drift of 0,01 is not exceeded in any case. This means that the entire building and particularly the diagrids are well designed.

The diagrids will show non-linear behavior but the gravitational system will remain elastic and therefore undamaged. The behavior obtained is consistent with the design objectives. Moreover the graph indicates that the structure can actually be pushed more than supposed as long as IDI_5^{LS} is not exceeded.

10.3 Base shear vs displacement



Figure 58: Overview of the base shear vs displacement diagrams for the 10 ground motions

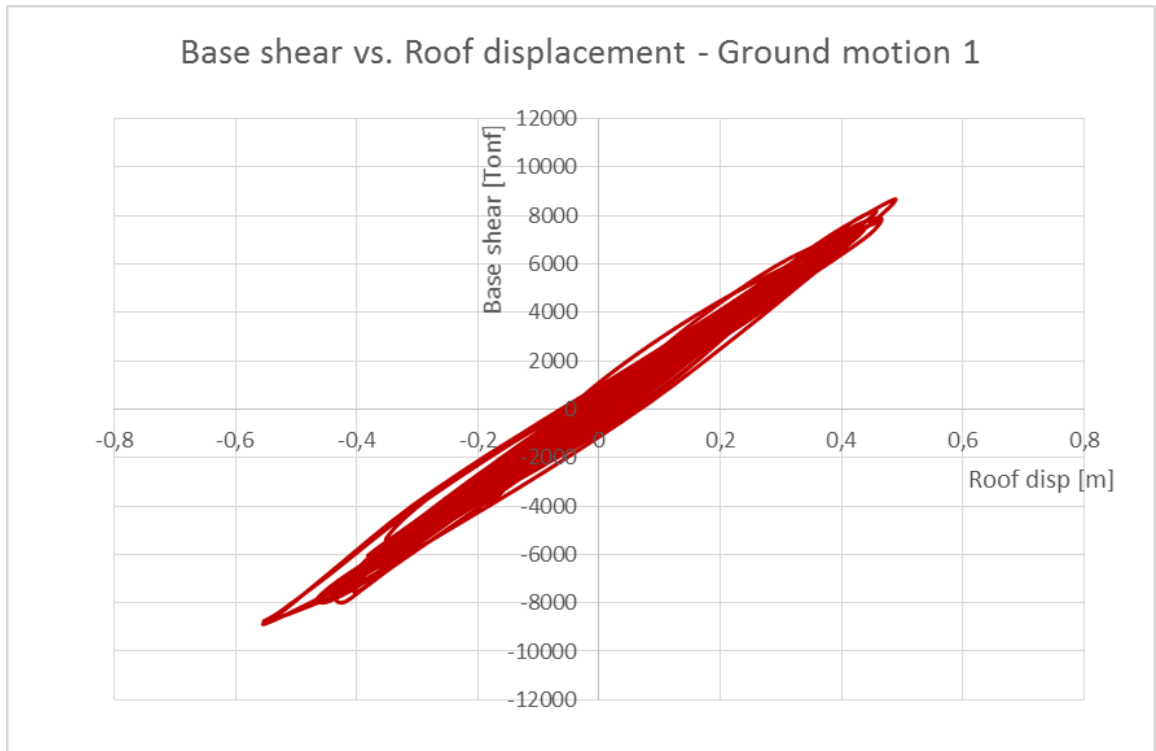


Figure 59: Base shear vs Roof displacement - Ground motion 1

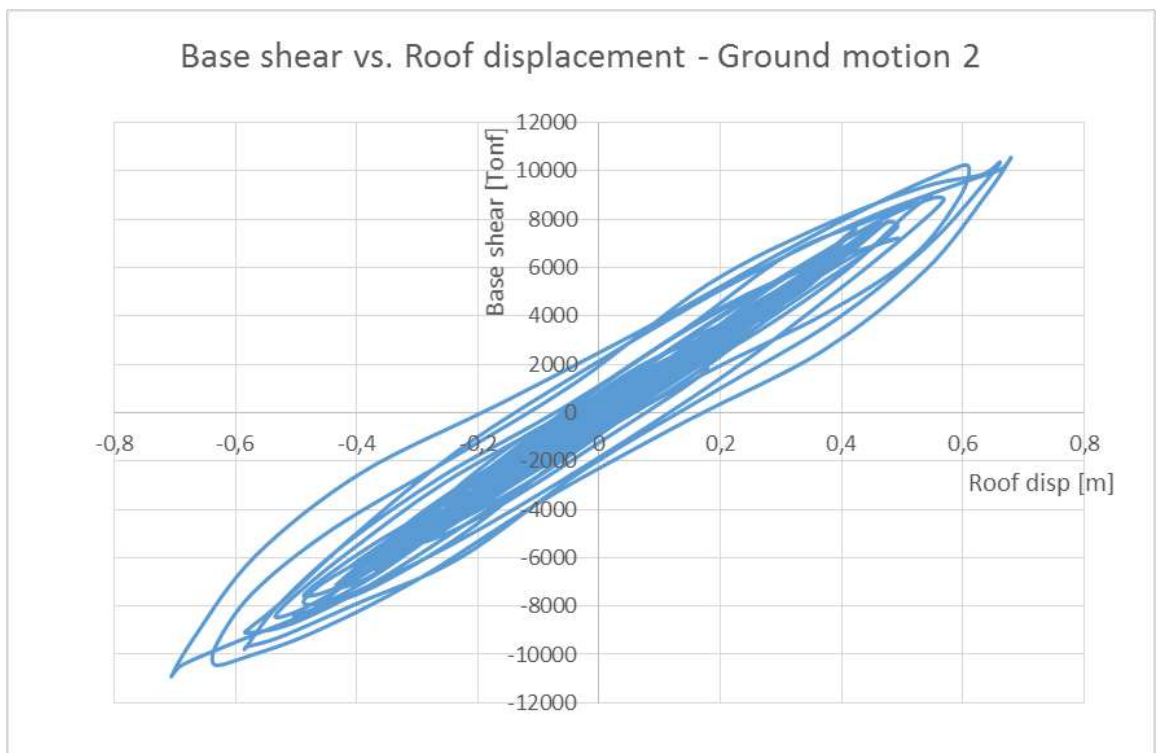


Figure 60: Base shear vs Roof displacement - Ground motion 2

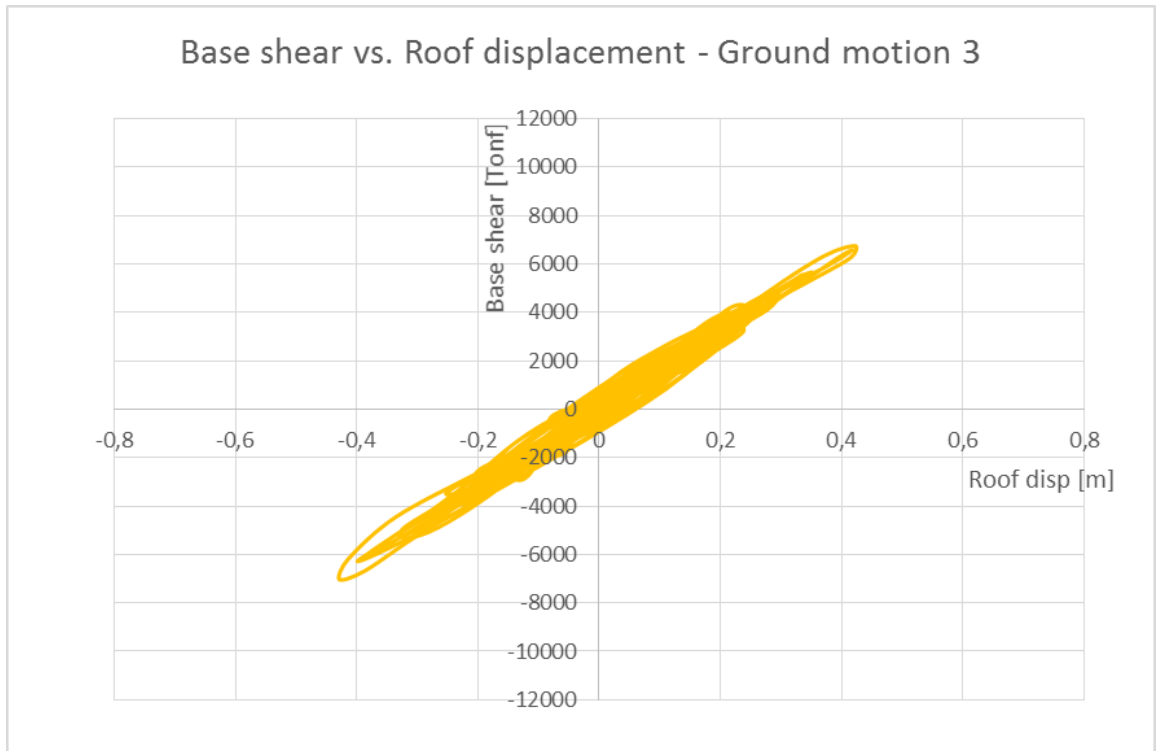


Figure 61: Base shear vs Roof displacement - Ground motion 3

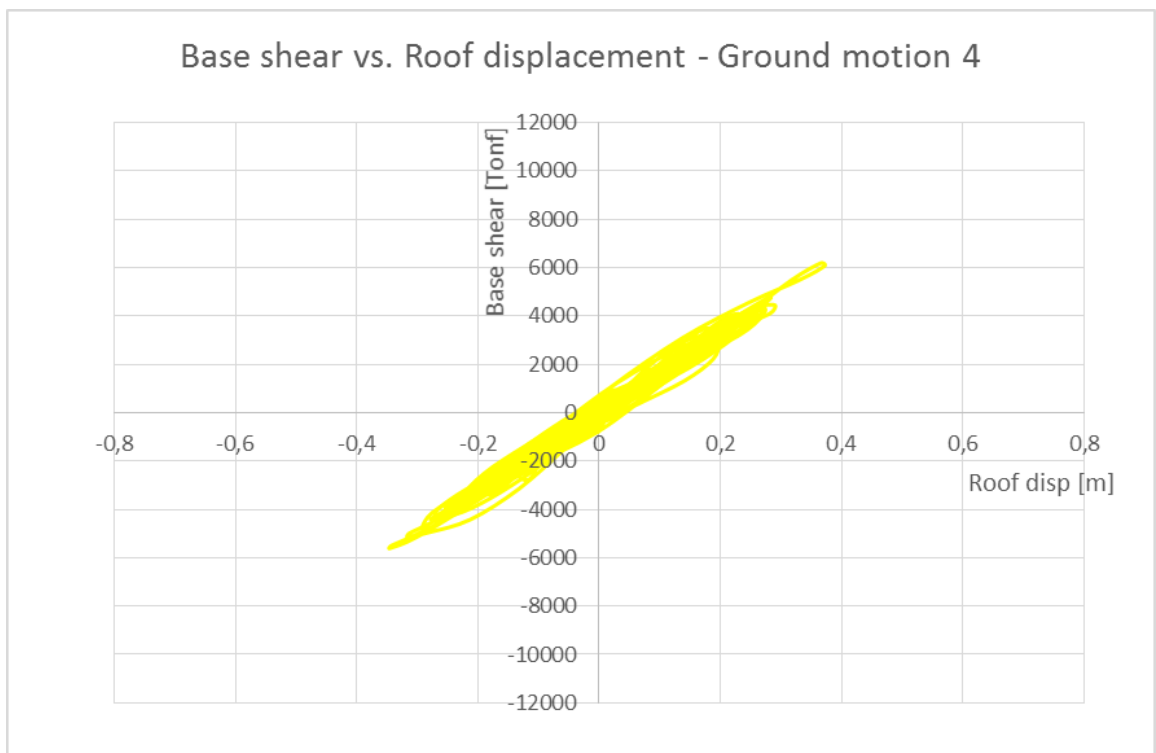


Figure 62: Base shear vs Roof displacement - Ground motion 4

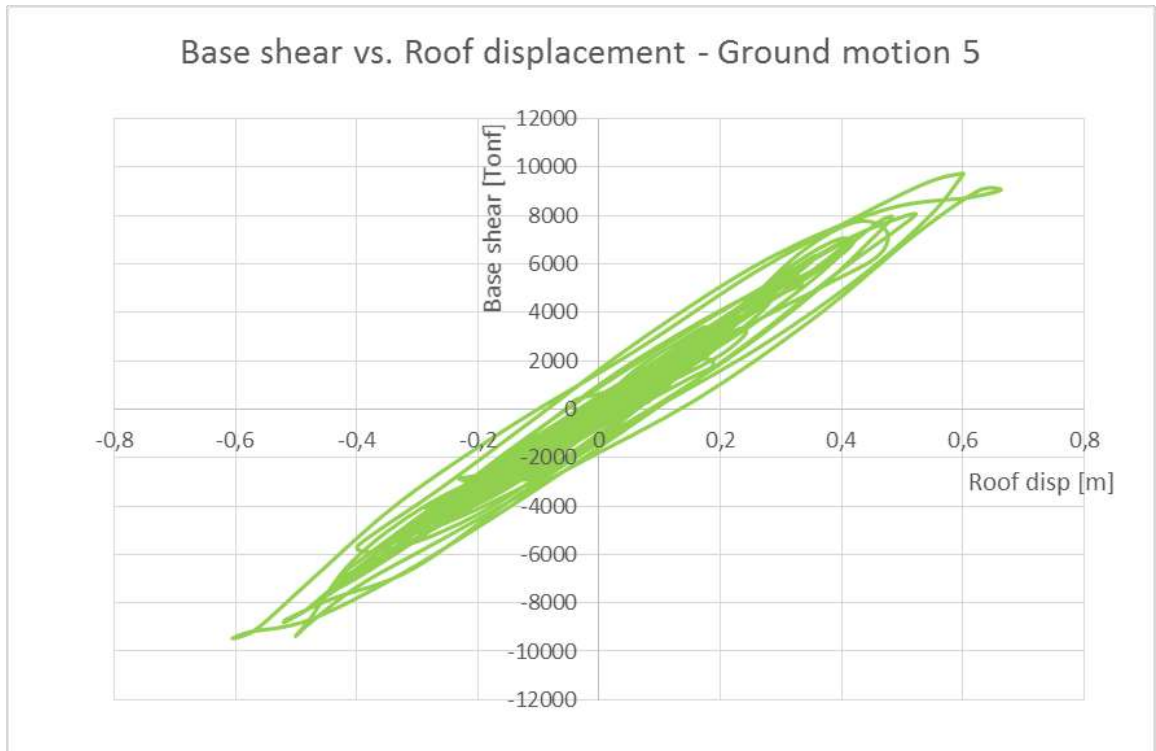


Figure 63: Base shear vs Roof displacement - Ground motion 5

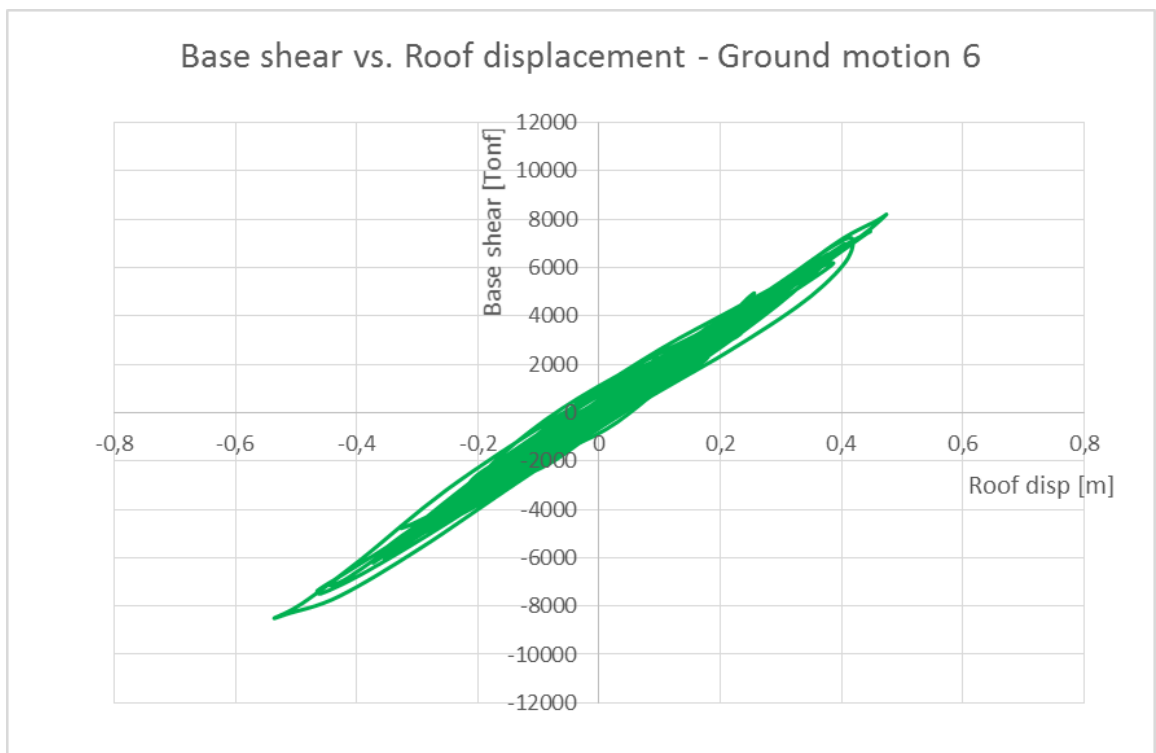


Figure 64: Base shear vs Roof displacement - Ground motion 6

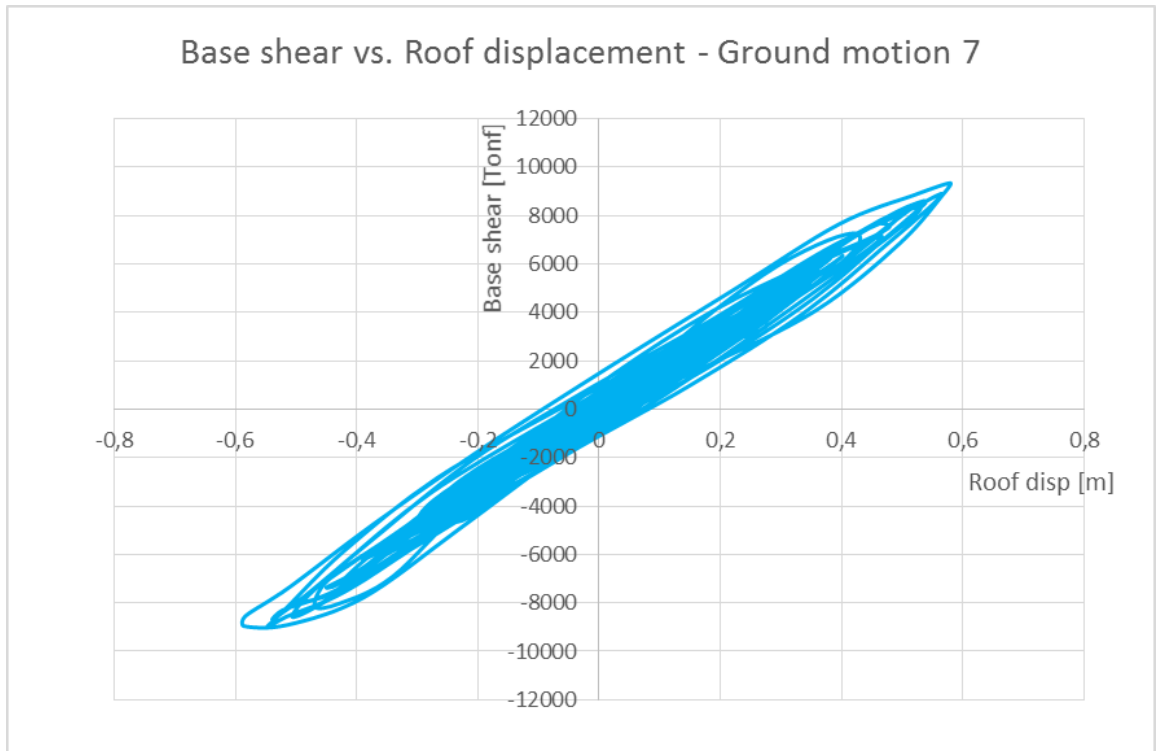


Figure 65: Base shear vs Roof displacement - Ground motion 7

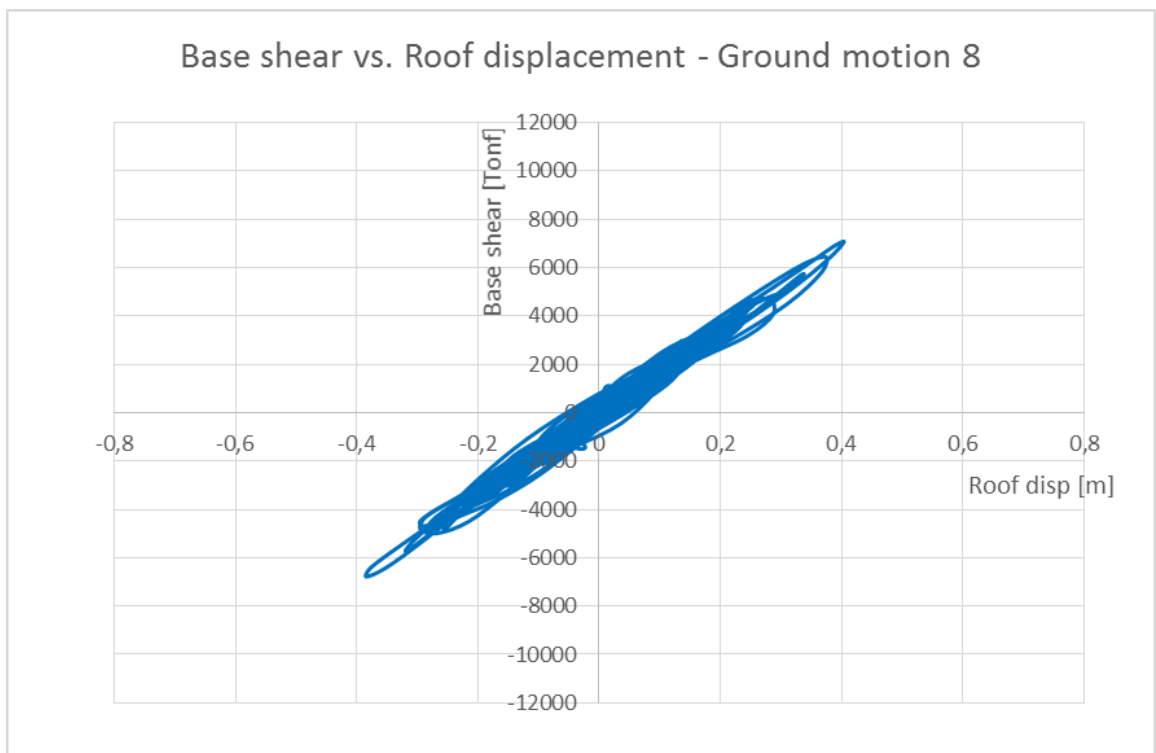


Figure 66: Base shear vs Roof displacement - Ground motion 8

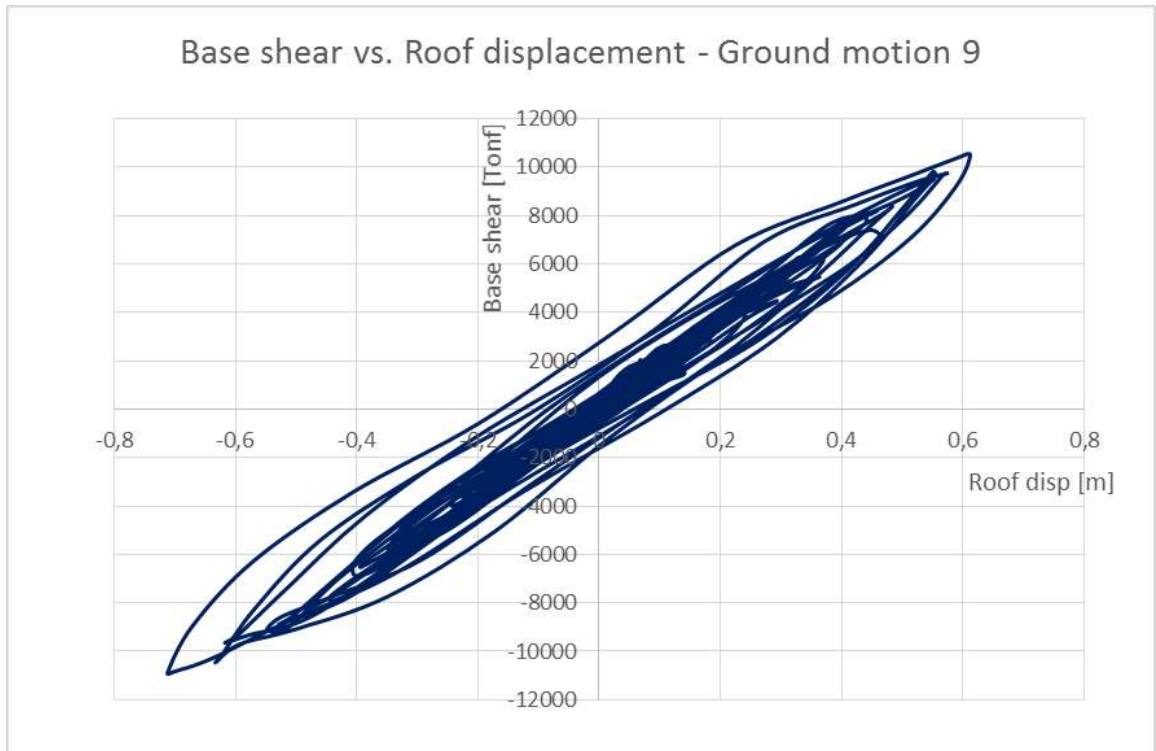


Figure 67: Base shear vs Roof displacement - Ground motion 9

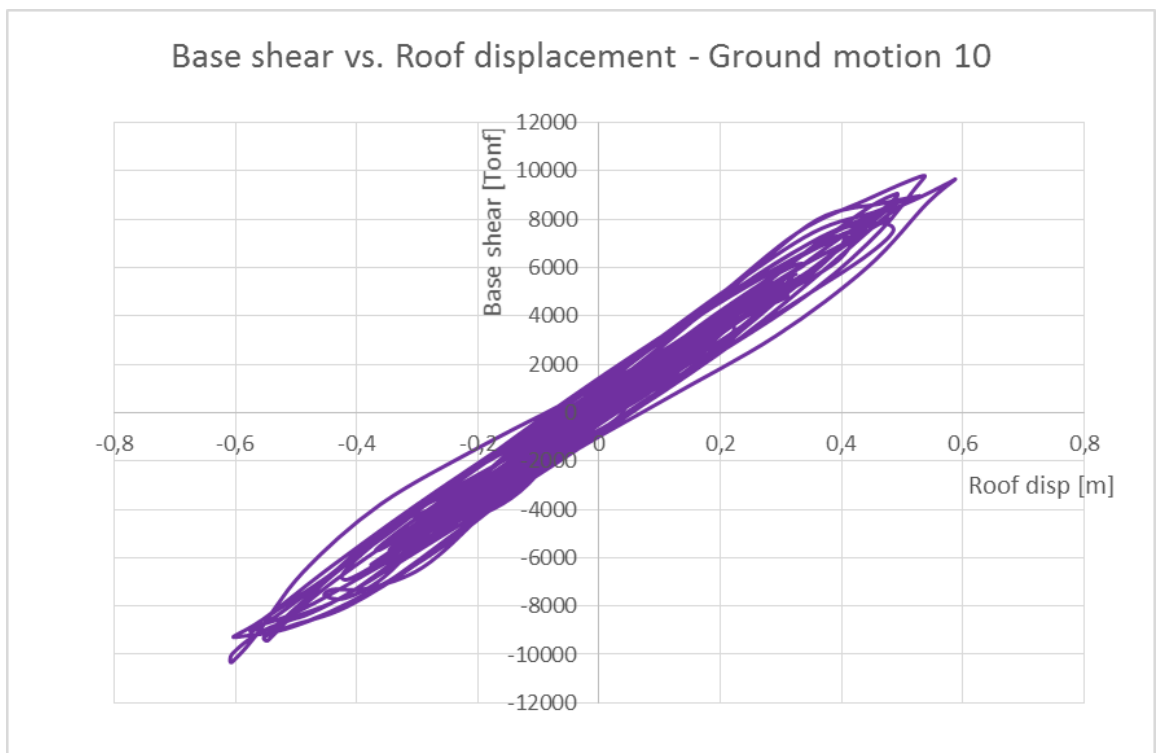


Figure 68: Base shear vs Roof displacement - Ground motion 10

The hysteresis drawn in the previous diagrams give information about the overall stability of the diagrid building. For all the ground motions the curves are near to an idealized diagonal straight line. This means that the building and especially the diagrids are stable during an earthquake and do not tend to degrade due to the presence of plastic deformations.

11. INITIAL PROPOSAL/POSSIBLE OPTIMIZATION

The sizing of the diagonal structural members derived from the conceptual methodology can be used directly by the structural engineer to establish the final design of the diagrid structural system or as an initial solution for methodologies aimed at optimizing the seismic performance of the building. The process of optimization should be undertaken carefully under the consideration of the uncertainties involved

The diagrid areas defined in this thesis are only an initial proposal for a preliminary design. A certain “liberty” is given for the design. If the structural engineer wants to have the plastic hinges better spread along the building’s height, it is possible to increase the diagrid area at the base and decrease the ones at the top to achieve a better repartition. It doesn’t mean that the actual design is bad, it is just that plastic behavior tends to concentrate in the diagonals located at the base of the building. But from a practical point of view, it could be an advantage for the replacement of the damaged diagonals since the work height is not so high.

12. NEW COEFFICIENT OF DISTORTION FOR DIAGRID BUILDINGS

In order to make a preliminary design of the diagrids, a coefficient of distortion (COD) equal to 1,5 according to table 13 was taken. However the values in the table 13 are typical value for building with braces and columns and not for diagrid edifices. 1,5 was chosen since there was no precedent value available for diagrid structures. With the results derived from the nonlinear analysis carried out, it is possible to compute the COD for the several ground motions and then take the average of all of them (because all the stories have the same height).

Table 26: Computation of the COD for the diagrid building

Ground motion	COD
1	1,088945
2	1,130133
3	1,106704
4	1,111057
5	1,084973
6	1,096324
7	1,081132
8	1,098824
9	1,157772
10	1,089834
Average COD	1,10457

The average of COD is 1,1. To be on the conservative side, a value of 1,2 should be taken for a diagrid building with a ductility of $\mu = 1,5$

With this new COD it is possible to review the computation done before and express the new roof displacement in function of a $COD = 1,2$

Roof displacement for life safety:

$$\delta_S^{LS} = \frac{IDI_S^{LS}(H)}{COD^{LS}} = \frac{0,01(84m)}{1,2} = 0,70 m = 70 cm$$

$$S_d = \frac{\delta_S^{LS}}{\alpha_{Diagrids}} = \frac{0,70 m}{1,4} = 0,50 m = 50 cm$$

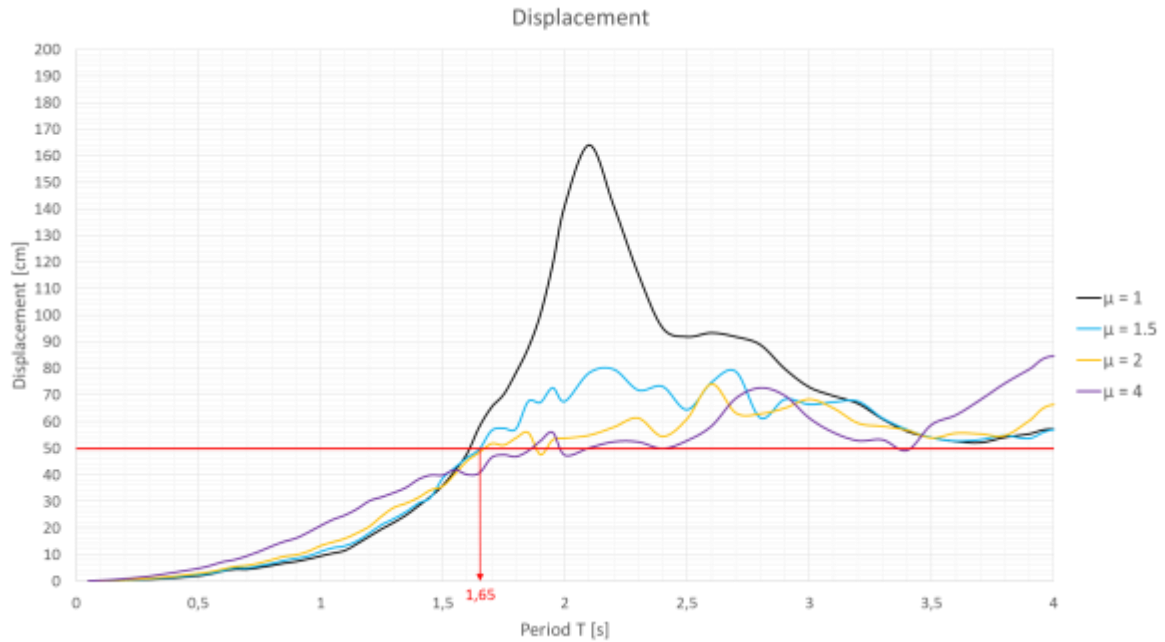


Figure 69: Displacement based design spectra for $\mu=1$, $\mu=1.5$, $\mu=2$ and $\mu=4$

Here $T_{T \text{ required}} = 1.65 \text{ s}$ so

$$k = \frac{T_{T \text{ required}} + 1.5}{2} \text{ if } 0.5 \text{ s} < T < 2.5 \text{ s}$$

$$k = \frac{T_{T \text{ required}} + 1.5}{2} = \frac{1.65 + 1.5}{2} = 1.575$$

$$T_S = 0.3621 \text{ s}; T_B = 0.279 \text{ s}$$

$$T_T^2 = T_S^2 + T_B^2 \Rightarrow T_T^0 = \sqrt{T_S^2 + T_B^2} = 0.457 \text{ s}$$

$$A = A^0 \left(\frac{T_T^0}{T_{T \text{ required}}} \right)^2$$

Table 27: Comparison of the diagrids area with a COD of 1,5 and 1,2

T = 1,55s		T = 1,65s	
$\mu = 2$		$\mu = 1,5$	
COD = 1,5		COD = 1,2	
Diagrids area required [m ²]	Diagrids area required [cm ²]	Diagrids area required [m ²]	Diagrids area required [cm ²]
0.01455	146	0.01279	128
0.01455	146	0.01279	128
0.01455	146	0.01279	128
0.01455	146	0.01279	128
0.02909	291	0.02557	256
0.02909	291	0.02557	256
0.02909	291	0.02557	256
0.02909	291	0.02557	256
0.04365	436	0.03836	384
0.04365	436	0.03836	384
0.04365	436	0.03836	384
0.04365	436	0.03836	384
0.05820	582	0.05115	512
0.05820	582	0.05115	512
0.05820	582	0.05115	512
0.05820	582	0.05115	512
0.07274	727	0.06393	639
0.07274	727	0.06393	639
0.07274	727	0.06393	639
0.07274	727	0.06393	639
0.08729	873	0.07672	767
0.08729	873	0.07672	767
0.08729	873	0.07672	767
0.08729	873	0.07672	767

13. CONCLUSION

In this thesis, the study of the lateral response of the particular case of a 24-stories diagrid building with a circular cross section has shown that a diagrid structural system offers an adequate solution for the design and construction of skyscrapers located in seismic areas.

Due to the fact that the diagrid facade acts also as a structural system which resist dynamic loads under an earthquake, the core can be discharged of the task of taking additional horizontal loads due to a ground motion. Because diagrids withstand both shear and bending forces in a singular manner - only by axial deformations and without the development of internal moments - the entire structural system shows a great stability. Besides this, the particular pattern of the diagrids created by diagonal steel members and horizontal bracing rings lead to a reduction of the amount of material used to build the structure.

Within the context of a displacement-based seismic design methodology, the sizes of the diagrids are determined as a function of: the definition of building performance, the maximal roof displacement and the required fundamental period of vibration. This is done in order to adequately control the level of damage in the building.

The results of the push-over analysis are stunning. The distribution of the interstory drift over the building height reach almost perfection. This is also supported by the excellent interstory ductility. The plastic behavior tends to accumulate in the diagrids located in the bottom stories of the building but since this work presents an initial design proposal, a further optimization is of course possible.

The study of the building dynamic response under an earthquake ground motion (time-history analysis) confirms the striking behavior of the edifice. Despite the fact that the lateral roof displacement is greater than expected, the distribution of the horizontal displacement through the building height is very similar. Nevertheless the prior criteria to confirm that building achieved the target fixed in terms of performance level is not the maximal roof displacement but the interstory drift index. The maximal allowable level of damage defined with an IDI value fixed at 0,01 for life safety was never reach or exceed. Moreover the repartition of distortion through the height is nearly identical in each story which is close to the better possibility attainable.

The period found after the modal analysis is greater than that considered initially but it has been shown that the difference was due to in inadequate definition of the coefficient of distortion since there was a lack of COD-value computed for diagrid buildings. However the study gave a new clue with a COD equal to 1,2 which can be now used for the design of further diagrid buildings located in high seismic zones.

A displacement-based methodology design for a 24-story diagrid building having a circular plan is applicable for the development and improvement of an adequate combination of sustainability and damage level control. All these results prove that the proposed methodology can be adopted for the preliminary design of a circular diagrid building located in an area of high seismicity.

14. APPENDIX

APPENDIX A.	DESIGN OF THE LOSACERO (STEEL-DECK)	87
APPENDIX B.	LIVE LOADS ACCORDING TO THE MEXICAN PROPOSAL	89
APPENDIX C.	AREAS DESIGNATION	90
APPENDIX D.	LOADS ON ONE FLOOR	91
APPENDIX E.	TABLES FOR CONCRETE DESIGN (U.S. CUSTOMARY UNITS)	93

Appendix A. Design of the Losacero (steel-deck)

Tables from (IMSA)

Section properties:

Propiedades de la Sección (Sin concreto)					
Cal.	PESO (Kg/m²)	I+ (cm⁴/m)	I- (cm⁴/m)	S+ (cm³/m)	S- (cm³/m)
24	5.70	57.12	52.68	13.86	14.10
22	8.00	74.60	69.39	18.62	19.23
20	9.54	90.95	86.51	23.66	24.78
18	12.59	121.09	119.12	33.26	36.24

Maximal span without shoring

Losacero Sección 4 Claros Máximos sin Apuntalamiento						
CALIBRE	APOYO	5cm	6cm	8cm	10cm	12cm
24	↑↑	1.77	1.70	1.59	1.50	1.42
	↑↑↑	2.38	2.29	2.15	2.03	1.93
	↑↑↑↑	2.41	2.32	2.17	2.05	1.95
22	↑↑	2.12	2.04	1.90	1.79	1.69
	↑↑↑	2.83	2.73	2.55	2.40	2.28
	↑↑↑↑	2.91	2.80	2.61	2.46	2.33
20	↑↑	2.46	2.36	2.19	2.06	1.95
	↑↑↑	3.20	3.08	2.89	2.72	2.58
	↑↑↑↑	3.31	3.19	2.98	2.81	2.67
18	↑↑	3.00	2.87	2.67	2.50	2.36
	↑↑↑	3.85	3.71	3.48	3.28	3.11
	↑↑↑↑	3.98	3.84	3.59	3.39	3.22

Maxmial admissible overload:

Losacero Sección 4 Sobrecargas Admisibles (kg/m²)														
Cal.	espesor de conc. (cm)	Separación entre apoyos (m)												
		1.8	2	2.2	2.4	2.6	2.8	3	3.2	3.4	3.6	3.8	4	
Con Conectores	24	5	1840	1462	1182	969	804	672	566	479	407	347	296	252
		6	2000	1649	1334	1094	907	759	640	542	461	393	335	286
		8	2000	2000	1638	1344	1115	933	787	667	586	485	414	354
		10	2000	2000	1941	1593	1323	1108	934	793	675	576	493	422
		12	2000	2000	2000	1843	1530	1282	1052	918	782	668	572	490
22	5	2000	1895	1465	1207	1006	846	717	612	525	452	390	337	
	6	2000	2000	1656	1356	1138	958	812	693	595	512	442	383	
	8	2000	2000	2000	1681	1402	1181	1002	856	735	634	548	474	
	10	2000	2000	2000	2000	1666	1404	1192	1019	875	755	653	566	
	12	2000	2000	2000	2000	2000	1627	1382	1182	1016	876	759	658	
20	5	2000	2000	1772	1464	1225	1035	882	756	652	565	492	429	
	6	2000	2000	2000	1660	1389	1174	1001	859	741	643	559	488	
	8	2000	2000	2000	2000	1717	1452	1238	1064	919	797	694	607	
	10	2000	2000	2000	2000	2000	1730	1476	1269	1096	952	830	725	
	12	2000	2000	2000	2000	2000	2000	1714	1473	1274	1107	965	844	
18	5	2000	2000	2000	1908	1603	1361	1165	1005	873	762	667	587	
	6	2000	2000	2000	2000	1826	1551	1328	1146	996	869	763	671	
	8	2000	2000	2000	2000	2000	1930	1655	1429	1242	1085	953	840	
	10	2000	2000	2000	2000	2000	2000	2000	1711	1488	1301	1143	1008	
	12	2000	2000	2000	2000	2000	2000	2000	2000	1735	1517	1334	1177	

Concrete volume:

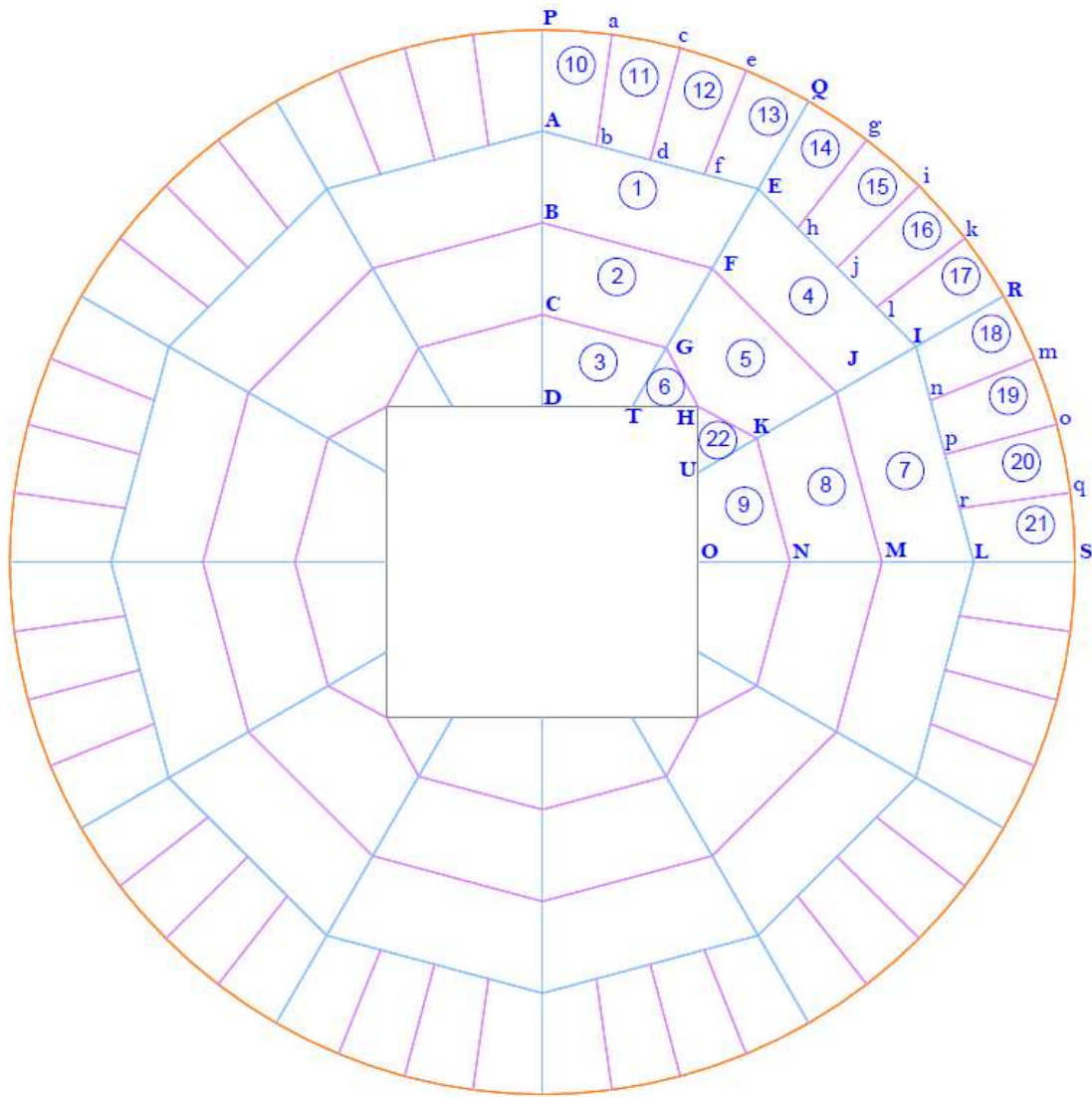
Losacero Sección 4(M³/M²)					
Espesor de concreto sobre la cresta	5cm	6cm	8cm	10cm	12cm
Volumen	0.085	0.095	0.115	0.135	0.155

Appendix B. Live loads according to the Mexican proposal

Tabla 6.1 Cargas vivas unitarias, kg/m² (kN/m²)

Destino de piso o cubierta	W	W_a	W_m	Observaciones
a) Habitación (casa–habitación, departamentos, viviendas, dormitorios, cuartos de hotel, internados de escuelas, cuarteles, cárceles, correccionales, hospitales y similares)	70 (0.7)	90 (0.9)	170 (1.7)	1
b) Oficinas, despachos y laboratorios	100 (1)	180 (1.8)	250 (2.5)	2
c) Aulas	100 (1)	180 (1.8)	250 (2.5)	
d) Comunicación para peatones (pasillos, escaleras, rampas, vestíbulos y pasajes de acceso libre al público)	40 (0.4)	150 (1.5)	350 (3.5)	3 y 4
e) Estadios y lugares de reunión sin asientos individuales	40 (0.4)	350 (3.5)	450 (4.5)	5
f) Otros lugares de reunión (templos, cines, teatros, gimnasios, salones de baile, restaurantes, bibliotecas, aulas, salas de juego y similares)	40 (0.4)	250 (2.5)	350 (3.5)	5
g) Cubiertas y azoteas con pendiente no mayor de 5 %	15 (0.15)	70 (0.7)	100 (1)	4 y 7
h) Cubiertas y azoteas con pendiente mayor de 5 %	5 (0.05)	20 (0.2)	40 (0.4)	4, 7 y 8
i) Volados en vía pública (marquesinas, balcones y similares)	15 (0.15)	70 (0.7)	300 (3)	
j) Garajes y estacionamientos (exclusivamente para automóviles)	40 (0.4)	100 (1)	250 (2.5)	9

Appendix C. Areas designation



Appendix D. Loads on one floor

(without self-weight of the steel and concrete elements)

Story											
Surface	Area [m ²]	Dead Load						Live Load for Gravitational system			
		Losacero Cal 22 [kg/m ²]	Losacero Cal 24 [kg/m ²]	Weight Losacero [kg]	Floor [kg/m ²]	Weight Floor [kg]	Dead Load [kg]	Dead Load/4 [kg]	Live Load W _m [kg/m ²]	Live Load W _m [kg]	Live Load W _m /4 [kg]
1	18,25	212		3869,00	153	2792	6661	1665	250	4563	1141
2	13,90	212		2946,80	153	2127	5074	1268	250	3475	869
3	8,58	212		1818,96	153	1313	3132	783	250	2145	536
4	18,25	212		3869,00	153	2792	6661	1665	250	4563	1141
5	15,15	212		3211,80	153	2318	5530	1382	250	3788	947
6	1,99	212		421,88	153	304	726	182	250	498	124
7	18,25	212		3869,00	153	2792	6661	1665	250	4563	1141
8	13,90	212		2946,80	153	2127	5074	1268	250	3475	869
9	8,58	212		1818,96	153	1313	3132	783	250	2145	536
22	1,99	212		421,88	153	304	726	182	250	498	124
10	6,87		209,7	1440,64	153	1051	2492	623	250	1718	429
11	7,40		209,7	1551,78	153	1132	2684	671	250	1850	463
12	7,40		209,7	1551,78	153	1132	2684	671	250	1850	463
13	6,87		209,7	1440,64	153	1051	2492	623	250	1718	429
14	6,87		209,7	1440,64	153	1051	2492	623	250	1718	429
15	7,40		209,7	1551,78	153	1132	2684	671	250	1850	463
16	7,40		209,7	1551,78	153	1132	2684	671	250	1850	463
17	6,87		209,7	1440,64	153	1051	2492	623	250	1718	429
18	6,87		209,7	1440,64	153	1051	2492	623	250	1718	429
19	7,40		209,7	1551,78	153	1132	2684	671	250	1850	463
20	7,40		209,7	1551,78	153	1132	2684	671	250	1850	463
21	6,87		209,7	1440,64	153	1051	2492	623	250	1718	429
204,46				For one quadrant		[kg]	74431				51115
						[t]	74,431				51,115
				For one floor		[t]	297,724				204,460

(without self-weight of the steel and concrete elements)

Roof											
Surface	Area [m ²]	Dead Load							Live Load for Gravitational system		
		Losacero Cal 22 [kg/m ²]	Losacero Cal 24 [kg/m ²]	Weight Losacero [kg]	Floor [kg/m ²]	Weight Floor [kg]	Dead Load [kg]	Dead Load/4 [kg]	Live Load W _m [kg/m ²]	Live Load W _m [kg]	Live Load W _m /4 [kg]
1	18,25	212		3869,00	153	2792	6661	1665	100	1825	456
2	13,90	212		2946,80	153	2127	5074	1268	100	1390	348
3	8,58	212		1818,96	153	1313	3132	783	100	858	215
4	18,25	212		3869,00	153	2792	6661	1665	100	1825	456
5	15,15	212		3211,80	153	2318	5530	1382	100	1515	379
6	1,99	212		421,88	153	304	726	182	100	199	50
7	18,25	212		3869,00	153	2792	6661	1665	100	1825	456
8	13,90	212		2946,80	153	2127	5074	1268	100	1390	348
9	8,58	212		1818,96	153	1313	3132	783	100	858	215
22	1,99	212		421,88	153	304	726	182	100	199	50
10	6,87		209,7	1440,64	153	1051	2492	623	100	687	172
11	7,40		209,7	1551,78	153	1132	2684	671	100	740	185
12	7,40		209,7	1551,78	153	1132	2684	671	100	740	185
13	6,87		209,7	1440,64	153	1051	2492	623	100	687	172
14	6,87		209,7	1440,64	153	1051	2492	623	100	687	172
15	7,40		209,7	1551,78	153	1132	2684	671	100	740	185
16	7,40		209,7	1551,78	153	1132	2684	671	100	740	185
17	6,87		209,7	1440,64	153	1051	2492	623	100	687	172
18	6,87		209,7	1440,64	153	1051	2492	623	100	687	172
19	7,40		209,7	1551,78	153	1132	2684	671	100	740	185
20	7,40		209,7	1551,78	153	1132	2684	671	100	740	185
21	6,87		209,7	1440,64	153	1051	2492	623	100	687	172
204,46				For one quadrant		[kg]	74431		20446		
						[t]	74,431		20,446		
				For one floor		[t]	297,724		81,784		

Appendix E. Tables for concrete design (U.S. Customary Units)

TABLE A.1 Values of Modulus of Elasticity for Normal-Weight Concrete

U.S. Customary Units	
f'_c (psi)	E_c (psi)
3,000	3,160,000
3,500	3,410,000
4,000	3,640,000
4,500	3,870,000
5,000	4,070,000

Figure 70: Values of Modulus of Elasticity for Normal-Weight Concrete (McCormac, Brown 2013, p. 631)

TABLE A.2 Designations, Areas, Perimeters, and Weights of Standard Bars

Bar No.	U.S. Customary Units		
	Diameter (in.)	Cross-Sectional Area (in. ²)	Unit Weight (lb/ft)
3	0.375	0.11	0.376
4	0.500	0.20	0.668
5	0.625	0.31	1.043
6	0.750	0.44	1.502
7	0.875	0.60	2.044
8	1.000	0.79	2.670
9	1.128	1.00	3.400
10	1.270	1.27	4.303
11	1.410	1.56	5.313
14	1.693	2.25	7.650
18	2.257	4.00	13.600

Figure 71: Designations, Areas, Perimeters, and Weights of Standard Bars (McCormac, Brown 2013, p. 631)

TABLE A.4 Areas of Groups of Standard Bars (in.²)— U.S. Customary Units

Bar No.	Number of Bars								
	2	3	4	5	6	7	8	9	10
4	0.39	0.58	0.78	0.98	1.18	1.37	1.57	1.77	1.96
5	0.61	0.91	1.23	1.53	1.84	2.15	2.45	2.76	3.07
6	0.88	1.32	1.77	2.21	2.65	3.09	3.53	3.98	4.42
7	1.20	1.80	2.41	3.01	3.61	4.21	4.81	5.41	6.01
8	1.57	2.35	3.14	3.93	4.71	5.50	6.28	7.07	7.85
9	2.00	3.00	4.00	5.00	6.00	7.00	8.00	9.00	10.00
10	2.53	3.79	5.06	6.33	7.59	8.86	10.12	11.39	12.66
11	3.12	4.68	6.25	7.81	9.37	10.94	12.50	14.06	15.62
14	4.50	6.75	9.00	11.25	13.50	15.75	18.00	20.25	22.50
18	8.00	12.00	16.00	20.00	24.00	28.00	32.00	36.00	40.00

Bar No.	Number of Bars									
	11	12	13	14	15	16	17	18	19	20
4	2.16	2.36	2.55	2.75	2.95	3.14	3.34	3.53	3.73	3.93
5	3.37	3.68	3.99	4.30	4.60	4.91	5.22	5.52	5.83	6.14
6	4.86	5.30	5.74	6.19	6.63	7.07	7.51	7.95	8.39	8.84
7	6.61	7.22	7.82	8.42	9.02	9.62	10.22	10.82	11.43	12.03
8	8.64	9.43	10.21	11.00	11.78	12.57	13.35	14.14	14.92	15.71
9	11.00	12.00	13.00	14.00	15.00	16.00	17.00	18.00	19.00	20.00
10	13.92	15.19	16.45	17.72	18.98	20.25	21.52	22.78	24.05	25.31
11	17.19	18.75	20.31	21.87	23.44	25.00	26.56	28.12	29.69	31.25
14	24.75	27.00	29.25	31.50	33.75	36.00	38.25	40.50	42.75	45.00
18	44.00	48.00	52.00	56.00	60.00	64.00	68.00	72.00	76.00	80.00

Figure 72: Areas of Groups of Standard Bars (in²) (McCormac, Brown 2013, p. 634)

15. PUBLICATION BIBLIOGRAPHY

- Ali, Mir M.; Moon, Kyoung Sun (2007): Structural Developments in Tall Buildings. Current Trends and Future Prospects. In *Architectural Science Review* 50 (3), pp. 205–223. DOI: 10.3763/asre.2007.5027.
- Amador Terán Gilmore: Capacity design.
- Amador Terán Gilmore: Elementos de concreto reforzado.
- Amaya Aguilar, Nabot J. (2015): Uso de rejillas rígidas como sistema estructural en edificios altos ubicados en zonas sísmicas.
- Autodesk: AutoCAD. Version 2016. Mill Valley, California, USA.
- Boake, Terri Meyer (2014): Diagrid structures. Systems, connections, details. Basel, Switzerland: Birkhäuser Verlag GmbH.
- Computers & Structure, Inc.: SAP2000. Version Ultimate 15.0.0. Berkeley, California, USA.
- FEMA 356 Prestandard and Commentary for the Seismic Rehabilitation of Buildings.
- IMSA: Losacero Sección 4 y Sección 36/15.
- Kim, Jinkoo; Lee, Young-Ho (2012): Seismic performance evaluation of diagrid system buildings. In *Struct. Design Tall Spec. Build.* 21 (10), pp. 736–749. DOI: 10.1002/tal.643.
- Kohrs-Sansorny, C. (2005): A Two-Stage Method for Ground-Motion Simulation Using Stochastic Summation of Small Earthquakes. In *Bulletin of the Seismological Society of America* 95 (4), pp. 1387–1400. DOI: 10.1785/0120040211.
- McCormac, Jack C.; Brown, Russell H. (2013): Design of reinforced concrete. Ninth edition, ACI 318-11 Code Edition.
- Mele, Elena; Toreno, Maurizio; Brandonisio, Giuseppe; Luca, Antonello de (2014): Diagrid structures for tall buildings: case studies and design considerations. In *Struct. Design Tall Spec. Build.* 23 (2), pp. 124–145. DOI: 10.1002/tal.1029.
- Moon, Kyoung Sun; Connor, Jerome J.; Fernandez, John E. (2007): Diagrid structural systems for tall buildings characteristics and methodology for preliminary design. DOI: 10.1002/tal.311.
- 2004: Normas Técnicas Complementarias para Diseño y Construcción De Estructuras de Concreto.
- Abril 2001: Normas Técnicas Complementarias sobre Criterios y Acciones para el Diseño Estructural de las Edificaciones.
- Olivera, Josimar S. (2015): Bases para un diseño sísmico basado en rigidez de rejillas rígidas de planta circular para edificios de gran altura ubicados en zonas de alta sismicidad.
- Pushover. Available online at wiki.csiamerica.com/display/kb/Pushover.
- Segui, William T. (2007): Steel design. 4th ed. Toronto, Ontario, Canada: Thomson; Nelson.

Terán Gilmore, Amador; Coeto, Guillermo (2011): Displacement-Based Preliminary Design of Tall Buildings Stiffened with a System of Buckling-Restrained Braces. In *Earthquake Spectra* 27 (1), pp. 153–182. DOI: 10.1193/1.3543854.

Terán Gilmore, Amador; Quiroz Ramírez, Arturo; Díaz Martínez, Gerardo (2014): Uso de rejillas perimetrales (Diagrid) para estructurar edificios altos de acero ubicados en zonas de alta sismicidad.